THREE ESSAYS ON ESTIMATION OF RISK NEUTRAL MEASURES USING OPTION PRICING MODELS

DISSERTATION

Presented in Partial Fulfillment of the Requirements for

the Degree Doctor of Philosophy in the

Graduate School of The Ohio State University

By

Seung Hwan Lee, M.A.

* * * * *

The Ohio State University
2008

Dissertation Committee:

J. Huston McCulloch, Adviser

Paul Evans

Pok-sang Lam

Approved by

Adviser
Graduate Program in
Economics

ABSTRACT

This dissertation develops two new parametric and nonparametric methods for estimating risk-neutral measures (RNM) which embody important information about market participants' sentiments concerning prices of the underlying asset in the future, and investigates empirical performance of parametric RNM estimation methods.

The first essay, "Estimation of Risk Neutral Measures using the Generalized Two-Factor Log-Stable Option Pricing Model", constructs a simple representative agent model to provide a theoretical framework for the log-stable option pricing model and then implements a new parametric method for estimating the RNM using a generalized two-factor log-stable option pricing model. Under the generalized two-factor log-stable uncertainty assumption, the RNM for the log of price is a convolution of two exponentially tilted stable distributions. Since the RNM for generalized two-factor log-stable uncertainty is expressed in terms of its Fourier Transform, I introduce a simple extension of the Fast Fourier Transform inversion procedure in order to reduce computational errors. The generalized two-factor log-stable RNM has a very flexible parametric form for approximating other probability distributions. Thus, this model provides a sufficiently accurate tool for estimating the RNM from observed option prices even if the log-stable assumption might not be satisfied. I estimate the RNM using the S&P 500 index options and find that the generalized two-factor log-stable model gives better performance than the Black-Scholes model (1973), the finite moment log-stable model (Carr and Wu, 2003), and the orthogonal log-stable model (McCulloch, 2003) in fitting the observed option prices.

The second essay, "Parametric Risk Neutral Measure Estimation Methods: A Horse Race", implements 12 parametric RNM estimation methods by means of the closed-form or characteristic function of RNM distributions and then compares the empirical performance under three criteria—the root mean squared error (RMSE) for the goodness-of-fit, likelihood ratio (LR) for the model selection, and the root mean integrated squared error (RMISE) for the accuracy and stability of the estimated RNMs. The empirical results show that the generalized two-factor log-stable model outperforms other alternative parametric RNM estimation methods. Even though the jump diffusion model with stochastic volatilities dominates other models in the RMSEs and the LR tests, it is vulnerable to over-fitting problems due to a large number of parameters. Monte-Carlo experiments reveal that the jump diffusion model with stochastic volatilities suffers from serious over-fitting problems and also show that the generalized two-factor log-stable model outperforms the alternatives.

The third essay, "Nonparametric Estimation of Risk-Neutral Measures using Quartic B-Spline CDFs with Power Tails", proposes a new nonparametric (BSP) method which overcomes the problems with the smoothed implied volatility smile (SML) method which is the most widely used nonparametric technique for estimating RNMs. I model a RNM cumulative distribution function (CDF) using quartic B-splines with power tails so that the resulting RNM probability density function (PDF) has continuity C^2 and arbitrage-free properties. Since the number of knots is selected optimally in constructing the quartic B-spline RNM CDF, my method avoids both overfitting and oversmoothing. To improve computational efficiency and accuracy I introduce a 3-step RNM estimation procedure that transforms a nonlinear optimization problem into a convex quadratic program, which is efficiently solved by numerical optimization software. The Monte-Carlo experiments suggest that the BSP method performs considerably better than the SML method as a technique for estimating option implied RNMs. The BSP method always produces arbitrage-free RNM estimators and almost perfectly recovers the actual RNM PDFs for all hypothetical distributional assumptions.

To my parents and my family

ACKNOWLEDGMENTS

I wish to thank my adviser, Professor J. Huston McCulloch, for his strong support, faithful encouragement, and many insightful comments that made this dissertation possible. I am indebted to my dissertation committee members, Professor Paul Evans and Professor Pok-sang Lam for their guidance and invaluable comments which were instrumental in completing the dissertation. I would also like to thank Professor Robert L. Kimmel who was my advisory committee member and provided me with the theoretical foundations of asset pricing and fiance.

I am grateful to the Bank of Korea for financial support and the Department of Economics for offering me the Graduate Teaching Associate position as well as the JMCB travel grant.

I would also like to thank my parents, Chunbong Lee and Okmoon Hyun, as well as mother-in-law, Sungja Kang, for their unconditional love. Perhaps most importantly, I must thank my dear wife, Jungmin, and two wonderful children Jiwon and Jaehyun. Without their love and support this dissertation might never have been written.

VITA

July 23, 1968	Born - Jeju, Korea
1993	B.A. Economics, Sogang University, Korea
1993-2003	Economist, The Bank of Korea
2005	M.A. Economics, The Ohio State University
2005-present	Graduate Teaching Associate, The Ohio State University

FIELDS OF STUDY

Major Field: Economics

Studies in:

Financial Economics

Macroeconomics

Econometrics

TABLE OF CONTENTS

Appendices:

LIST OF TABLES

LIST OF FIGURES

CHAPTER 1

INTRODUCTION

Investors and researchers have long used option prices to infer market expectations about the volatilities and correlations of the underlying assets by recovering risk neutral distributions from observed option prices. A European option is a contingent claim whose value is dependent upon the investor's risk preference and the statistical probability measure, the so-called frequency (probability) measure (FM), which governs the empirically observable distribution of the underlying asset prices at the maturity of the option contract. In a complete arbitrage-free market, the valuation of European options is equivalent to computing the discounted value of expected payoff under the risk-adjusted probability measure, the so-called risk-neutral measure (RNM), regardless of the investor's risk preference. The RNM allows us to price any derivative of the particular underlying asset with the same time to maturity by a present value of their expected payoffs at a risk free interest rate. Inversely, the implied RNM may be extracted from the derivative prices by reversing the process of obtaining prices from pricing models.

Since the RNM embodies important information about market participants' sentiments concerning prices of the underlying asset in the future, a number of methods have been developed to estimate the RNM from observed option prices. Generally, these methods are divided into two broad groups of parametric and nonparametric methods. The parametric methods make particular assumptions on the form or family of the RNM and then typically use a non-linear regression technique to estimate the parameters of the RNM which mini-

mizes sum of squared pricing errors. On the other hand, the nonparametric methods make no strong assumptions about the RNM since they are flexible data-driven methods.

This dissertation implements a new parametric RNM estimation method by using the generalized two-factor log-stable option pricing model; investigates the empirical performance of parametric RNM estimation methods; and also proposes a new non-parametric RNM estimation method by constructing a quartic B-spline RNM cumulative distribution function with power tails.

In the first essay, "Estimation of Risk Neutral Measures using the Generalized Two-Factor Log-Stable Option Pricing Model", I construct a simple representative agent model to provide a theoretical framework for the log-stable option pricing model and then implement a new parametric method for estimating the RNM using a generalized two-factor log-stable option pricing model.

The Generalized Central Limit Theorem (GCLT) provides support for stable distributions as a financial asset's log return process since financial asset returns may be considered as the multiplicatively cumulative outcome of many stochastic events. Furthermore, stable distributions can easily accommodate heavy tails and skewness of asset returns, which are commonly observed in the financial data. It is therefore reasonable to assume that log asset returns are governed by a stable distribution. In turn, asset prices themselves follow a log-stable distribution.

I construct a simple representative agent model in an Arrow-Debreu world to provide a theoretical framework for the log-stable option pricing model. I also introduce the generalized two-factor log-stable option pricing model by relaxing the orthogonal log-stable assumption of McCulloch (2003). Since the RNM for generalized two-factor log-stable uncertainty is expressed in terms of its Fourier Transform, I implement a simple extension of the Fast Fourier Transform inversion procedure in order to reduce computational errors. Under the generalized two-factor log-stable uncertainty assumption, the RNM for the log of price is a convolution of two exponentially tilted stable distributions. The generalized

two-factor log-stable RNM has a very flexible parametric form for approximating other probability distributions. Thus, this model provides a sufficiently accurate tool for estimating the RNM from observed option prices even if the log-stable assumption might not be satisfied.

To illustrate the empirical performance of the generalized two-factor log-stable model, I estimate the RNM from observed S&P 500 index option prices by using four option pricing models: the BS log-normal model, the finite moment log-stable model, the orthogonal log-stable model, and the generalized two-factor log-stable model. I evaluate the models on the basis of the goodness-of-fit and find that the generalized two-factor log-stable model outperforms the others.

In the second essay, "Parametric Risk Neutral Measure Estimation Methods: A Horse Race", I implement 12 parametric RNM estimation methods by means of the closed form of RNM distributions or RNM characteristic functions and then compare the empirical performance of the 12 parametric RNM estimation methods. First, the goodness-of-fits are examined by means of the root mean squared errors (RMSE). Second, I perform likelihood ratio (LR) tests for the nested and non-nested model selection. Finally, I conduct Monte-Carol experiments to compare the accuracy and stability of the parametric RNM estimation methods by focusing the root mean integrated squared error (RMISE) criterion.

The empirical results from the RMSEs and the LR tests show that the generalized two-factor log-stable model and the jump diffusion model with stochastic volatilities dominate other models. However, the jump diffusion model with stochastic volatilities has so many free parameters that it is vulnerable to over-fitting problems, which create spurious oscillations due to sampling noises. The Monte-Carlo experiments reveal that the jump diffusion model with stochastic volatilities suffers from serious over-fitting problems and also show that the two-factor generalized model outperforms the alternatives.

In the final essay, "Nonparametric Estimation of Risk Neutral Measures using Quartic B-Spline CDFs with Power Tails", I propose a new nonparametric approach which over-

comes the drawbacks of the smoothed implied volatility smile (SML) method which is the most widely used nonparametric technique for estimating RNMs. First, I model a probability distribution outside the traded strike range as power tails, which may be estimated from far-from-the-money option prices. With the power tails, the RNM has the nonnegative tail probabilities and also reflects information about true tail probabilities. Second, the RNM cumulative distribution function (CDF) is constructed by using quartic B-spline functions with power tails so that the resulting RNM PDF has continuity C^2. The advantage of constructing the RNM CDF with power tails is that the sum of RNM probabilities is guaranteed to be unity. Lastly, by choosing an optimum number of knots, this method can avoid both overfitting and oversmoothing. To select optimal tradeoff between smoothness and fit, I use a minimum number of knots which attains zero bid-ask pricing errors in constructing the B-spline RNM CDF. This method is termed the B-spline RNM CDF with power tails (BSP), which is nonparametric because any probability distribution is a possible solution.

This nonparametric method involves solving a highly nonlinear optimization problem with a number of constraints due to the power tails. To improve computational efficiency and accuracy I develop a 3-step estimation procedure that transforms a nonlinear optimization problem into a convex quadratic program which can be efficiently solved by numerical optimization software.

To compare the performance of the BSP method with the SML method for estimating option implied RNMs, I evaluate the two methods on the basis of the flexibility of the estimated RNM and conduct Monte-Carlo experiments based on 12 hypothetical true distributions. I find that the BSP method dominates the SML method as a technique for estimating option implied RNMs. The SML method violates the no-arbitrage constraints, and it is significantly biased, particularly under the scenarios that the true RNM is a fat-tailed distribution. In contrast, the BSP method always produces arbitrage-free RNM estimators, and it almost perfectly recovers the actual RNM PDFs for all hypothetical distributional assumptions.

CHAPTER 2

ESTIMATION OF RISK NEUTRAL MEASURES USING THE GENERALIZED TWO-FACTOR LOG-STABLE OPTION PRICING MODEL

2.1 Introduction

Derivative prices provide a valuable source of information for measuring market participants' perception of future development of underlying asset prices. Particularly, cross section data on options, all of which expire at the same time but have different strike prices, contain rich information about the underlying asset price distribution in the future. Call (put) options are only valuable to the extent that there is a chance that the underlying asset will be worth more (less) than the strike price so that the option comes to be exercised. Thus, the market prices of the options provide information about the probability that market attaches to an asset being within a range of possible prices at maturity date.

The option values are determined by the investors' risk preference and the statistical probability distribution of the underlying asset price, the so-called Frequency (probability) Measure (FM).[1] Alternatively, the value of option may be evaluated as a discounted expected value of the future payoffs of the option under the risk-adjusted distribution of the underlying asset price, the so-called Risk-Neutral (probability) Measure (RNM), as in the risk-neutral valuation of Ross (1976) and Cox and Ross (1976). The RNM allows us to

[1]The FM governs the empirically observable distribution of underlying asset prices. It is also called the physical probability measure, the objective probability measure, or the real world probability measure.

price any derivative of the particular underlying asset with the same time to maturity by a present value of their expected payoffs in an arbitrage-free market. Inversely, the implied RNM may be extracted from the derivative prices by reversing the process of obtaining prices from pricing models. In a complete arbitrage-free market, a unique RNM can be recovered from a complete set of European option prices using the relationship proposed in Ross (1976) and Breeden and Litzenberger (1978).

The famous Black-Scholes (BS) option pricing model (1973) provides a market's *ex-ante* estimate of the underlying asset's price distribution at maturity under the log-normal assumption. The lognormal assumption suggests that implied volatilities[2] should be constant for all strike prices because only one volatility parameter governs the underlying stochastic process on which all options are priced. However, practitioners and researchers have noted that option prices tend to systematically violate the constant volatility assumption in the BS model. Rubinstein (1985) documented the first such systematic violations of BS model prices. The typical market volatilities implied from option prices often have an asymmetric U-shaped structure with respect to strike prices, commonly referred to as the "volatility smile" or "volatility smirk."[3] The observed deviations of implied volatilities from the Black-Scholes assumption provide some information about the shape of the RNM density function implied by option prices. The volatility smirk suggests that the log returns of the underlying asset at maturity should have a skewed and leptokurtic distribution rather than a normal distribution. Thus, it is necessary to make an alternative assumption for the asset's return distribution which is consistent with the implied volatility structure. To relax the log-normal assumption of the BS model, many option pricing models have been de-

[2]Among the parameters entering the Black-Scholes formula only the volatility cannot be observed. However, using an observed option price an implied volatility can be computed by inverting the option pricing formula. Often the implied volatility is called the Black-Scholes implied volatility.

[3]Before 1987, the implied volatility of the US equity index options, as a function of strike for a certain maturity, behaves like a symmetric smiled curve. The phenomenon is called the implied volatility smile. After the market crash in 1987, the implied volatility as a function of strike price is skewed towards the left. The phenomenon is regarded as implied volatility smirk.

veloped by introducing additional factors such as (i) the stochastic interest rate [Amin and Jarrow (1992)]; (ii) the jump-diffusion [Bates (1991)]; (iii) the stochastic volatility [Heston (1993)]; (iv) the stochastic volatility and stochastic interest rate [Bakshi and Chen (1997)]; (v) jump diffusion with the stochastic volatility [Bates (1996)].

However, the Generalized Central Limit Theorem (GCLT)[4] provides support for stable distributions as a financial asset's log return process since financial asset returns may be considered as the multiplicatively cumulative outcome of many stochastic events. Furthermore, stable distributions can easily accommodate heavy tails and skewness of asset returns, which are commonly observed in the financial data. It is therefore reasonable to assume that log asset returns are governed by a stable distribution. In turn, asset prices themselves follow a log-stable distribution. The normal or Gaussian distribution is the most familiar member and the only one with finite variance of the stable class, but inappropriate for modeling extreme events because the probability of a substantial change is considerably smaller than the frequency observed in financial asset returns. In addition, observed asset returns are often too skewed to be normal as mentioned above. Thus, the non-Gaussian stable distributions are preferable for modeling log returns of financial assets.

In the early 1960s the asset pricing models driven by log-stable distributions had already been proposed by Fama (1963), and Mandelbrot and Taylor (1967) as an alternative to the log-normal assumption, but the fact that expected payoffs on assets and call options are infinite under most log-stable distributions led both Paul Samuelson (as quoted by Smith 1976) and Robert Merton (1976) to conjecture that assets and derivatives could not be reasonably priced under these distributions, despite their attractive feature as limiting distributions under the Generalized Central Limit Theorem. These concerns of Samuelson and Merton come from the misunderstanding about the shape of the RNM. The RNM cor-

[4]According to the Generalized Central Limit Theorem, if the sum of a large number of identically and independently distributed (IID) random variables has a non-degenerate limiting distribution after appropriate scaling and shifting, the limiting distribution must be a member of the stable class. See Zolotarev (1986).

responding to a log-stable FM is not a simple location shift of the FM. Instead, the RNM in general has a different shape with finite moments, and leads to reasonable asset and option prices.

The option pricing model with log-stable distributions was first proposed by McCulloch (1978, 1985, 1987, 1996) using a utility maximization setting with the orthogonal log-stable uncertainty assumption.[5] Janicki et al. (1997), Popova and Ritchken (1998), and Hurst et al. (1999) have developed option pricing models under the symmetric log-stable assumption. Carr and Wu (2003) propose the finite moment log-stable (FMLS) option pricing model by making the very restrictive assumption that the RNM for log prices have maximally negative skewness[6], which is a parametric special case of the orthogonal log-stable assumption. McCulloch (2003) reformulated the orthogonal log-stable option pricing model in the RNM context and showed how the RNM can be derived from the underlying distribution of marginal utilities in a simple representative agent model. The orthogonal log-stable uncertainty assumption allows the RNM of log-stable returns to be the convolution of two densities: one is a maximally negatively skewed stable density, and the other is an exponentially tilted maximally positively skewed stable density. However, the orthogonal assumption is too restrictive for the RNM to fit option prices observed in the markets, which makes it inappropriate to estimate the RNM from observed option prices.

In this chapter, we construct the numeraire and asset choice model in an Arrow-Debreu world to provide a theoretical framework for the log-stable option pricing model. We also introduce the generalized two-factor log-stable option pricing model by relaxing the orthogonal assumption. The orthogonal assumption can be generalized by introducing two factors which are independent maximally negatively skewed standard stable variates and

[5]It is assumed that the marginal utilities of numeraire and asset follow a log-stable distribution with maximum negative skewness, respectively, and are also independently distributed so that it is called the orthogonal log-stable uncertainty assumption.

[6]They assume the max-negative skewness in order to give the returns themselves finite moments. They also incorporate max-negative skewness directly into the stable distribution describing the RNM of the underlying asset without assumptions on the frequency measure (FM).

affect both the log marginal utility of numeraire and the log marginal utility of asset. This assumption allows the log marginal utilities to be dependent upon each other and also provides a flexible RNM probability distribution function, which is the convolution of two exponentially tilted stable distributions. Furthermore, since the generalized two-factor stable RNM is sufficiently flexible to fit observed option prices, the generalized two-factor log-stable option pricing model provides a new parametric method for estimating the RNM from a cross-section of option price data.

Since there are no known closed form expressions for general stable densities, we numerically evaluate log-stable options from the characteristic function (CF) by modifying the inverse Fourier Transform approach of Carr and Madan (1999). This chapter also introduces a simple extension of the Fast Fourier Transform inversion procedure in order to reduce computational errors.

To illustrate the empirical performance of the generalized two-factor log-stable model, we estimate the RNM from observed S&P 500 index option prices. We then conduct model specification tests and compare the fitting performance of four models: the BS log-normal model, the finite moment log-stable model, the orthogonal log-stable model, and the generalized two-factor log-stable model. We evaluate the models on the basis of the goodness-of-fit and find that the generalized two-factor log-stable model outperforms the others.

The rest of the chapter is organized as follows. Section 2.2 discusses the theoretical relationship between option prices and the RNM. Section 2.3 presents a simple general equilibrium model for the log-stable option pricing by constructing a numeraire and asset choice problem in the Arrow-Debreu world. Section 2.4 introduces the generalized two-factor log-stable option pricing model. In Section 2.5 we estimate the RNM from S&P 500 index option prices and compare the performance of the models. Section 2.6 concludes.

2.2 Option prices and the RNM

The fundamental building block in modern financial economic theory is a contingent claim. The contingent claim is an asset or security whose return depends on the state of nature at a point in the future. An option is such a contingent claim because the payoff of the option depends on the price of the underlying asset at maturity date. The price of the option therefore contains information about the market participants' probability assessment of the outcome of the underlying asset price at the future maturity date. This is the basic idea behind the RNM estimation from option prices.

A particular simple and important example of the contingent claim is the Arrow-Debreu security, which pays one unit in one specific state of nature and nothing in other state. For each state, the prices of Arrow-Debreu securities, the so-called state-prices, are proportional to the RNM probability densities for the realization of the state. In a continuum of states the state prices thus are proportional with the continuous RNM probability density function (PDF).[7] Since the state prices are determined by the combination of investors' preferences, budget constraints, information structures, and the imposition of market-clearing conditions, i.e., general equilibrium, the RNM contains additional information than the statistical probability measure (FM).

A number of estimation methods have been developed to back out the RNM from option prices based on seminal work by Ross (1976), Cox and Ross (1976), and Breeden and Litzenberger (1978). Ross (1976) showed that a portfolio[8] of European call-options can be used to construct synthetic Arrow-Debreu securities, thereby establishing a relation between option prices and the RNM. By ruling out arbitrage possibilities, Cox and Ross

[7] By construction, the RNMs have a probability-like interpretation, which are nonnegative and integrating to unity. For this reason the RNM density is sometimes called the risk-neutral probability density (RND).

[8] These portfolios are butterfly spreads that are composed of two long and two short call options. The strike price of both short calls is halfway in between the strike prices of the two long call options. In the limit as the difference between the strike prices goes to zero the butterfly spread's payoff becomes a Dirac-Delta function, e.g. Merton (1999).

(1976) showed that options in general, independently of investors' risk preferences, can be priced as if investors were risk neutral.[9] Consider a general European call option whose payoff is $\max(S_T - K)$, where S_T is the value of an underlying asset on maturity date T, and K is the strike price. In a complete arbitrage-free market, the price of a European call option $C(K)$ can then be computed as the discounted value of the option's expected payoff under the RNM. Formally,

$$\begin{aligned} C(K) &= e^{-r_f T} E^Q \left[\max(S_T - K, 0)\right] \\ &= e^{-r_f T} \int_K^\infty (S_T - K)\, \mathrm{r}(S_T)\, dS_T, \end{aligned} \tag{2.1}$$

where r_f is the risk free interest rate, $\mathrm{r}(S_T)$ is the RNM PDF, and E^Q is the conditional expectation on time 0 information under the RNM. As shown by Breeden and Litzenberger (1978), the RNM density $\mathrm{r}(S_T)$ can be isolated by differentiating (2.1) twice, yielding[10]

$$\mathrm{r}(S_T) = e^{r_f T} \left.\frac{\partial^2 C(K)}{\partial K^2}\right|_{K=S_T}. \tag{2.2}$$

Equation (2.2) states that the RNM is proportional to the second derivative of the call pricing function with respect to the strike price.

Since the RNM might embody important information about market participants' expectations concerning prices of the underlying asset in the future, methods have been developed to estimate the RNM PDF from observed option prices. As pointed out in Chang and Melick (1999), Equation (2.1) and (2.2) provide two different approaches for estimating the RNMs from observed option prices. The methods based on Equation (2.1) make assumptions about the form or family of the RNM for evaluating the integral in (2.1) and

[9] However, it does not mean that agents are assumed to be risk neutral. We are not assuming that investors are actually risk-neutral and risky assets are actually expected to earn the risk-free rate of return.

[10] By similar reasoning, the cumulative distribution function (CDF) can be obtained by differentiating a single time. This technique is used by Neuhaus (1995).

then typically use a non-linear optimization method to estimate the parameters of the RNM that minimize pricing errors, which are differences between the predicted option prices and the observed option prices. On the other hand, the methods based on Equation (2.2) use a variety of means to generate the call option price function $C(K)$ and then differentiate the function (either numerically or analytically) to obtain the RNM PDF. Computing the RNM by (2.2) requires call prices being available for continuous strike prices, but in reality just a few discretely spaced strike prices are available. These methods therefore entail directly or indirectly the construction of a continuous option pricing function from observed prices.

In this chapter, we follow the first approach to estimate the RNM by making a parametric assumption that the log marginal utilities of numeraire and asset are affected by two independent standard stable variates.

2.3 State Prices, Pricing Kernels and the RNM

In this section, we construct a numeraire and asset choice model in the Arrow-Debreu general equilibrium economy to provide a theoretical framework for the relationship between state prices, pricing kernels, and the RNM.

2.3.1 Numeraire and Asset Choice Model

The fundamental investment-selection problem for an individual is to determine the optimal allocation of his/her wealth among the available investment opportunities. Under the expected utility maximization paradigm, each individual's consumption and investment decision is characterized as if he/she determines the probabilities of possible asset pay-offs, assigns a utility index to each possible consumption outcome, and chooses the consumption and investment policy to maximize the expected value of the index.

Consider a representative agent model in the Arrow-Debreu world, in which only a single consumption good N (numeraire) and a single underlying asset A exist. We assume

that the utility function of the representative agent is random, given by:

$$U^s(N, A)$$

with random marginal utility of consumption U^s_N and random marginal utility of asset U^s_A, where s is a state variable which represents a state of random utility function.[11]

Let $S_T(s)$, which is affected by the state variable s, be the asset price at future time T and introduce Arrow-Debreu securities which pay one unit of numeraire in specified states, $S_T(s) \in [x, x + dx)$, and no payout in other states, $S_T(s) \notin [x, x + dx)$, with unconditional payment of $p(x)dx$ unit of numeraire to be made at present time 0. The price of the Arrow-Debreu security $p(x)dx$ is called the state price, which can be thought of as the insurance premium that the agent is prepared to pay in order for him/her to enjoy one unit of consumption if $S_T(s) \in [x, x + dx)$.

We assume that the representative agent receives one unit of both numeraire and asset as endowment; makes forward contracts on the asset at the forward price F; and buys/sells the Arrow-Debreu securities prior to the realization of a state s of the random utility function. The representative agent then buys/sells the asset, and consumes the numeraire after the realization of a state s.

Thus, the representative agent faces a consumption-asset choice problem as followings:[12]

$$\max_{\{N(s),A(s),B,G,Q(x)\}_{s\in\Omega,x\in[0,\infty]}} EU(N, A) \equiv \int_\Omega U(N(s), A(s))\omega(s)ds$$

$$\text{s.t.} \quad 1 = N_0 + \int_0^\infty p(x)(B + Q(x))dx$$

$$N_0 + B + S_T(s)(1 - A(s)) + (S_T(s) - F)G + 1_{S_T(s)\in[x,x+dx)}Q(x) = N(s), \quad \forall s,$$

[11] In the analysis of preference for flexibility (Kreps (1979), Dekel, Lipman and Rustichini's (2001)) the realization of the agent's random utility function corresponds to the realization of his subjective (emotional) state.

[12] For brevity the superscripts on the utility function $U^s(N, A)$ have been suppressed.

where s is the *state* of the random utility function, $s \in \Omega$; $N(s)$ is the consumption (numeraire); $A(s)$ is the amount of asset holding;[13] $S_T(s)$ is the spot price of the asset; $\omega(s)$ is the density of the state variable s, which is conditional on time 0 information; N_0 is the amount of numeraire holding before the realization of the state; B is the amount of bond holding; $1_{S_T(s)\in[x,x+dx)}$ is the payoff of the $A-D$ security (1 if $S_T(s) \in [x, x+dx)$, 0 otherwise); $p(x)dx$ is the state price of $A-D$ security; $Q(x)$ is the amount of $A-D$ security holding; F is the forward price of the asset; and G is the amount of forward contracts[14] on the asset. Asset prices, forward prices, state prices, pricing kernels, and the RNM can be easily derived from the first order conditions for the representative agent problem.

The asset price S_T at future time T may be expressed as the ratio of the marginal utilities:

$$S_T = \frac{U_A}{U_N}, \tag{2.3}$$

where U_N is the random future marginal utility of the numeraire in which the asset is priced, and U_A is the random future marginal utility of the asset itself.

On the other hand, the forward price F at present time 0, which is the numeraire price to be paid at time T for a contract to deliver 1 unit of the asset at future time T, may be written as the ratio of the expected marginal utilities:

$$F = \frac{\int_\Omega U_A \omega(s) ds}{\int_\Omega U_N \omega(s) ds} = \frac{EU_A}{EU_N}. \tag{2.4}$$

The state price $p(x)dx$, which is the unconditional payment of $p(x)dx$ units of numeraire to be made at time 0 for an Arrow-Debreu security which pays 1 if $S_T(s) \in [x, x+dx)$,

[13] Here, we assume no dividend for the underlying asset. Even if we introduced the dividend, the results would be same.

[14] The forward contract is an contract between two parties in which the buyer agrees to pay the seller unconditional payment of F units of numeraire, in exchange for 1 unit of the asset at future time T.

otherwise 0, can be decomposed in the following way:

$$p(x)dx \quad = \quad m(x) \cdot f(x)dx, \tag{2.5}$$

where $f(x)dx$ is the probability of $S_T(s) \in [x, x + dx)$, i.e., the FM probability, while $m(x)$ is the price that we would pay to enjoy 1 unit of numeraire at time T under the condition that we know that future's state is going to be $S_T(s) \in [x, x+dx)$.[15] We call $m(x)$ the pricing kernel, which is a stochastic discount factor for the asset pricing formula.

Since the first order conditions imply that the state price is

$$\begin{aligned} p(x)dx &= \int_0^\infty p(x)dx \cdot \frac{\int_\Omega 1_{S_T(s)\in[x,x+dx)}\, U_N \frac{\omega(s)}{f(x)} ds}{\int_\Omega U_N\, \omega(s) ds}\, f(x)dx \\ &= \frac{1}{R_f}\, \frac{E(U_N|U_A/U_N = x)}{EU_N}\, f(x)dx, \end{aligned}$$

where R_f $(= e^{r_f T})$[16] is the gross risk-free interest rate to time T, the pricing kernel $m(x)$ is taken to be:

$$m(x) \;=\; \frac{p(x)dx}{f(x)dx} \;=\; \frac{1}{R_f}\, \frac{E(U_N|U_A/U_N = x)}{EU_N}. \tag{2.6}$$

Equation (2.6) shows how the preferences define the pricing kernel, translating the state changes into changes in the MRS between conditional and unconditional expected marginal utilities[17] of consumption of the representative agent.

[15] It is very important to note that although the agent defines $m(x)$ as if she knew S_T, it will not be equal to the price of the bond. This is because different states imply different effects on his/her utility.

[16] In the Arrow-Debreu economy, the bond price is determined by the sum of state prices:

$$\frac{1}{R_f} \quad = \quad e^{-r_f T} \quad = \quad \int_0^\infty p(x)dx.$$

[17] Rigorously, the unconditional expected marginal utility, EU_N, is a conditional expectation based on information at time 0. On the other hand, the conditional expected marginal utility, $E(U_N|U_A/U_N = x)$, is a conditional expectation on time 0 information and the fact that the asset price is going to be x, $S_T(s) \in [x, x + dx)$.

Consider a European call option that has state dependent cash flows $\max(x-K,0)$ when $S_T(s) \in [x, x+dx)$. The price of this call option $C(K)$ may be determined by the state prices and the possible cash flows:

$$C(K) = \int_0^\infty \max(x-K,0)\, p(x)\, dx. \tag{2.7}$$

Substituting (2.5) into (2.7), we have

$$\begin{aligned} C(K) &= \int_0^\infty m(x)\ \max(x-K,0)\, f(x)\, dx, \\ &= E[m(x)\ \max(x-K,0)] \end{aligned} \tag{2.8}$$

where E is the conditional expectation on time 0 information under the FM $f(x)$. Equation (2.8) implies that the option price should equal the expected discounted value of the option's payoff, using the investor's stochastic marginal utility to discount the payoff.

Let $\mathrm{r}(x)$ be the density of the RNM at time 0 for state-contingent claims at time T. By definition of the RNM,

$$\begin{aligned} C(K) &= \frac{1}{R_f}\int_0^\infty \max(x-K,0)\, \mathrm{r}(x)\, dx \\ &= \frac{1}{R_f} E^Q[\max(x-K,0)] \end{aligned} \tag{2.9}$$

where E^Q is the conditional expectation on time 0 information under the RNM $r(x)$. Combining (2.6), (2.8) and (2.9), we finally get the RNM PDF:

$$\begin{aligned} \mathrm{r}(x) &= R_f\, p(x) = R_f\, m(x)\, f(x) \\ &= \frac{E(U_N | U_A/U_N = x)}{EU_N}\, f(x). \end{aligned} \tag{2.10}$$

Equation (2.10) states that the RNM is simply the FM, adjusted by the risk-free interest

rate and the pricing kernel.

Further, combining (2.3), (2.4) and (2.10) yields the mean-forward price equality condition (i.e., the mean of the risk neutral distribution should equal the currently observed forward price of the underlying asset):

$$F = \frac{EU_A}{EU_N} = \int_0^\infty x\,\mathrm{r}(x)\,dx. \tag{2.11}$$

2.3.2 FM and RNM under Random Future Marginal Utilities

To derive the RNM from the FM and pricing kernels, we start from the joint distributions of the random future marginal utilities U_N and U_A instead of assuming the random utility function $U^s(N, A)$ explicitly.

Let $g(U_N, U_A)$ be the joint PDF of U_N and U_A conditional on information at present time 0. Equation (2.3) implies that the FM cumulative distribution function (CDF) of S_T is

$$\begin{aligned} F(x) &= \Pr(S_T \le x) = \Pr(U_A \le xU_N) \\ &= \int_0^\infty \int_0^{xU_N} g(U_N, U_A)\,dU_A dU_N. \end{aligned}$$

Therefore, the FM probability density function (PDF) for S_T is

$$\begin{aligned} f(x) &= \int_0^\infty U_N\, g(U_N, U_A)\,dU_N \\ &= \frac{1}{x}\int_{-\infty}^\infty h(v_N, v_N + \log x)\,dv_N, \end{aligned}$$

where $h(v_N, v_A) = U_N U_A\, g(U_N, U_A)$ is the joint PDF of $v_N = \log U_N$ and $v_A = \log U_A$.

The FM, in terms of the PDF for $\log S_T$, is then

$$\begin{aligned} \varphi(z) &= e^z\, f(e^z) \\ &= \int_{-\infty}^\infty h(v_N, v_N + z)\,dv_N, \end{aligned}$$

where $z \equiv \log x$. Since

$$\begin{aligned} E(U_N|U_A/U_N = x) &= E(e^{v_N}|v_A = v_N + \log x) \\ &= \frac{\int_{-\infty}^{\infty} e^{v_N}\, h(v_N, v_N + \log x)\, dv_N}{\int_{-\infty}^{\infty} h(v_N, v_N + \log x)\, dv_N}, \end{aligned}$$

Equation (2.10) follows that

$$\begin{aligned} \mathrm{r}(x) &= \frac{E(U_N|U_A/U_N = x)}{EU_N} f(x) \\ &= \frac{1}{xEU_N} \int_{-\infty}^{\infty} e^{v_N}\, h(v_N, v_N + \log x)\, dv_N. \end{aligned}$$

The RNM PDF for the *log* of price is then

$$\begin{aligned} q(z) &= e^z\, r(e^z) \\ &= \frac{1}{EU_N} \int_{-\infty}^{\infty} e^{v_N}\, h(v_N, v_N + z)\, dv_N. \end{aligned} \tag{2.12}$$

2.4 Generalized Two-Factor Log-Stable Option Pricing Model

To derive a generalized two-factor log-stable RNM PDF, we rely on basic properties of stable distributions. In this section, we first present a brief review of the basic properties of stable distributions, which are essential to construct the log-stable option pricing model.

2.4.1 Basic Properties of Stable Distributions

Stable distributions[18] are a rich class of probability distributions that allow skewness and heavy tails and have many interesting mathematical properties. According to the Generalized Central Limit Theorem, if the sum of a large number of i.i.d. random variates has

[18]The stable distribution was developed by Paul Lévy, so it is also called the Lévy skew alpha-stable distribution.

a limiting distribution after appropriate shifting and scaling, the limiting distribution must be a member of the stable class. A random variable X is stable if for X_1 and X_2 independent copies of X and any positive constants a and b,

$$a X_1 + b X_2 \stackrel{d}{=} c X + d \tag{2.13}$$

holds for some positive c and some $d \in R$, where the symbol $\stackrel{d}{=}$ means equality in distribution, i.e., both expressions have the same probability law. Equation (2.13) implies that the shape of the distribution is preserved up to scale and shift under addition.

Stable distributions $S(x;\alpha,\beta,c,\delta)$ are determined by four parameters: the characteristic exponent $\alpha \in (0,2]$, the skewness parameter $\beta \in [-1,1]$, the scale parameter $c \in (0,\infty)$, and the location parameter $\delta \in (-\infty,\infty)$. If X has a distribution $S(x;\alpha,\beta,c,\delta)$, we write $X \sim S(x;\alpha,\beta,c,\delta)$ and use $s(x;\alpha,\beta,c,\delta)$ for the corresponding densities.

The characteristic exponent governs the tail behavior and indicates the degree of leptokurtosis. When $\alpha = 2$, its maximum permissible value, the normal distribution results, with variance $2c^2$. For $\alpha < 2$, the population variance is infinite. When $\alpha > 1$, the mean of the distribution $E(X)$ is δ. For $\alpha \leq 1$, the mean is undefined. The skewness parameter β is 0 when the distribution is symmetrical, positive when the distribution is skewed to the right, and negative when the distribution is skewed to the left. As α approaches 2, β loses its effect, and the distribution becomes symmetrical regardless of β. The location parameter δ merely shifts the distribution left or right, and the scale parameter c expands or contracts the distribution about δ in proportion to c. Figure 2.1 depicts stable densities with different parameter values. The left panel shows bell-shaped symmetric stable densities with $\alpha = 1.3,\ 2$. When $\alpha = 2$, the normal density results as mentioned above. As α decreases, three things occur to the density: the peak gets higher, the regions flanking the peak get lower, and the tails get heavier. The right panel shows maximally skewed stable densities with $\alpha = 1.5$ and $\beta = -1,\ 1$. The stable density is max-negatively skewed when $\beta = -1$, and max-positively skewed when $\beta = 1$.

Since there are no known closed form expressions for general stable densities[19], the most concrete way to describe all possible stable distributions is through the characteristic function (CF) or Fourier transform (FT).[20] The log CF of the general stable distribution $S(x;\alpha,\beta,c,\delta)$ is

$$\begin{aligned}\log cf_{\alpha,\beta,c,\delta}(t) &= \log E[e^{iXt}] \\ &= \begin{cases} i\delta t - |ct|^{\alpha}\left[1 - i\beta \mathrm{sgn}(t)\tan\left(\frac{\pi\alpha}{2}\right)\right], & \alpha \neq 1 \\ i\delta t + |ct|\left[1 + i\beta\frac{2}{\pi}\mathrm{sgn}(t)\log|ct|\right], & \alpha = 1, \end{cases}\end{aligned}$$

where $\alpha \in (0,2]$ is the characteristic exponent, $\beta \in [-1,1]$ is the skewness parameter, $c \in (0,\infty)$ is the scale parameter, and $\delta \in (-\infty,\infty)$ is the location parameter.[21]

Two properties of stable distributions are important for deriving the generalized two-factor log-stable RNM:

---

[19]There are only three cases where one can write down closed form expressions for the density: stable-normal, Cauchy and Lévy distributions.

[20]For a random variable X with density function $f(x)$, the characteristic function is defined by

$$cf(t) = E[e^{iXt}] = \int_{-\infty}^{\infty} e^{iXt}dx.$$

The function $cf(t)$ completely determines the distribution of X.

[21]The sgn function is defined as

$$\mathrm{sgn}(t) = \begin{cases} -1, & t < 0 \\ 0, & t = 0 \\ 1, & t > 0 \end{cases}$$

Property 1: Convolution[22]

$$\begin{aligned} X &= \sum_{j=1}^{n} a_j X_j, \quad X_j \sim ind.\, S(\alpha, \beta_j, c_j, \delta_j) \quad \Rightarrow \\ X &\sim \underset{j=1}{\overset{n}{\ast}} S(\alpha, \mathrm{sgn}(a_j)\beta_j, |a_j| c_j, a_j \delta_j) \\ &\sim S(\alpha, \beta, c, \delta), \end{aligned}$$

where

$$\begin{aligned} \beta &= \frac{\sum_{j=1}^{n} |a_j|^\alpha c_j^\alpha \mathrm{sgn}(a_j)\beta_j}{c^\alpha}, \\ c &= \left(\sum_{j=1}^{n} |a_j|^\alpha c_j^\alpha \right)^{1/\alpha}, \text{ and} \\ \delta &= \sum_{j=1}^{n} a_j \delta_j. \end{aligned}$$

Property 2: Two-sided Laplace transform

$$\begin{aligned} X &\sim S(\alpha, \beta, c, \delta), \quad \lambda \text{ complex with } Re(\lambda) \geq 0 \quad \Rightarrow \\ Ee^{-\lambda X} &= \begin{cases} -\infty, & \alpha < 2,\ \beta < 1 \\ \exp\left(-\lambda\delta - \lambda^\alpha c^\alpha \sec\left(\frac{\pi\alpha}{2}\right)\right), & \beta = 1, \end{cases} \end{aligned}$$

or equivalently,

$$Ee^{\lambda X} = \begin{cases} \infty, & \alpha < 2,\ \beta > -1 \\ \exp\left(\lambda\delta - \lambda^\alpha c^\alpha \sec\left(\frac{\pi\alpha}{2}\right)\right), & \beta = -1. \end{cases}$$

[22]The convolution of f and g is written as $f \ast g$. If X and Y are two independent random variables with probability distributions f and g, respectively, then the probability distribution of the sum $z = X + Y$ is given by the convolution:

$$(f \ast g)(z) = \int f(\tau) g(z - \tau) d\tau.$$

To describe the generalized two-factor log-stable RNM, it is also necessary to introduce an exponentially tilted stable distribution.[23] An exponentially tilted positively skewed stable density with parameters α, c, δ, and $\lambda > 0$ has density

$$ts_+(x;\alpha,c,\delta,\lambda) \quad = \quad ke^{-\lambda x}s(x;\alpha,+1,c,\delta),$$

where k is a normalizing constant to be determined. Its CF, using Property 2(Two-sided Laplace transform) with $\alpha \neq 1$, is

$$\begin{aligned} cf_{ts+}(t) &= k\int_{-\infty}^{\infty} e^{ixt}e^{-\lambda x}s(x;\alpha,+1,c,\delta)dx \\ &= k\int_{-\infty}^{\infty} e^{-(\lambda-it)x}s(x;\alpha,+1,c,\delta)dx \\ &= k\exp\left(-(\lambda-it)\delta-(\lambda-it)^{\alpha}c^{\alpha}\sec\left(\frac{\pi\alpha}{2}\right)\right). \end{aligned}$$

Since for any CF, $cf(0) \equiv 1$, we must have

$$\begin{aligned} k &= \exp\left(\lambda\delta+\lambda^{\alpha}c^{\alpha}\sec\left(\frac{\pi\alpha}{2}\right)\right) \quad \text{so that} \\ \log cf_{ts+}(t) &= i\delta t + c^{\alpha}\sec\left(\frac{\pi\alpha}{2}\right)(\lambda^{\alpha}-(\lambda-it)^{\alpha}). \end{aligned}$$

Similarly, an exponentially tilted negatively skewed stable density with parameters α, c, δ, and $\lambda > 0$ is expressed as follows:[24]

$$\begin{aligned} ts_-(x;\alpha,c,\delta,\lambda) &= ke^{\lambda x}s(x;\alpha,-1,c,\delta), \\ k &= exp\left(-\lambda\delta+\lambda^{\alpha}c^{\alpha}\sec\left(\frac{\pi\alpha}{2}\right)\right), \text{ and} \\ \log cf_{ts-}(t) &= i\delta t + c^{\alpha}\sec\left(\frac{\pi\alpha}{2}\right)(\lambda^{\alpha}-(\lambda+it)^{\alpha}). \end{aligned}$$

[23] Tilted stable distributions have already been used in the context of option pricing by Vinogaradov (2002), and Createa and Howison (2003).

[24] It is not possible to tilt a stable distribution with $\beta \in (-1,1)$ in either direction, since then $\int e^{\lambda x}s(\alpha,\beta,c,\delta)dx$ would be infinite for any value of $\lambda \neq 0$.

Figure 2.2 illustrates exponentially tilted positively skewed stable densities with different tilting parameters $\lambda = 0,\ 0.5$, and 1. As λ increases, the upper tails get thinner. In contrast, for the exponentially tilted negatively skewed stable densities, as λ increases, the lower tails get thinner.

2.4.2 Generalized Two-Factor Log-Stable RNM

The generalized two-factor log-stable option pricing formula is based on distributional assumptions on the log marginal utilities of the asset $v_A(\equiv \log U_A)$ and of the numeraire $v_N(\equiv \log U_N)$. Let the two factors u_1 and u_2 be independent maximally negatively skewed standard stable variates[25], which affect both v_A and v_N with a scale matrix C and a location vector D:

$$\begin{aligned}\begin{bmatrix} v_A \\ v_N \end{bmatrix} &= C\begin{bmatrix} u_1 \\ u_2 \end{bmatrix} + D \\ &= \begin{bmatrix} c_{A1} & c_{A2} \\ c_{N1} & c_{N2} \end{bmatrix}\begin{bmatrix} u_1 \\ u_2 \end{bmatrix} + \begin{bmatrix} \delta \\ 0 \end{bmatrix}, \quad u_j \sim ind.S(\alpha, -1, 1, 0), \end{aligned} \tag{2.14}$$

where $\forall c_{ij} \geq 0$, $i = A, N$ and $j = 1, 2$.[26] By Property 1 (Convolution) of stable distributions, both v_A and v_N are also maximally negatively stable with different scale parameters c_A and

[25] In order for the expectations in (15) to be finite, v_N and v_A must both be maximally negatively skewed, i.e., have $\beta = -1$. Therefore we have no choice but to make this assumption in order to evaluate log stable options. Nevertheless, this restriction does not prevent $\log S_T$ itself from having the general stable distribution as in (2.16).

[26] The scale parameters c_{ij} are not annualized. If annualized scale parameters are known, the scale parameters c_{ij} can be calculated from the annualized one:

$$c_{ij} = \bar{c}_{ij} T^{1/\alpha},$$

where $\bar{c}_{ij}$ are the annualized scale parameters and T is the remaining time to maturity.

c_N, but the same exponent α:

$$\begin{aligned} v_A &= c_{A1}u_1 + c_{A2}u_2 + \delta \sim S(\alpha, -1, c_A, \delta) \qquad \text{and} \\ v_N &= c_{N1}u_1 + c_{N2}u_2 \sim S(\alpha, -1, c_N, 0), \end{aligned}$$

where $c_A = (c_{A1}^{\alpha} + c_{A2}^{\alpha})^{1/\alpha}$ and $c_N = (c_{N1}^{\alpha} + c_{N2}^{\alpha})^{1/\alpha}$. By Property 2 (Two-sided Laplace transform) of stable distributions, the expected marginal utilities of numeraire and asset are taken to be

$$\begin{aligned} EU_A &= Ee^{v_A} = e^{\delta - c_A^{\alpha}\sec\left(\frac{\pi\alpha}{2}\right)} \qquad \text{and} \\ EU_N &= Ee^{v_N} = e^{-c_N^{\alpha}\sec\left(\frac{\pi\alpha}{2}\right)}. \end{aligned} \tag{2.15}$$

Using the forward price equation (2.4), we have

$$F = \frac{EU_A}{EU_N} = e^{\delta + (c_N^{\alpha} - c_A^{\alpha})\sec\left(\frac{\pi\alpha}{2}\right)},$$

which is the finite mean of the generalized two-factor log-stable RNM distribution by the mean-forward price equality condition (2.12).

Since v_A and v_N are both stable with a same characteristic exponent α , Property 1 implies that the FM for $\log S_T$ also follows a stable distribution with the same exponent α:[27]

$$\begin{aligned} \log S_T &= v_A - v_N = \sum_{j=1}^{2}(c_{Aj} - c_{Nj})u_j + \delta \\ &\sim \underset{j=1}{\overset{2}{\circledast}} S\left(\alpha, \operatorname{sgn}(c_{Nj} - c_{Aj}), |c_{Nj} - c_{Aj}|, \delta_j\right) \\ &\sim S(\alpha, \beta, c, \delta), \end{aligned} \tag{2.16}$$

[27]Carr and Wu (2003) evaluate the option price under log-stable uncertainty, but only by making the very restrictive assumption that log returns have maximally negative skewness, i.e $\beta = -1$, in order to give the returns themselves finite moments. They incorporate maximum negative skewness directly into the stable distribution describing the RNM of the underlying asset.

where

$$\begin{aligned}
\beta &= \frac{\sum_{j=1}^{2} \text{sgn}(c_{Nj} - c_{Aj})|c_{Nj} - c_{Aj}|^{\alpha}}{c^{\alpha}}, \\
c &= \left(\sum_{j=1}^{2} |c_{Nj} - c_{Aj}|^{\alpha} \right)^{1/\alpha}, \\
\delta_1 &= \delta, \text{ and } \delta_2 = 0.
\end{aligned}$$

Finally, the RNM PDF (2.12) and model (2.14) imply that the RNM PDF for $\log S_T$ is

$$\begin{aligned}
q(z) &= \frac{1}{EU_N} \int_{-\infty}^{\infty} e^{v_N} h(v_N, v_N + z) dv_N \\
&= \frac{1}{EU_N} \int_{-\infty}^{\infty} e^{-\frac{c_{N2}c_{A1} - c_{N1}c_{A2}}{c_{N1} - c_{A1}} u_2 - \frac{c_{N1}}{c_{N1} - c_{A1}}(z - \delta)} \cdot s(u_2; \alpha, -1, 1, 0) \\
&\quad s(z; \alpha, \text{sgn}(c_{N1} - c_{A1}), |c_{N1} - c_{A1}|, \delta - (c_{N2} - c_{A2})u_2) du_2. \qquad (2.17)
\end{aligned}$$

The derivation of (2.17) may be found in Appendix A. The RNM PDF $q(z)$ proves to be a convolution of two exponentially tilted stable distributions:

$$q(z) = \underset{j=1}{\overset{2}{\circledast}} ts_{\text{sgn}(c_{Nj} - c_{Aj})} \left(z_j; \alpha, |c_{Nj} - c_{Aj}|, \delta_j, \left| \frac{c_{Nj}}{c_{Nj} - c_{Aj}} \right| \right) \qquad (2.18)$$

where $ts(\cdot)$ is the exponentially tilted stable density. Since the closed form expression of stable distributions does not exist, the RNM PDF (2.18) can be described by its log CF:[28]

$$\begin{aligned}
\log cf_q(t) &= i\delta t + |c_{N1} - c_{A1}|^{\alpha} \sec\left(\frac{\pi\alpha}{2}\right) \left[\left| \frac{c_{N1}}{c_{N1} - c_{A1}} \right|^{\alpha} - \left(\left| \frac{c_{N1}}{c_{N1} - c_{A1}} \right| - \text{sgn}(c_{N1} - c_{A1}) it \right)^{\alpha} \right] \\
&+ |c_{N2} - c_{A2}|^{\alpha} \sec\left(\frac{\pi\alpha}{2}\right) \left[\left| \frac{c_{N2}}{c_{N2} - c_{A2}} \right|^{\alpha} - \left(\left| \frac{c_{N2}}{c_{N2} - c_{A2}} \right| - \text{sgn}(c_{N2} - c_{A2}) it \right)^{\alpha} \right] \qquad (2.19)
\end{aligned}$$

The proof of (2.18) and the derivation of (2.19) are given in Appendix A.

The parameters of the two exponentially tilted stable distributions are determined by

[28] Unless $\beta = 0$, the case $\alpha = 1$ require special treatment of both the CF and the location parameter. Therefore, the RNM PDF equation may not apply in that special case. In practice, however, this does cause problems because $\alpha = 1$ is irrelevant for an asset return's distribution.

the relative magnitude of elements in the scale matrix C: The skewness parameter β_j is determined by the sign of $c_{Nj} - c_{Aj}$; the scale parameter c_j depends on the absolute value of $c_{Nj} - c_{Aj}$; and the tilting factor λ_j is also affected by the relative magnitude of c_{Nj} and c_{Aj}. The location parameter δ of the RNM can be solved from the mean-forward price equality condition:

$$F = \frac{EU_A}{EU_N} = e^{\delta + (c_N^\alpha - c_A^\alpha)\sec\left(\frac{\pi\alpha}{2}\right)} = S_0 e^{(r_f - d)T}, \tag{2.20}$$

where S_0 is the asset price at time 0, d is the dividend rate of asset, and $S_0 e^{(r-d)T}$ is the implicit forward price. This condition always holds if there are no arbitrage opportunities. Solving (2.20) for the location parameter δ of the RNM yields

$$\delta = \log\left(S_0 e^{(r_f - d)T}\right) - (c_N^\alpha - c_A^\alpha)\sec\left(\frac{\pi\alpha}{2}\right).$$

Finally, the generalized two-factor log-stable RNM of $\log S_T$ may be simply expressed as a function of the five free parameters $(\alpha, c_{N1}, c_{N2}, c_{A1}, c_{A2})$:

$$q(z) = q(z; \alpha, c_{N1}, c_{N2}, c_{A1}, c_{A2} | S_0, r_f, d, T),$$

where S_0 is the asset price at time 0, r_f is the risk-free interest rate, d is the dividend rate of asset, and T is the remaining time to maturity.

The generalized two-factor log-stable RNM has a very flexible parametric form with five free parameters for approximating other probability distributions, so it provides a new parametric method for estimating the RNM from a cross-section of option data. As shown in (18), the generalized two-factor log-stable RNM $q(z)$ has two additional tilting parameters which control the shapes of upper and lower tail respectively. This model thus allows a considerably accurate tool for estimating the RNM from the observed option prices even if the log-stable assumption might not be satisfied.

2.4.3 Special cases

The Black-Scholes log-normal Model (1973), the finite moment log-stable Model [Carr and Wu (2003)] and the Orthogonal log-Stable Model [McCulloch (1978, 1985, 1987, and 2003) and Hales (1997)] may be considered as special cases of the generalized two-factor log-stable model. In this section we describe these three models under the generalized two-factor log-stable model framework.

a. Orthogonal Log-Stable Model

The orthogonal log-stable model of McCulloch (1978, 1985, 1987, 1996 and 2003) and Hales (1997) assumes that v_A and v_N are independent with

$$\begin{aligned} v_A &\sim S(\alpha, -1, c_A, \delta) \text{ and} \\ v_N &\sim \textit{ind.}\, S(\alpha, -1, c_N, 0). \end{aligned}$$

The orthogonal assumption can be expressed as a diagonal scale matrix in terms of the generalized two-factor framework:

$$\begin{bmatrix} v_A \\ v_N \end{bmatrix} = \begin{bmatrix} c_A & 0 \\ 0 & c_N \end{bmatrix} \begin{bmatrix} u_1 \\ u_2 \end{bmatrix} + \begin{bmatrix} \delta \\ 0 \end{bmatrix}, \quad u_j \sim \textit{ind.}\, S(\alpha, -1, 1, 0), \quad j = 1, 2.$$

By the convolution property of stable distributions, the FM PDF of the orthogonal log-stable model, which is a convolution of max-positively stable density and max-negatively skewed density, is also a stable distribution:

$$\begin{aligned} \varphi(z) &= s(z_1 : \alpha, -1, c_A, \delta) * s(z_2 : \alpha, 1, c_N, 0) \\ &= s(z : \alpha, \beta, c, \delta), \end{aligned}$$

where $\beta = \frac{c_N^\alpha - c_A^\alpha}{c^\alpha}$ and $c = (c_N^\alpha + c_A^\alpha)^{1/\alpha}$.

The generalized log-stable RNM equation (2.18) implies that the RNM of the orthogonal log-stable model is a convolution of the max-negatively skewed stable density and exponentially tilted max-negatively skewed stable density:

$$\begin{aligned} q(z) &= \mathop{\circledast}_{j=1}^{2} ts\left(z_j; \alpha, \operatorname{sgn}(c_{Nj} - c_{Aj}), |c_{Nj} - c_{Aj}|, \delta_j, \left|\frac{c_{Nj}}{c_{Nj} - c_{Aj}}\right|\right) \\ &= ts_{-}(z_1; \alpha, c_A, \delta, 0) \circledast ts_{+}(z_2; \alpha, c_N, 0, 1) \\ &= s(z_1; \alpha, -1, c_A, \delta) \circledast ts_{+}(z_2; \alpha, c_N, 0, 1). \end{aligned}$$

With the mean-forward price equality condition:

$$F = \frac{EU_A}{EU_N} = e^{\delta + (c_N^\alpha - c_A^\alpha)\sec\left(\frac{\pi\alpha}{2}\right)} = S_0 e^{(r_f - d)T},$$

the location parameter of the RNM can be solved as:

$$\delta = \log(S_0 e^{(r_f - d)T}) - \beta c^\alpha \sec\left(\tfrac{\pi\alpha}{2}\right).$$

Therefore, the orthogonal stable RNM of $\log S_T$ is directly expressed as a function of the three parameters (α, β, c) of the FM[29]:

$$q(z) = q(z; \alpha, \beta, c | S_0, r_f, d, T).$$

b. Finite Moment Log-Stable Model

The finite moment log-stable model of Carr and Wu (2003) assumes that the RNM is a max-negatively skewed log-stable distribution, i.e., $\beta = -1$. When $\beta = -1$, the RNM and FM have common density:

$$q(z) = \varphi(z) = s\left(z; \alpha, -1, c, \log F + c^\alpha \sec\left(\frac{\pi\alpha}{2}\right)\right).$$

[29]The free parameters (β, c) are equivalent to (c_A, c_N), since $\beta = \frac{c_N^\alpha - c_A^\alpha}{c^\alpha}$ and $c = (c_N^\alpha + c_A^\alpha)^{1/\alpha}$.

The finite moment assumption, $\beta = -1$, can be expressed as the following scale matrix under the generalized two-factor framework:

$$\begin{bmatrix} v_A \\ v_N \end{bmatrix} = \begin{bmatrix} c & 0 \\ 0 & 0 \end{bmatrix} \begin{bmatrix} u_1 \\ u_2 \end{bmatrix} + \begin{bmatrix} \delta \\ 0 \end{bmatrix}, \quad u_j \sim ind.\, S(\alpha, -1, 1, 0), \quad j = 1, 2.$$

With the mean-forward price equality condition:

$$F = \frac{EU_A}{EU_N} = e^{\delta - c^\alpha \sec\left(\frac{\pi\alpha}{2}\right)} = S_0 e^{(r_f - d)T},$$

the location parameter of the RNM can be solved as:

$$\delta = \log(S_0 e^{(r_f - d)T}) + c^\alpha \sec\left(\frac{\pi\alpha}{2}\right).$$

Therefore, the finite moment log-stable RNM of $\log S_T$ is simply expressed as a function of the two free parameters (α, c):

$$q(z) = q(z; \alpha, c | S_0, r_f, d, T).$$

c. Black-Scholes Log-Normal Model

The Black-Scholes option pricing model (1973) assumes the log price follows a normal distribution. When $\alpha = 2$, a stable distribution results normal with mean δ and variance $\sigma^2 = 2c^2$. Therefore, the log-normal case can be considered as a special case of the generalized two-factor stable model. The log-normal assumption can be expressed as a generalized form:

$$\begin{bmatrix} v_A \\ v_N \end{bmatrix} = \begin{bmatrix} c_{A1} & 0 \\ c_{N1} & c_{N2} \end{bmatrix} \begin{bmatrix} u_1 \\ u_2 \end{bmatrix} + \begin{bmatrix} \delta \\ 0 \end{bmatrix}, \quad u_j \sim ind.\, S(\alpha = 2, -1, 1, 0), \quad j = 1, 2.$$

We can pin down the location parameter from the mean-forward price equality condition:

$$\begin{aligned}\delta &= \log F - (c_N^\alpha - c_A^\alpha)\sec\left(\frac{\pi\alpha}{2}\right) \\ &= \log F - \frac{1}{2}\left(\frac{c_{N1}^2 - c_{A1}^2 + c_{N2}^2}{(c_{N1} - c_{A1})^2 + c_{N2}^2}\right)\sigma^2.\end{aligned}$$

Thus, the FM of $\log S_T$ is

$$\begin{aligned}\varphi(z) &= s(z; \alpha = 2, \beta, c, \delta) \\ &= \phi(z; \delta, \sigma^2 = 2c^2) \\ &= \phi\left(z; \log F - \frac{1}{2}\left(\frac{c_{N1}^2 - c_{A1}^2 + c_{N2}^2}{(c_{N1} - c_{A1})^2 + c_{N2}^2}\right)\sigma^2, \sigma^2\right).\end{aligned}$$

The RNM of $\log S_T$ is

$$\begin{aligned}q(z) &= ts_{\mathrm{sgn}(c_{N1}-c_{A1})}\left(z_1; 2, |c_{N1} - c_{A1}|, \delta, \left|\frac{c_{N1}}{c_{N1} - c_{A1}}\right|\right) * ts_+(z_2; 2, c_{N2}, 0, 1) \\ &= \phi\left(z; \log F - \frac{\sigma^2}{2}, \sigma^2\right),\end{aligned}$$

where $F = e^{(r_f - d)T} S_0$ and $\phi(\cdot)$ is the PDF of normal distributions.[30] Accordingly, the Black-Scholes log-normal RNM can be expressed as a function of only one free parameter σ:

$$q(z) = q(z; \sigma | S_0, r, d, T).$$

[30] In the log-normal case, the RNM and FM therefore both have the same Gaussian shape in terms of log price, with the same variance. They differ only in location, by the observable risk premium

$$\left(1 - \frac{c_{N1}^2 - c_{A1}^2 + c_{N2}^2}{(c_{N1} - c_{A1})^2 + c_{N2}^2}\right)\frac{\sigma^2}{2}$$

that is determined by the scale matrix, i.e., by the relative standard deviation of $\log U_N$ and $\log U_A$. This comes about because a exponentially tilted normal distribution is just another normal back again, with same variance but different mean.

2.5 RNM Estimation from Option Market Prices

In this section, we estimate the conditional RNM from a cross-section of S&P 500 index option prices using the BS lognormal model, the finite moment log-stable model, the orthogonal stable model, and the generalized two-factor stable model under the modified least square criterion. We also conduct a simple likelihood ratio test for the model selection among the competing nested models.

2.5.1 OTM Option value functions

Let $C(K)$ be the value, in units of numeraire to be delivered at time 0, of a European call option which gives right to the holder to purchase 1 unit of the asset in question at time T at strike price K. By the definition of the RNM, its value must be the discounted expectation of its payoff under either $\mathrm{r}(x)$ or $q(z)$:

$$\begin{aligned} C(K) &= e^{-r_f T} \int_0^\infty \max(x-K,0)\mathrm{r}(x)dx \\ &= e^{-r_f T} \int_{-\infty}^\infty \max(e^z-K,0)q(z)dz. \end{aligned} \tag{2.21}$$

Similarly, let $P(K)$ be the value of a European put option which allows the owner to sell one unit of the asset at time T at strike price K so that

$$\begin{aligned} P(K) &= e^{-r_f T} \int_0^\infty \max(K-x,0)\mathrm{r}(x)dx \\ &= e^{-r_f T} \int_{-\infty}^\infty \max(K-e^z,0)q(z)dz. \end{aligned} \tag{2.22}$$

Define the out-of-the-money (OTM) option value function by

$$V(K;\boldsymbol{\theta}) = \begin{cases} P(K;\boldsymbol{\theta}) & \text{for } K < F \\ C(K;\boldsymbol{\theta}) & \text{for } K \geq F \end{cases}, \tag{2.23}$$

where $\boldsymbol{\theta}$ is the vector of the RNM parameters. Using the put-call parity[31], we can rewrite (2.23) as:

$$V(K;\boldsymbol{\theta}) \quad = \quad \min\left(C(K;\boldsymbol{\theta}), P(K;\boldsymbol{\theta})\right). \tag{2.24}$$

The OTM option value function $V(K)$ is continuous at F, and is also monotonic and convex on either side of F under the arbitrage-free condition. Figure 2.3 illustrates option value functions using S&P 500 index options on Sep 13, 2006 (F=1,325.7). The left panel shows the call option value function $C(K)$ and the put option value function $P(K)$. The right panel shows the OTM option value function $V(K) = \min(C(K), P(K))$.

Since there are no known closed form expressions for general stable densities, the option value function $V(K)$ may be evaluated through the characteristic function (CF) or Fourier transform (FT). With no loss of generality, we may measure the asset in units such that $F = 1$. Modifying Carr and Madan (1999),[32] the Fourier Transform of $v(z) \equiv V(e^z)$ is then

$$\phi_v(t) \quad = \quad e^{-rT}\left[\frac{cf_q(t-i)-1}{it-t^2}\right], \quad t \neq 0, \tag{2.25}$$

where cf_q is the CF of the RNM pdf $q(z)$. When $t = 0$, this formula takes the value $0/0$, but the limit may be evaluated by means of l'Hôpital's rule. In the case of the generalized

[31] In the absence of arbitrage opportunities, the following relationship holds for European option:

$$C(K) + e^{-r_f T}K \quad = \quad P(K) + e^{-dT}S_0,$$

so that $C(K) = P(K)$ at $K = F$. The put-call parity implies that $C(K)$, $P(K)$, and $V(K)$ are equivalent, so we use $V(K)$ instead of $C(K)$ and $P(K)$.

[32] Carr and Madan in fact base their (14) on a function which equals $P(K)$ when K is less than the spot price S_0 and $C(K)$ otherwise. This unnecessarily creates a small discontinuity which can only aggravate the Fourier inversion. The present function $V(K)$ avoids this problem, with the consequence that (2.25) is in fact somewhat simpler than their (14).

two-factor generalized log-stable model, this becomes

$$\begin{aligned}\phi_v(0) &= e^{-rT}\frac{cf_q'(-i)}{i} \\ &= e^{-rT}\left[\left(-\sum_{j=1}^{2}(c_{Nj}{}^{\alpha} - c_{Aj}{}^{\alpha})\sec\left(\frac{\pi\alpha}{2}\right)\right) + \alpha\sum_{j=1}^{2}\operatorname{sgn}(c_{Nj}-c_{Aj})|c_{Nj}-c_{Aj}|^{\alpha}\sec\left(\frac{\pi\alpha}{2}\right)\cdot \right. \\ &\qquad \left.\left(\left|\frac{c_{Nj}}{c_{Nj}-c_{Aj}}\right| - \operatorname{sgn}(c_{Nj}-c_{Aj})\right)^{\alpha-1}\right].\end{aligned}$$

Unfortunately, however, the function $v(z)$ has a cusp at $z = 0$ corresponding to that in $V(K)$ at $K = F$, so that numerical inversion of (2.25) by means of the discrete inverse FFT results in pronounced spurious oscillations in the vicinity of the cusp. The problem is that the ultra-high frequencies required to fit the cusp and its vicinity are omitted from the discrete Fourier inversion, which only integrates over a finite range of integration instead of the entire real line. Increasing the range of integration progressively reduces these oscillations, but never entirely eliminates them. However, the fact that increasing the range of integration does give improved results allows the FFT inversion results to be "Romberged" to give satisfactory results, as follows: Start with a large number of points $N = N_1$, with a log-price step $\Delta z = c\sqrt{2\pi/N}$ (or a round number in that vicinity if desired), and a frequency-domain step $\Delta t = 2\pi/(N\Delta z)$. Then quadruple N to $N_2 = 4N_1$, and then again to $N_3 = 16N_1$, halving both step sizes each time, so as to double the range of integration each time, while obtaining values for the original z grid. Each of the original N_1 z values now has 3 approximate function values v_1, v_2, and v_3 that are converging on the true value at an approximately geometric rate as the grid fineness and range of integration are successively doubled. The true value may then be approximated to a high degree of precision at each of these points simply by extrapolating the geometric series implied by the three values to infinity:

$$v_\infty = v_3 + \frac{\rho}{1-\rho}(v_3 - v_2),$$

where $\rho = (v_3 - v_2)/(v_2 - v_1)$. The residual error may then be conservatively estimated by computing v_0 using $N_0 = N_1/4$, repeating the above procedure using v_0, v_1, and v_2, and assuming that the absolute discrepancy between the two results is an upper bound on the error. It was found that for $\alpha \geq 1.3$, $N_1 = 2^{10}$ usually gives a maximum estimated error less than .0001 relative to $F = 1$, though occasionally $N_1 = 2^{14}$ is necessary.[33] Put-call parity may then be used to recover $C(K)$ and/or $P(K)$, as desired, from $V(K) \equiv v(\log K)$. The above procedure gives the value of $v(z)$ at N_1 closely spaced values of z, and therefore $V(K)$ at N_1 closely spaced values of K. Unfortunately, however, these will ordinarily not precisely include the desired exercise prices, and because of the convexity of $V(K)$ on each side of the cusp, linear interpolation may give an interpolation error in excess of the Fourier inversion computational error. Nevertheless, cubic interpolation on $C(K)$ and/or $P(K)$ using two points on each side of each desired exercise price gives very satisfactory results.

2.5.2 Modified Least Square Criterion

By using the OTM option value function (2.23), option pricing models can be expressed as a non-linear regression with the parameters of the RNM:

$$\begin{aligned} V_i &= V(K_i; \boldsymbol{\theta} | S_0, r_f, d, T) + \epsilon_i, \quad i = 1, \ldots, N \\ &= V_i(\boldsymbol{\theta}) + \epsilon_i, \end{aligned} \tag{2.26}$$

where $\boldsymbol{\theta}$ is the vector of the RNM parameters, V_i is an observed OTM option price, $V_i(\boldsymbol{\theta})$ is the theoretical OTM option price, and ϵ_i is the pricing error of the OTM option with strike price K_i. Consequently, we may apply non-linear regression techniques to the model (2.26) in order to estimate the parameters $\boldsymbol{\theta}$ of the RNM.

[33] For the financially less relevant values of $\alpha < 1.3$, the infinite first derivative of the imaginary part of (2.25) at the origin causes additional computational problems. These problems become even worse for $\alpha < 1$, when the imaginary part becomes discontinuous at the origin.

If we observe transaction prices for all options across strike prices at the same time, the Non-linear Least Squares (NLS) criterion would be proper for estimating the RNM parameters:

$$\begin{aligned} \min_{\boldsymbol{\theta}\in\boldsymbol{\Theta}} \quad L(SSE) &= \sum_{i=1}^{N} (V_i - V_i(\boldsymbol{\theta}))^2 \\ &= \boldsymbol{\epsilon}^\top \boldsymbol{\epsilon}, \end{aligned}$$

where $\boldsymbol{\epsilon} = [\epsilon_1 \ \epsilon_2 \ \cdots \ \epsilon_N]^\top$ is the vector of pricing errors.[34]

Unfortunately the transaction prices are recorded with substantial measurement errors due to non-synchronous trading so that we instead use bid and ask quote prices. The bid-ask average prices have been used as an alternative of the transaction prices in many studies. The NLS criterion, however, does not fully exploit the additional information coming from the individual bid and ask quote prices because it only utilizes the bid-ask average OTM option prices. In our study we therefore use a modified least squares (MLS) criterion under which the loss value (Modified SSE, MSSE) increases only when the theoretical prices fall outside of the bid-ask price range. However, since multiple solutions are possible under the MLS criterion, we add an arbitrary small ordinary least square term to guarantee a unique solution:

$$\min_{\boldsymbol{\theta}\in\boldsymbol{\Theta}} \quad L(MSSE) = \sum_{i=1}^{N} \left[\left(V_i^B - V_i(\boldsymbol{\theta})\right)_+^2 + \left(V_i(\boldsymbol{\theta}) - V_i^A\right)_+^2 + \lambda \left(\bar{V}_i - V_i(\boldsymbol{\theta})\right)^2 \right],$$

where V_i^B is the OTM option bid price, V_i^A is the OTM option ask price, $\bar{V}_i = (V_i^B + V_i^A)/2$ is the OTM option bid-ask average price at strike price K_i, $X_+ = \max(0, X)$, and λ is a small constant[35]. Figure 2.4 illustrates the loss functions based on the two criteria. The left panel

[34] We cannot use the weighted least square criterion because the variance structure of pricing errors is not known. To construct variance structure of pricing errors, it is necessary to consider different source of pricing errors: non-synchronous trading, price discreteness, and the bid-ask bounce. Unfortunately, there is no simple or generally accepted manner for modeling all of these effects.

[35] In our study, we set $\lambda = 0.01$.

shows the NLS loss function, and the right panel presents the MLS loss function.

2.5.3 Empirical results of the RNM estimation

a. Data

We have estimated the parametric risk-neutral density using the cross-section data on the S&P 500 index options traded at the Chicago Board of Options Exchange (CBOE). The transaction prices are recorded with substantial measurement errors due to non-synchronous trading so that we use daily closing bid and ask price quotes. We have obtained 100 sets of cross-section data on the S&P 500 index options which are transacted with 2 months to maturity in 2006. We have filtered the data using the arbitrage violation conditions since the existence of arbitrage possibilities can lead to negative risk-neutral probabilities. By checking the monotonicity and convexity of the option pricing functions, we may eliminate option prices which violate the arbitrage-free condition. After eliminating the violating data, we have 8,468 option price quotes.

Since risk-free interest rates for a time of maturity exactly matching the options' time to maturity generally can not be observed, we compute implicit risk-free interest rates from the European put-call parity as suggested by Jackwerth and Rubinstein (1996). The estimation of the RNM is conducted by using the four models separately for each cross section data set.

b. Goodness-of-fit

In this section, we compare the goodness-of-fit of the RNM estimations of the four option pricing models: the BS log-normal option pricing model (BS), the finite moment log-stable option pricing model (FS), the orthogonal log-stable option pricing model (OS), and the generalized two-factor log-stable option model (GS). If option prices are exact and continuous, and if the pricing model holds exactly for every single option, the RNM

parameters can be recovered with zero pricing errors between the estimated and observed prices. However, model and market imperfections introduce pricing errors. In order to compare these pricing errors, we first estimate the RNM by applying the four option pricing models to S&P 500 index (European) options under the modified least square criterion (MLS). Then, the four models are compared by examining the pricing errors associated with each model in terms of the Modified Root Mean Squared Error (MRMSE), which represents the average pricing error:

$$MRMSE = \sqrt{\frac{1}{N-k} MSSE},$$

where $MSSE$ is the modified sum of squared errors, N is the number of strike prices, i.e., the number of observations, and k is the number of free parameters of the RNM.

The estimated RNM density functions for the four models are illustrated in Figure 2.5, and the estimated average RNM parameters are reported in Table 2.1. Also, given the RNM density from the each model, Equation (2.21) and (2.22) give predicted values for the option prices. These model predictions and the actual bid-ask prices are plotted in the upper panels in Figure 2.6 for an illustrative date. We calculate the volatility smiles from the predicted prices and the actual bid-ask prices, and they are plotted in the lower panels in Figure 2.6. Since the Black-Scholes option price is monotonically increasing in volatility, deviations of estimated volatilities from actual implied volatilities are also related with pricing errors of the option pricing model. Options with actual implied volatility above (below) the estimated volatility are underpriced (overpriced) by the option pricing model.[36]

The fitting performances of the four models are reported in Table 2.2 in terms of the Modified Root Mean Squared Error (MRMSE). Table 2.2 shows that the GS model outperforms the BS, FS and OS model with respect to the goodness-of-fit for all data sets. Note

[36]This is based on the assumption that there is no mispricing in the observed option prices. If the model is correctly specified and the observed option prices are mispriced, options with actual implied volatility above (below) the estimated volatility are overpriced (underpriced).

that the fitting performance of the FS and OS models are identical. This implies that there is no additional improvement from introducing an additional parameter c_N of the OS model relative to the FS model. That is to say, the S&P 500 returns have maximally negative skewness.

The BS model overprices options around the ATM price, while it underprices options with relatively large or small exercise prices. The FS and OS models perform relatively better around the ATM price, but exhibits pricing bias in both the upper and lower tails. On the other hand, the GS model shows almost perfect goodness-of-fit for all exercise prices. The first terms of the MSSE are almost zero for the GS model. This result indicates that the theoretical option prices based on the estimated RNM could fall into the bid-ask option price range across almost all strike prices.

c. Likelihood Ratio Test

Using the Kullback-Leibler Information Criterion (KLIC), Vuong (1989) proposed simple likelihood-ratio tests for the model selection among the competing models, which are non-nested or nested. We assume that the pricing errors are i.i.d. normally distributed with variance σ^2. Under such assumptions, minimizing the sum of squared pricing error is equivalent to maximizing the log likelihood function. Thus, the NLS estimates can be regarded as maximum likelihood estimates.[37]

Consider two competing models **F** and **G** whose log density functions are given by, respectively:

$$\begin{aligned} \log f(e_{\theta i};\boldsymbol{\theta}) &= -\frac{1}{2}\log\left(2\pi\sigma_f^2\right) - \frac{e_{\theta i}^2}{2\sigma_f^2} \quad \text{and} \\ \log g(e_{\gamma i};\boldsymbol{\gamma}) &= -\frac{1}{2}\log\left(2\pi\sigma_g^2\right) - \frac{e_{\gamma i}^2}{2\sigma_g^2}, \end{aligned}$$

[37] Under the MLS criterion it is not possible to compute the LR statistics so that we use NLS criterion for the model selection test.

where $e_{\theta i}$ and $e_{\gamma i}$ denote the pricing error on the ith option under the model $\mathbf{F}$ and $\mathbf{G}$, respectively, and $\boldsymbol{\theta}$ and $\boldsymbol{\gamma}$ are the parameter vectors of $\mathbf{F}$ and $\mathbf{G}$, respectively. Since the maximum likelihood estimate for σ^2 is simply the mean squared pricing error: mse = $\mathbf{e}^\top\mathbf{e}/N$, the log likelihood functions are given by, respectively:

$$\begin{aligned}
\mathcal{L}_f(\mathbf{e}_\theta;\boldsymbol{\theta}) &= \sum_{i=1}^{N}\log f(e_{\theta i};\boldsymbol{\theta}) = -\frac{N}{2}\left[1+\log(2\pi)+\log\left(\frac{\mathbf{e}_\theta{}^\top\mathbf{e}_\theta}{N}\right)\right] \quad \text{and}\\
\mathcal{L}_g(\mathbf{e}_\gamma;\boldsymbol{\gamma}) &= \sum_{i=1}^{N}\log g(e_{\gamma i};\boldsymbol{\gamma}) = -\frac{N}{2}\left[1+\log(2\pi)+\log\left(\frac{\mathbf{e}_\gamma{}^\top\mathbf{e}_\gamma}{N}\right)\right],
\end{aligned}$$

where $\mathbf{e}_\theta$ and $\mathbf{e}_\gamma$ are the pricing error vectors for each model. Furthermore, the likelihood ratio between the two models ($\mathbf{F}$ and $\mathbf{G}$) is given by:

$$\begin{aligned}
LR\left(\hat{\boldsymbol{\theta}},\hat{\boldsymbol{\gamma}}\right) &= \mathcal{L}_f(\hat{\mathbf{e}}_\theta;\hat{\boldsymbol{\theta}}) - \mathcal{L}_g(\hat{\mathbf{e}}_\gamma;\hat{\boldsymbol{\gamma}})\\
&= -\frac{N}{2}\left[\log\left(\frac{\hat{\mathbf{e}}_\theta^\top\hat{\mathbf{e}}_\gamma}{N}\right)-\log\left(\frac{\hat{\mathbf{e}}_\gamma^\top\hat{\mathbf{e}}_\gamma}{N}\right)\right]\\
&= -\frac{N}{2}\left[\log\left(\frac{\hat{\mathbf{e}}_\theta^\top\hat{\mathbf{e}}_\theta}{\hat{\mathbf{e}}_\gamma^\top\hat{\mathbf{e}}_\gamma}\right)\right].
\end{aligned}$$

If the model $\mathbf{G}$ is nested in the model $\mathbf{F}$, any conditional density $g(\cdot;\boldsymbol{\gamma})$ is also a conditional density $f(\cdot;\boldsymbol{\theta})$ for some $\boldsymbol{\theta}$ in $\boldsymbol{\Theta}$. Based on the KLIC, we consider the following hypotheses and definitions:[38]

$$\begin{aligned}
H_0 &: E\left[\log\frac{f(e_{\theta i};\boldsymbol{\theta})}{g(e_{\gamma i};\boldsymbol{\gamma})}\right] = 0 : \mathbf{F} \text{ and } \mathbf{G} \text{ are equivalent}\\
H_A &: E\left[\log\frac{f(e_{\theta i};\boldsymbol{\theta})}{g(e_{\gamma i};\boldsymbol{\gamma})}\right] > 0 : \mathbf{F} \text{ is better than } \mathbf{G}.
\end{aligned}$$

[38] Since $\mathbf{G}$ can never be better than $\mathbf{F}$, H_A does not include the case such that $\mathbf{G}$ is better than $\mathbf{F}$.

If **G** is nested in **F** and **F** is correctly specified, then

$$\begin{aligned} \text{under } H_0 \quad &: \quad 2LR(\hat{\boldsymbol{\theta}}, \hat{\boldsymbol{\gamma}}) \xrightarrow{D} \chi^2_{p-q}, \\ \text{under } H_A \quad &: \quad 2LR(\hat{\boldsymbol{\theta}}, \hat{\boldsymbol{\gamma}}) \xrightarrow{a.s.} +\infty, \end{aligned}$$

where p and q are the number of parameters in models **F** and **G**, respectively.

The three stable type models (BS, FS, and OS) are nested in the GS model; the BS and FS model are nested in the OS model; and the BS model is nested in the FS model. The LR test statistics and the corresponding P-values between nested models are reported in Table 2.3. The test results indicate that the GS model is significantly better the BS, FS, and OS models and the OS and FS model are significantly better the BS model. However, the OS model and FS model are equivalent even though the OS model has an additional parameter relative to the FS model.

2.6 Concluding Remarks

The generalized two-factor log-stable option pricing model is a highly integrated approach to evaluating contingent claims in the sense that it provides state prices, pricing kernels, and the risk neutral measure explicitly. The RNM can be simply derived by adjusting the FM for the state-contingent value of the numeraire. Under generalized two-factor log-stable uncertainty the RNM is expressed as a convolution of two exponentially tilted stable distributions, while the FM itself is a pure stable distribution. Furthermore, the generalized two-factor log-stable RNM has a very flexible parametric form for approximating other probability distributions. Thus, this model also provides a considerably accurate tool for estimating the RNM from the observed option prices even though the two-factor log-stable assumption might not be satisfied.

The empirical results of the RNM estimation from the S&P 500 index options shows that the generalized two-factor log-stable model gives better performance than the Black-Scholes log-normal model, the finite moment log-stable model and the orthogonal log-stable model in fitting the observed option prices. Moreover, the distributional assumption for the generalized stable model is consistent with the implied volatility structure, which violates the lognormal assumption of the Black-Scholes model.

The Black-Scholes log-normal model, the finite moment log-stable model, and the orthogonal log-stable model are nested by the generalized two-factor log-stable model. In order to verify the empirical performance of the generalized two-factor log-stable model, it is necessary to compare it with other parametric models which are not nested by it. Also, we need to examine the stability or robustness of the RNM parameter through the Monte Carlo experiment or the Bootstrap technique. Chapter 3 investigates these issues to verify the empirical performance of the generalized two-factor log-stable option pricing model.[39]

[39] See Chapter 3.

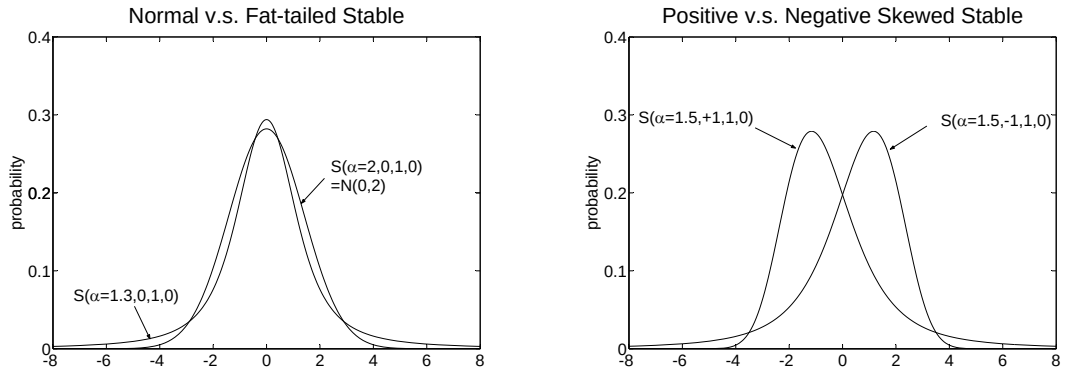

Figure 2.1: Illustrations of Stable Distributions with Different Parameter Values

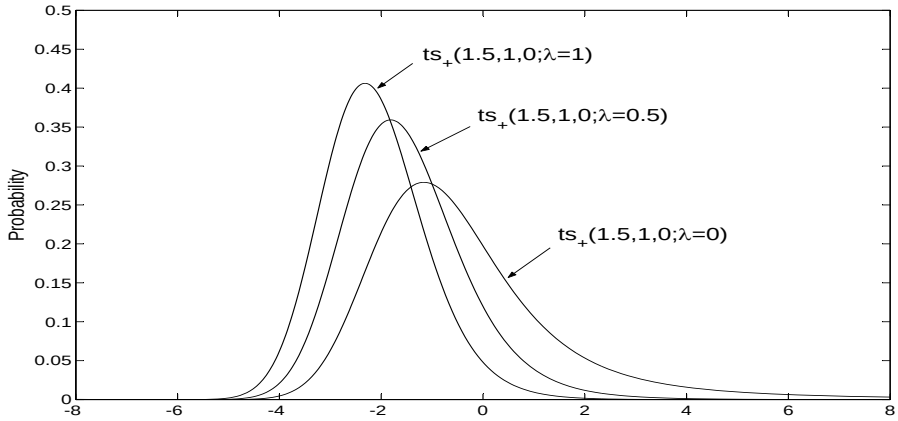

Figure 2.2: Exponentially Tilted Positively Skewed Stable Densities with Different Tilting Factor Values

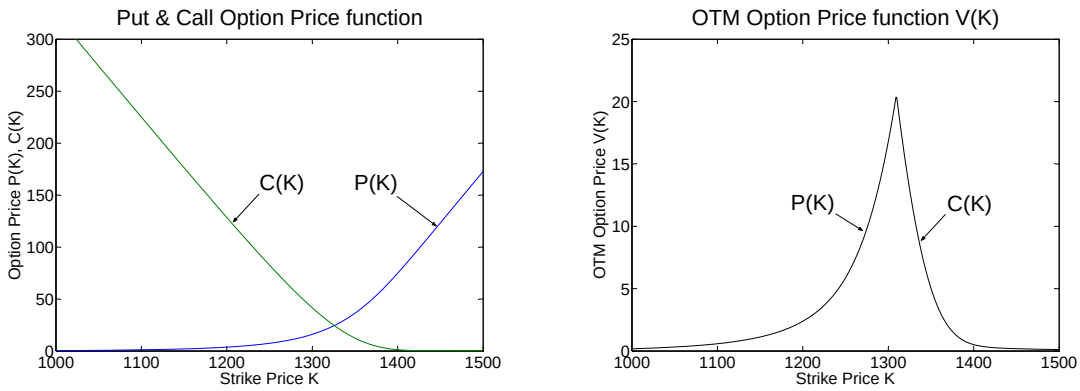

Figure 2.3: Option Value Functions for S&P 500 Index Options on Sep 13, 2006 (F=1,325.7)

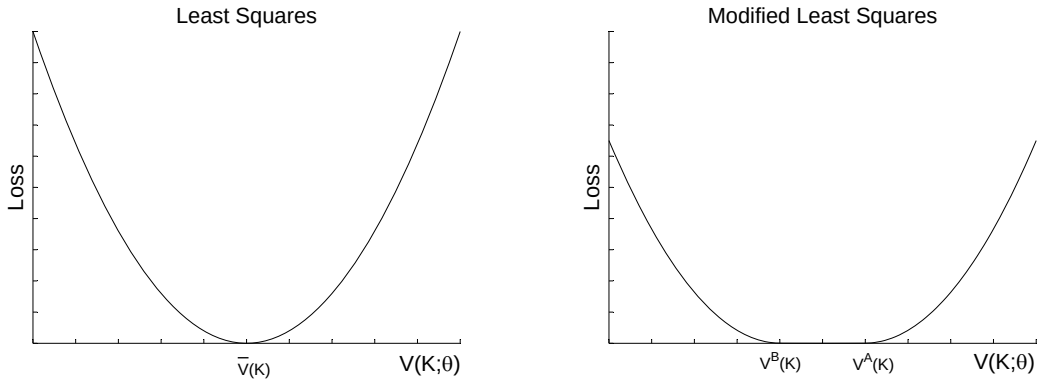

Figure 2.4: Loss Functions of NLS and MLS

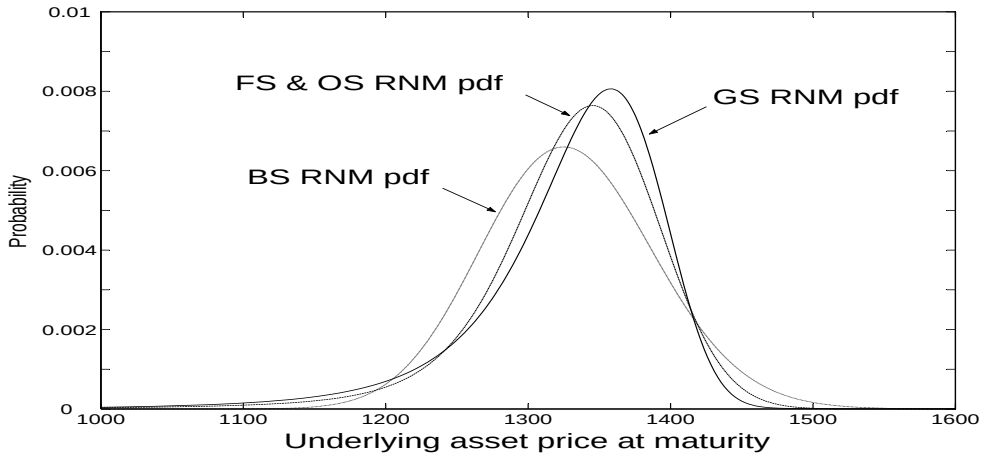

Figure 2.5: Estimated RNM Densities for S&P 500 Index Options on Sep. 13, 2006

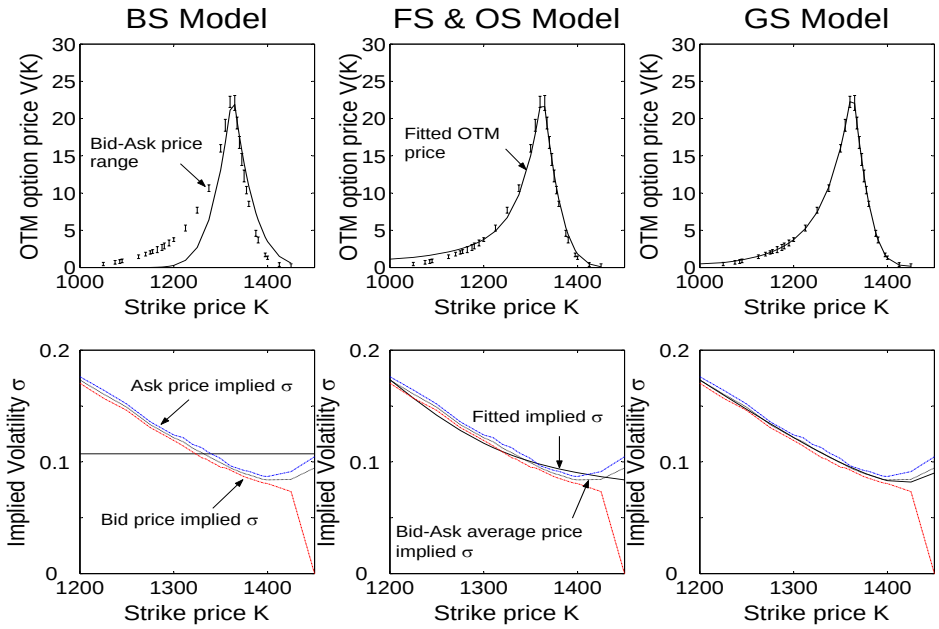

Figure 2.6: Fitted Option Prices and Volatility Smiles for S&P 500 Index Options on Sep. 13, 2006

BS	FS		OS[a]			GS[b]				
σ	α	c	α	c_N	c_A	α	c_{N1}	c_{N2}	c_{A1}	c_{A2}
0.12	1.74	0.08	1.74	0	0.08	1.34	0.41	0.63	0.40	0.75

a Implied FM parameters of the OS model: $\alpha = 1.74, \beta = -1$, and $c = 0.08$.
b Implied FM parameters of the GS model: $\alpha = 1.34, \beta = -0.96$, and $c = 0.12$.
Note: The entries report the sample average of the estimated parameters. The sample contains 100 sets of cross-section data on S&P 500 index options with 2 months to maturity, which are traded in 2006.

Table 2.1: Estimated RNM Parameters for S&P 500 Index Options

	BS	FS	OS	GS
MRMSE	150.848	3.480	3.480	0.013
(1st term)	148.716	3.334	3.334	0.004
(2nd term)	2.132	0.146	0.146	0.009

Note: The 1st term of MSSE is $\sum_{i=1}^{N}\left[\left(V_i^B - V_i(\boldsymbol{\theta})\right)_+^2 + \left(V_i(\boldsymbol{\theta}) - V_i^A\right)_+^2\right]$, and the 2nd term is the ordinary least square term $\sum_{i=1}^{N}\lambda\left(\bar{V}_i - V_i(\boldsymbol{\theta})\right)^2$. The entries report the sample average of the test statistics and the corresponding P-values. The sample contains 100 sets of cross-section data on S&P 500 index options with 2 months to maturity, which are traded in 2006.

Table 2.2: Goodness-of-fit of the Option Pricing Models

		Model **G**					
		BS		FS		OS	
		2LR	P-value	2LR	P-value	2LR	P-value
Model **F**	FS	121.7	0.000	–	–	–	–
	OS	121.7	0.000	0.0	1.000	–	–
	GS	266.3	0.000	144.5	0.000	144.5	0.000

Note: The test statistic is asymptotically chi-square distributed with $p - q$ degree of freedom. The entries report the sample average of the test statistics and the corresponding P-values. The sample contains 100 sets of cross-section data on S&P 500 index options with 2 months to maturity, which are traded in 2006.

Table 2.3: Likelihood Ratio Tests for Nested Models

CHAPTER 3

PARAMETRIC RISK-NEUTRAL MEASURE ESTIMATION METHODS: A HORSE RACE

3.1 Introduction

A European option is a contingent claim whose value is dependent upon the investor's risk preference and the statistical probability measure, the so-called frequency (probability) measure (FM), which governs the empirically observable distribution of the underlying asset prices at the maturity of the option contract. In a complete arbitrage-free market, the valuation of European options is equivalent to computing the discounted value of expected payoff under the risk-adjusted probability measure, the so-called risk-neutral measure (RNM), regardless of the investor's risk preference. This risk-neutral pricing framework implies that the probability measure used to price assets is adjusted so as to make the expected return on a risky asset equal to the risk free interest rate.[1]

The RNM has been used for numerous applications. First, standard or complex derivative assets, with the same time-to-maturity, can be priced easily under RNMs [Longstaff (1995) and Rosenberg (1998)]. Second, classical risk management tools, such as Value-at-Risk (VaR), can be computed using RNMs [Aït-Sahalia and Lo (2000)]. Third, RNMs can be used to assess the market sentiments about political and economic events [Campa and Chang (1996), Melick and Thomas (1997), and Söderlind (2000)]. Fourth, RNMs can

[1] However, it does not mean that agents are assumed to be risk neutral. We are not assuming that investors are actually risk-neutral and that risky assets are actually expected to earn the risk-free rate of return.

also be used to estimate the implied risk aversion function from the joint observation of the risk-neutral and the historical densities [Aït-Sahalia and Lo (2000), Jackwerth (2000), and Rosenberg and Engle (2002)]. Finally, parameters of the underlying stochastic process can be estimated using the RNM [Bates (1996)].

Recently, various methodologies have been developed to derive the risk-neutral distribution of the future underlying asset price from the observed option prices. Generally, all methods can be divided into parametric and nonparametric ones. The parametric methods make particular assumptions on the form or family of the RNM and then typically use a non-linear regression technique to estimate the parameters of the RNM which minimize sum of squared pricing errors. On the other hand, the nonparametric methods make no strong assumptions about the RNM since they are flexible data-driven methods. However, the nonparametric approaches are so data-intensive that they usually lead to over-fitting problems and are not effective in small samples. For surveys of existing methods, see Mayhew (1995), Jackwerth (1999), Bliss and Panigirtzoglou (2002), Markose and Alentorn (2005) among others.

The celebrated Black-Scholes model (1973) evaluate the price of a European option on the basis of the parametric assumption that the underlying asset price process is the geometric Brownian motion, resulting in the terminal lognormal density as a FM. Girsanov's theorem[2] states that the RNM corresponding to the geometric Brownian motion is also lognormal. However, it is common knowledge that the implied RNMs are not lognormal, as exhibited by the so-called "volatility smirk". The volatility smirk suggests that the underlying asset prices on maturity should follow a left-skewed and leptokurtic distribution rather

[2]The Girsanov's theorem implies that the Black-Scholes model has the unique RNM, which is specified by:

$$\frac{dQ}{dP} = \varepsilon\left(\int_0^t \frac{r-\mu}{\sigma} dW\right),$$

where Q is the RNM, P is the FM, $\varepsilon(X)$ is the stochastic exponential of X with respect to W, W is the Brownian motion under the FM.

than a lognormal distribution.

Parametric estimations of the RNM with non-lognormality assumptions have been attempted to accommodate skewness and excess kurtosis by many researchers. Parametric RNM estimation methods can be classified into four categories:

- specific distributions—the lognormal distribution [Black and Scholes (1973)], the Weibull distribution [Savickas (2002)], and the max-negatively skewed stable distribution [Carr and Wu (2003)];

- mixture distributions—the mixture log-normals [Ritchey (1990), Melick and Thomas (1997), Bahra (1997)] and the mixture of log-stables [Lee (2007)];

- generalized distributions—the generalized gamma distribution [Tunaru and Albota (2005)], the generalized beta distribution [Rebonato (1999)], the orthogonal log-stable distribution [McCulloch (1985, 1987, 1996, 2003)], the generalized two-factor log-stable distribution [McCulloch and Lee (2008)]; and

- jump diffusion risk-neutral processes— the variance-gamma process [Madan and Milne (1991) and Madan, Carr, and Chang (1998)], the poisson jump diffusion process [Merton (1976), Naik and Lee (1990), and Bates (1991)], and the jump diffusion process with stochastic volatilities [Bates (1996), Bakshi, Cao, and Chen (1997), and Scott (1997)].

The value of a European option can be easily priced using a parametric option pricing model if a closed form RNM distribution function exists and is known, but in many cases a closed form RNM distributions are messy or unknown. However, even though a closed form of a distribution function is unknown, once an analytical form for the characteristic function exists, a European option can then be priced by efficient numerical procedures such as the "Romberged" Inverse Fast Fourier Transform (IFFT) method developed by Carr and Madan (1999) and McCulloch (2003).

In this chapter, we investigate the empirical performance of 12 parametric RNM estimation methods reviewed above using observed prices of cross section of S&P500 Index options traded at Chicago Board Option Exchange (CBOE). First, the goodness-of-fits are examined by means of the root mean squared errors (RMSE). Second, we perform likelihood ratio (LR) tests for nested and non-nested model selection. Finally, we conduct Monte-Carlo experiments to compare the accuracy and stability of the parametric RNM estimation methods by focusing the root mean integrated squared errors (RMISE) criterion.

The empirical results from the RMSEs and the LR tests show that the generalized two-factor log-stable model and the jump diffusion model with stochastic volatilities dominate other models. However, the jump diffusion model with stochastic volatilities has so many free parameters that it is vulnerable to over-fitting problems, which create spurious oscillations due to sampling noises. The over-fitting problems may be detected by Monte-Carlo experiments. Our Monte-Carlo experiments reveal that the jump diffusion with stochastic volatilities suffers from serious over-fitting problems and also show that the generalized two-factor log-stable model outperforms the alternatives.

The rest of the chapter is organized as follows. Section 3.2 discusses the option pricing approaches with the RNM. Section 3.3 presents 12 alternative parametric option pricing models for estimating the RNM. Section 3.4 describes the RNM estimation techniques under the non-linear regression framework. In Section 3.5, we conduct model selection tests and Monte-Carlo experiments to compare the performance of the alternative parametric models using S&P 500 index options. Section 3.6 concludes.

3.2 Option Pricing with the RNM

3.2.1 Closed Form Distribution Approach

By ruling out arbitrage possibilities, Cox and Ross (1976) showed that options can be priced as if investors were risk neutral, regardless of investors' risk preferences. Consider

a general European call option whose terminal payoff is $\max(0, S_T - K)$, where S_T is the underlying asset price at maturity, T is the time to maturity, and K is the strike price. In a complete arbitrage-free market, the price of a European call option $C(K)$ can then be computed as the discounted value of the option's expected payoff under the RNM. Formally,

$$\begin{aligned} C(K) &= e^{-r_f T} E^Q \left[\max(0, S_T - K)\right] \\ &= e^{-r_f T} \int_K^\infty (x - K)\, \mathrm{r}(x)\, dx, \end{aligned} \tag{3.1}$$

where r_f is the risk free rate, E^Q is the conditional expectation on time 0 information under the RNM, and $\mathrm{r}(x)$ is the risk-neutral density of the underlying asset price at maturity.

In the arbitrage-free market, the expected price at maturity under the RNM should equal the forward price of the underlying asset with the same time to maturity, i.e. the RNM must satisfy the so-called mean-forward price equality condition:

$$E^Q(x) = \int_0^\infty x\, \mathrm{r}(x) dx = S_0 e^{(r_f - d)T}, \tag{3.2}$$

where S_0 is the underlying asset price at time 0, d is the annual dividend rate of the underlying asset, and $S_0 e^{(r_f - d)T}$ is the implicit forward price.

Imposing a no-arbitrage condition (3.2) on (3.1), the call option price may be decomposed into two parts:

$$\begin{aligned} C(K) &= e^{-r_f T} \int_K^\infty x\, \mathrm{r}(x)\, dx - K e^{-r_f T} \int_K^\infty \mathrm{r}(x)\, dx \\ &= S_0 e^{-dT} \Pi_1 - K e^{-r_f T} \Pi_2, \end{aligned} \tag{3.3}$$

where

$$\Pi_1 = 1 - \frac{\int_0^K x\, \mathrm{r}(x)\, dx}{\int_0^\infty x\, \mathrm{r}(x)\, dx} \qquad \text{and} \tag{3.4}$$

$$\Pi_2 = 1 - \int_0^K \mathrm{r}(x)\, dx. \tag{3.5}$$

In a similar manner the price of a European put option $P(K)$ can be decomposed as:

$$\begin{aligned} P(K) &= e^{-r_f T} \int_0^K (K - x)\, \mathrm{r}(x)\, dx \\ &= -e^{-r_f T} \int_0^K x\, \mathrm{r}(x)\, dx + K e^{-r_f T} \int_0^K \mathrm{r}(x)\, dx \\ &= -S_0 e^{-dT}[1 - \Pi_1] + K e^{-r_f T}[1 - \Pi_2]. \end{aligned}$$

The option price may be also evaluated in terms of the RNM for the log of price, whose density is:

$$q(z) = e^z \mathrm{r}(e^z),$$

where $z = \log S_T$. Accordingly, Π_1 and Π_2 can be also expressed in terms of $q(z)$ as:

$$\Pi_1 = 1 - \frac{\int_{-\infty}^{k} e^z\, q(z)\, dz}{\int_{-\infty}^{\infty} e^z\, q(z)\, dz} \qquad \text{and} \tag{3.6}$$

$$\Pi_2 = 1 - \int_0^k q(z)\, dz, \tag{3.7}$$

where $k = \log K$.

The first term in (3.3) is the present value of expected the underlying asset upon optimal exercise, and the second term is the present value of the expected strike-price payment. Furthermore, $e^{-dT}\Pi_1$ can be seen as a delta (Δ) of the option which measures sensitivity to the underlying asset price, while Π_2 can be interpreted as a risk-neutral probability of finishing in-the-money, i.e., $\Pr(S_T > K)$.[3]

If the closed form cumulative distribution function (CDF) of the RNM is known, the option prices can be computed by simply evaluating Π_1 and Π_2 under the distributional assumptions for the RNM.

[3]The Π_1 and Π_2 can be interpreted as a cumulative funtions of the strike price K. As $K \to 0, \Pi_1 \to 1$, and when $K \to \infty, \Pi_1 \to 0$. In a similar manner as $K \to 0, \Pi_2 \to 1$, and when $K \to \infty, \Pi_2 \to 0$.

3.2.2 Characteristic Function Approach

If the CDF of the RNM is messy or unknown, it is computationally inefficient or impossible to evaluate Π_1 and Π_2 directly from the CDF. However, even though the closed form of the distribution function is unknown, once we have the closed form of the characteristic function, there exist fast numerical procedures for evaluating Π_1 and Π_2.

The characteristic function(CF) or Fourier Transform (FT) of density of $z = \log S_T$ is defined by:

$$\begin{aligned} cf_q(u) &= E[e^{iuz}] \\ &= \int_{-\infty}^{\infty} e^{iuz} q(z) dz \end{aligned}$$

The risk neutral probabilities, Π_1 and Π_2, are numerically recovered by inverting the characteristic function, which is known analytically:[4]

$$\Pi_1 = \frac{1}{2} + \frac{1}{\pi} \int_0^{\infty} \mathrm{Re}\left[\frac{e^{-iuk} cf_q(u-i)}{iuc f_q(-i)} \right] du \qquad \text{and} \tag{3.8}$$

$$\Pi_2 = \frac{1}{2} + \frac{1}{\pi} \int_0^{\infty} \mathrm{Re}\left[\frac{e^{-iuk} cf_q(u)}{iu} \right] du, \tag{3.9}$$

where $k = \log K$.

The Fast Fourier Transform (FFT) algorithm allows us to invert the characteristic functions with considerable computational speed advantages.[5] Unfortunately, as Carr and Madan

[4] See Heston(1993), Bates(1996), Bakshi and chen(1997), and Scott(1997) for more details.

[5] The Fast Fourier Transform(FFT) is one of the most fundamental advances in scientific computing, which allows to compute quickly the discrete Fourier transform (DFT) and its inverse. The FFT is an efficient algorithm for computing the DFT:

$$X(k) = \sum_{j=1}^{N} e^{-i\frac{2\pi}{N}(j-1)(k-1)} x(j) \quad \text{for } k = 1, \ldots, N,$$

The FFT makes pricing methods that use FFT much faster than other methods by reducing the number of multiplications from an order of N^2 to an order of $N \log_2 N$ in the DFT. See Carr and Madan (1999) for more detail.

(1999) pointed out, the FFT cannot be used to evaluate the two probabilities Π_1 and Π_2 in (3.8) and (3.9), since the integrand is singular at $u = 0$. To take advantage of the computational power of the FFT, Carr and Madan (1999) developed a new technique, which is designed to use the FFT in the inversion of the FT of the out-of-the-money (OTM) option prices. However, OTM option price function creates a small discontinuity at the spot price S_0 which can only aggravate the Fourier inversion. To avoid this problem McCulloch (2003) defines the OTM option price function $V(K)$ based on the forward price F:

$$V(K) \equiv F\, v(\tilde{k}) = \begin{cases} P(K) & \text{for } K < F \\ C(K) & \text{for } K \geq F \end{cases} \tag{3.10}$$

where $\tilde{k} = \log(K/F)$ and $v(\tilde{k}) = V(K)/(S_0 e^{(r_f - d)T})$.

With no loss of generality, we may measure the underlying asset in units such that $F = S_0 e^{(r_f - d)T} = 1$. Let $\phi_v(u)$ denote the FT of $v(\tilde{k})$:[6]

$$\begin{aligned} \phi_v(u) &= \int_{-\infty}^{\infty} e^{iu\tilde{k}} v(\tilde{k}) d\tilde{k} \\ &= \begin{cases} e^{-r_f T}\left[\frac{cf_q(u-i)-1}{iu-u^2}\right], & u \neq 0 \\ e^{-r_f T}\frac{cf_q'(-i)}{i}, & u = 0. \end{cases} \end{aligned}$$

[6]When $u = 0$, $\phi_v(u)$ takes the value 0/0, but the limit may be evaluated by means of l'Hôpital's rule:

$$\begin{aligned} \lim_{u\to 0}\phi_v(u) &= e^{-r_f T}\lim_{u\to 0}\left[\frac{d(cf_q(u-i)-1)/du}{d(iu-u^2)/du}\right] \\ &= e^{-r_f T}\frac{cf_q'(-i)}{i}. \end{aligned}$$

If the RNM CF $cf_q(u)$ takes the form of $e^{f(u)}$, it is more useful to use the following expression:

$$\lim_{u\to 0}\phi_v(u) = e^{-r_f T}\frac{\left.\frac{d\log cf_q(u)}{du}\right|_{u=-i}}{i}.$$

The prices of OTM options are obtained by inverting this Fourier transform:

$$\begin{aligned} V(K) &= F\, v(\tilde{k}) \\ &= S_0 e^{(r_f - d)T} \frac{1}{2\pi} \int_{-\infty}^{\infty} e^{-iu\tilde{k}} \phi_v(u) du. \end{aligned}$$

We evaluate the OTM option prices by means of the "Romberged" FFT algorithm[7] developed by McCulloch (2003) to improve the accuracy of numerical inversion.

Finally, the put-call parity condition[8] allows the call and put option prices to be computed across strike prices as:

$$\begin{aligned} C(K) &= I_{[K<F]} \left(V(K) + S_0 e^{-dT} - K e^{-r_f T} \right) + I_{[K \geq F]}\, V(K) \quad \text{and} \\ P(K) &= I_{[K<F]}\, V(K) + I_{[K \geq F]} \left(V(K) - S_0 e^{-dT} + K e^{-r_f T} \right), \end{aligned}$$

where $I_{[\cdot]}$ is the indicator function.

3.3 Parametric Distributions for the RNM

3.3.1 Specific Distributions

a. Black Scholes Log-Normal (BS) Model

The classic Black-Scholes (1973) model assumes that the price of the underlying asset follows a geometric Brownian motion (GBM) with a constant drift μ and volatility σ. The Black-Scholes GBM assumption implies the risk neutral distribution for S_T is lognormal:

$$\log S_T = z \sim N(\alpha, \beta), \quad \text{where } \beta = \sigma \sqrt{T}.$$

[7] Since increasing the range of integration results in a higher degree of precision, the "Romberged" FFT gives more satisfactory results. For details on the Romberg-FFT see McCulloch (2003).

[8] In the absence of arbitrage opportunities, the following relationship holds for European option:

$$C(K) + e^{-r_f T} K = P(K) + e^{-dT} S_0.$$

The risk neutral density function for $\log S_T$ is given by:

$$q(z) = \frac{1}{\beta\sqrt{2\pi}} e^{-\frac{(z-\alpha)^2}{2\beta^2}}.$$

By (3.6) and (3.7), the risk neutral probabilities Π_1 and Π_2 are:

$$\Pi_1 = \Phi\left(\frac{-k+\alpha+\beta^2}{\beta}\right) \quad \text{and}$$
$$\Pi_2 = \Phi\left(\frac{-k+\alpha}{\beta}\right),$$

where $\Phi(\cdot)$ is the cumulative distribution function for a standard normal variable.

Using the mean-forward price equality condition (3.2):

$$E^Q(S_T) = e^{\alpha+\beta^2/2} = S_0 e^{(r_f-d)T},$$

we have:

$$\alpha = \log S_0 + \left((r_f - d) - \frac{1}{2}\sigma^2\right)T,$$

so that the Black Scholes lognormal (BS) model has one free parameter—the volatility parameter β:

$$q(z) = bs(z;\beta),$$

where $bs(\cdot)$ denotes the risk neutral density of the BS model.

b. Weibull (WB) Model

Savickas (2002) values a European option under the assumption that the risk neutral distribution for the terminal underlying asset price S_T is a Weibull distribution:

$$S_T = x \sim \text{Weibull}(\alpha,\beta),$$

where $\alpha > 0$ is the scale parameter, and $\beta > 0$ is the peakedness parameter of the distribuiton. The risk neutral density function for S_T is given by:

$$r(x) = \begin{cases} \left(\frac{\beta}{\alpha}\right)\left(\frac{x}{\alpha}\right)^{\beta-1} e^{-\left(\frac{x}{\alpha}\right)^{\beta}}, & \text{for all } x \geq 0 \\ 0, & \text{for all } x < 0. \end{cases}$$

By (3.4) and (3.5), the risk neutral probabilities Π_1 and Π_2 are:

$$\begin{aligned} \Pi_1 &= 1 - I\left(1 + 1/\beta, \left(\frac{K}{\alpha}\right)^{\beta}\right) \qquad \text{and} \\ \Pi_2 &= e^{-\left(\frac{K}{\alpha}\right)^{\beta}}, \end{aligned}$$

where

$$\begin{aligned} \Gamma(a,b) &= \int_0^b u^{a-1}e^{-u}du \quad \text{(Incomplete gamma function)}, \\ \Gamma(a) &= \int_0^{\infty} u^{a-1}e^{-u}du \quad \text{(Gamma function), and} \\ I(a,b) &= \frac{\Gamma(a,b)}{\Gamma(a)} \quad \text{(Regularized Incomplete gamma function).} \end{aligned}$$

Using the mean-forward price equality condition (3.2):

$$E^Q(S_T) = \alpha\Gamma(1 + 1/\beta) = S_0 e^{(r_f - d)T},$$

we have:

$$\alpha = \frac{S_0 e^{(r_f - d)T}}{\Gamma(1 + 1/\beta)},$$

so that the Weibull (WB) model has one free parameter—the peakedness parameter β:

$$\mathrm{r}(x) = wb(x;\beta),$$

where $wb(\cdot)$ denotes the risk neutral density of the WB model.

c. Finite Moment Log-Stable (FS) Model

Carr and Wu (2003) are able to price options under log-stable uncertainty, but only by making the very restrictive assumption that log prices have maximally negative skewness:[9]

$$\log S_T \;=\; z \;\sim\; S(\alpha, -1, c\,T^{1/\alpha}, \delta),$$

where $\alpha \in (0, 2]$ is the peakedness parameter, $c \in (0, \infty)$ is the scale parameter, and $\delta \in (-\infty, \infty)$ is the location parameter. The risk neutral density function for $\log S_T$ is given by:

$$q(z) \;=\; s\left(z; \alpha, -1, c\,T^{1/\alpha}, \delta\right), \tag{3.11}$$

where $s(\cdot)$ is the stable density function.[10]

Under the risk neutral density (3.11), the characteristic function of $\log S_T$ is given by:

$$cf_q(u) \;=\; \exp\left[iu\left(\log S_0 + (r_f - d)T + c^\alpha \sec\left(\frac{\pi\alpha}{2}\right)T\right) - c^\alpha \sec\left(\frac{\pi\alpha}{2}\right)(iu)^\alpha T\right]$$

Using the mean-forward price equality condition (3.2):

$$E^Q(S_T) \;=\; e^{\delta - c^\alpha \sec\left(\frac{\pi\alpha}{2}\right)T} \;=\; S_0 e^{(r_f - d)T},$$

we have:

$$\delta \;=\; \log S_0 + (r_f - d)T + c^\alpha \sec\left(\frac{\pi\alpha}{2}\right)T,$$

so that the finite moment log-stable (FS) model has two free parameters—the peakedness

[9] They assume the max-negative skewness in order to give the returns themselves finite moments. They also incorporate max-negative skewness directly into the stable distribution describing the RNM of the underlying asset without assumptions on the frequency measure (FM).

[10] Since there are no known closed form expressions for stable density, the most concrete way to describe all possible stable distributions is through the characteristic function.

parameter α and the scale parameters c:

$$q(z) \quad = \quad fs(z;\alpha,c),$$

where $fs(\cdot)$ denotes the risk neutral density of the FS model.

3.3.2 Mixture Distributions

a. Mixture of Two Log-Normal (DN) Model

Ritchey (1990), Melick and Thomas (1997), and Bahra (1997) assume that the risk-neutral distribution is a mixture of univariate log-normals:

$$\log S_T \quad = \quad z \sim \begin{cases} N(\alpha_1,\beta_1) & \text{with pr. } \omega \\ N(\alpha_2,\beta_2) & \text{with pr. } 1-\omega. \end{cases}$$

The resulting risk neutral density function for $\log S_T$ is given by:

$$\begin{aligned} q(z) &= \omega\phi(z;\alpha_1,\beta_1) + (1-\omega)\phi(z;\alpha_2,\beta_2) \\ &= \omega\frac{1}{\beta_1\sqrt{2\pi}}e^{-\frac{(z-\alpha_1)^2}{2\beta_1^2}} + (1-\omega)\frac{1}{\beta_2\sqrt{2\pi}}e^{-\frac{(z-\alpha_2)^2}{2\beta_2^2}}, \end{aligned}$$

where $\beta_j = \sigma_j\sqrt{T}$.

By (3.6) and (3.7), the risk neutral probabilities Π_1 and Π_2 are:

$$\Pi_1 \quad = \quad \frac{\omega e^{\alpha_1+1/2\beta_1^2}\left[1-\Phi\left(\frac{k-(\alpha_1+\beta_1^2)}{\beta_1}\right)\right] + (1-\omega)e^{\alpha_2+1/2\beta_2^2}\left[1-\Phi\left(\frac{k-(\alpha_2+\beta_2^2)}{\beta_2}\right)\right]}{\omega e^{\alpha_1+1/2\beta_1^2} + (1-\omega)e^{\alpha_2+1/2\beta_2^2}} \quad \text{and}$$

$$\Pi_2 \quad = \quad \omega\,\Phi\left(\frac{-k+\alpha_1}{\beta_1}\right) + (1-\omega)\,\Phi\left(\frac{-k+\alpha_2}{\beta_2}\right),$$

where $\Phi(\cdot)$ is the cumulative distribution function for a standard normal variate.

Using the mean-forward price equality condition (3.2):

$$E^{Q}(S_T) \;=\; \omega e^{\alpha_1+\frac{1}{2}\beta_1^2} + (1-\omega)e^{\alpha_2+\frac{1}{2}{\beta_2}^2} \;=\; S_0 e^{(r_f-d)T},$$

we have:

$$\alpha_2 \;=\; \log\left[\frac{1}{1-\omega}\left(S_0 e^{(r_f-d)T} - \omega e^{\alpha_1+\frac{1}{2}\beta_1^2}\right)\right] - \frac{1}{2}{\beta_2}^2,$$

so that the mixture of two lognormal (DN) model has four free parameters—the location parameter α_1, the volatility parameters β_1 and β_2, and the weight parameter ω:

$$q(z) \;=\; dn(z;\alpha_1,\beta_1,\beta_2,\omega),$$

where $dn(\cdot)$ denotes the risk neutral density of the DN model.

b. Mixture of Two Log-Stable (DS) Model

Similarly to the mixture of lognormals, we may construct the FM of $\log S_T$ with a weighted sum of two maximally skewed log-stables: one is a maximally negatively skewed one and the other is a maximally positively skewed one. The RNM of the max-negatively skewed log-stable distribution is the FM itself. On the other hand, the RNM of the max-positively skewed log-stable distribution is an exponentially tilted positively skewed stable distribution. Consequently, the resulting RNM is the weighted sum of the max-negatively skewed log-stable distribution and the exponentially tilted positively skewed log-stable distribution:

$$\log S_T \;=\; z \sim \begin{cases} S(\alpha_1,-1,c_1T^{1/\alpha_1},\delta_1) & \text{with pr. } \omega \\ TS_+(\alpha_2,c_2T^{1/\alpha_2},\delta_2,1) & \text{with pr. } 1-\omega, \end{cases}$$

where $S(\cdot)$ is a stable distribution, and $TS_+(\cdot)$ is an exponentially tilted positively skewed stable distribution, $\alpha_1,\ \alpha_2 \in (0,2]$ are the peakedness parameters, $c_1, c_2 \in (0,\infty)$ are the scale parameters, and $\delta_1, \delta_2 \in (-\infty,\infty)$ are the location parameters.

The risk neutral density function for $\log S_T$ is given by:

$$\begin{aligned} q(z) &= \omega q_1(z) + (1-\omega) q_2(z) \\ &= \omega s(z; \alpha_1, -1, c_1 T^{1/\alpha_1}, \delta_1) + (1-\omega) t s_+(z; \alpha_2, c_2 T^{1/\alpha_2}, \delta_2, 1) \\ &= \omega s(z; \alpha_1, -1, c_1 T^{1/\alpha_1}, \delta_1) \\ &\quad + (1-\omega) e^{\delta_2 + {c_2}^{\alpha_2} T \sec\left(\frac{\pi\alpha_2}{2}\right)} e^{-z} s(z; \alpha_2, 1, c_2 T^{1/\alpha_2}, \delta_2), \end{aligned} \tag{3.12}$$

where $s(\cdot)$ is a stable density function, and $ts_+(\cdot)$ is an exponentially tilted positively skewed stable density.

Under the risk neutral density (3.12), the characteristic function of $\log S_T$ is given by:

$$\begin{aligned} cf_q(u) &= \omega cf_{q_1}(u) + (1-\omega) cf_{q_2}(u) \\ &= \omega e^{iu\delta_1 - {c_1}^{\alpha_1} \sec\left(\frac{\pi\alpha_1}{2}\right)(iu)^{\alpha_1} T} + (1-\omega) e^{iu\delta_2 + {c}^{\alpha_2} \sec\left(\frac{\pi\alpha_2}{2}\right)(1-(1-iu)^{\alpha_2})T} \end{aligned}$$

Using the mean-forward price equality condition (3.2):

$$E^Q(S_T) = (1-\omega) e^{\delta_2 + {c_2}^{\alpha_2} \sec\left(\frac{\pi\alpha_2}{2}\right)T} + \omega e^{\delta_1 - {c_1}^{\alpha_1} \sec\left(\frac{\pi\alpha_1}{2}\right)T} = S_0 e^{(r_f - d)T},$$

we have:

$$\delta_2 = \log\left[\frac{1}{1-\omega}\left(S_0 e^{(r_f-d)T} - \omega e^{\delta_1 - {c_1}^{\alpha_1}\sec\left(\frac{\pi\alpha_1}{2}\right)}\right)\right] - {c_2}^{\alpha_2} \sec\left(\frac{\pi\alpha_2}{2}\right),$$

so that the mixture of two-logstable (DS) model has six free parameters—the peakedness parameters α_1 and α_2, the scale parameters c_1 and c_2, the location parameter δ_1, and the weight parameter ω:

$$q(z) = ds(z; \alpha_1, \alpha_2, c_1, c_2, \delta_1, \omega),$$

where $ds(\cdot)$ denotes the risk neutral density of the DS model.

3.3.3 Generalized Distributions

a. Generalized Gamma (GG) Model

Tunaru and Albota (2005) propose the use of the generalized gamma distribution (GG) for the risk neutral distribution of the terminal underlying asset price S_T:

$$S_T = x \sim \text{GG}(\alpha, \beta, p),$$

where $\alpha > 0$ is the scale parameter, β is the peakedness parameter, and $p > 0$ is the index parameter of the distribution. The generalized gamma distribution nests several distributions: when $p = 1$, the Weibull distribution results; when $\beta = 1$, the gamma distribution results; when $\beta = p = 1$, the exponential distribution results; and when $\beta \to 0$ we arrive at the log-normal distribution.

The risk neutral density function for S_T is given by:

$$\text{r}(x) = \begin{cases} \frac{1}{\Gamma(p)} \left(\frac{|\beta|}{\alpha}\right) \left(\frac{x}{\alpha}\right)^{\beta p - 1} e^{-\left(\frac{x}{\alpha}\right)^{\beta}}, & \text{for all } x \geq 0 \\ \\ 0, & \text{for all } x < 0. \end{cases}$$

By (3.4) and (3.5), the risk neutral probabilities, Π_1 and Π_2, are:

$$\Pi_1 = 1 - I\left(p + 1/\beta, (K/\alpha)^{\beta}\right) \qquad \text{and}$$

$$\Pi_2 = 1 - I\left(p, (K/\alpha)^{\beta}\right)$$

where

$$\Gamma(a, b) = \int_0^b u^{a-1} e^{-u} du \quad \text{(Incomplete gamma function)},$$

$$\Gamma(a) = \int_0^{\infty} u^{a-1} e^{-u} du \quad \text{(Gamma function), and}$$

$$I(a, b) = \frac{\Gamma(a, b)}{\Gamma(a)} \quad \text{(Regularized Incomplete gamma function).}$$

Using the mean-forward price equality condition (3.2):

$$E^{Q}(S_T) = \alpha\frac{\Gamma(p+1/\beta)}{\Gamma(p)} = S_0 e^{(r_f-d)T},$$

we have:

$$\alpha = \frac{\Gamma(p)}{\Gamma(p+1/\beta)} S_0 e^{(r_f-d)T},$$

so that the generalized gamma (GG) model has two free parameters—the peakedness parameter β and the index parameter p:

$$\mathrm{r}(x) = gg(x;\beta,p),$$

where $gg(\cdot)$ denotes the risk neutral density of the GG model.

b. Generalized Beta (GB) Model

Bookstaber and McDonald (1987) develop a new generalized distribution, called the Generalized Beta Distribution of the Second Kind (GB2), which accommodates a fat-tail property and permits skewness as well. Rebonato (1999) valued the call option based on the assumption that the risk neutral distribution of the terminal underlying asset price S_T is a GB2 distribution:

$$S_T = x \sim \mathrm{GB2}(\alpha,\beta,p,q),$$

where $\alpha > 0$ is the scale parameter, β is the peakedness parameter, and $p > 0$ and $q > 0$ control the shape and skewness. The GB model nests the GG model since the generalized gamma is a limiting case of the GB2 distribution.[11]

[11] When $q \to \infty$, the generalized gamma distribution results:

$$\lim_{q\to\infty} GB2(x;\tilde{\alpha} = \alpha q^{1/\beta},\beta,p,q) = GG(x;\alpha,\beta,p)$$

The risk neutral density function for S_T is given by:

$$\mathrm{r}(x) = \begin{cases} \frac{|\beta| x^{\beta p-1}}{\alpha^{\beta p} B(p,q)\left[1+(x/\alpha)^{\beta}\right]^{p+q}}, & \text{for all } x \geq 0 \\ 0, & \text{for all } x < 0, \end{cases}$$

where

$$\begin{aligned} B(p,q) &= \frac{\Gamma(p)\Gamma(q)}{\Gamma(p+q)} = \int_0^{\infty} \frac{u^{p-1}}{(1+u)^{p+q}} du \quad \text{(Beta function)} \\ &= \int_0^1 w^{p-1}(1-w)^{q-1} dw, \quad w = \frac{1}{u+1}. \end{aligned}$$

By (3.4) and (3.5), the risk neutral probabilities Π_1 and Π_2 are:

$$\Pi_1 = I\left(p+\frac{1}{\beta}, q-\frac{1}{\beta}, \frac{1}{1+(K/\alpha)^{\beta}}\right) \qquad \text{and}$$

$$\Pi_2 = I\left(p, q, \frac{1}{1+(K/\alpha)^{\beta}}\right),$$

where

$$I(p,q,z) = \frac{B(p,q,z)}{B(p,q)} \quad \text{(Regularized Incomplete Beta function)} \quad \text{and,}$$

$$B(p,q,z) = \int_0^z w^{p-1}(1-w)^{q-1} dw \quad \text{(Incomplete Beta function).}$$

Using the mean-forward price equality condition (3.2):

$$E^Q(S_T) = \alpha \frac{B\left(p+\frac{1}{\beta}, q-\frac{1}{\beta}\right)}{B(p,q)} = S_0 e^{(r_f-d)T},$$

we have:

$$\alpha = \frac{B(p,q)}{B\left(p+\frac{1}{\beta}, q-\frac{1}{\beta}\right)} S_0 e^{(r_f-d)T},$$

so that the GB model has three free parameters—the peakedness parameter β, the shape

and skewness parameters p and q:

$$\mathrm{r}(x) \quad = \quad gb(x;\beta,p,q),$$

where $gb(\cdot)$ denotes the risk neutral density of the GB model.

c. Orthogonal Log-Stable Model (OS)

McCulloch (2003) reformulates his orthogonal stable option pricing model[12] in the RNM context. The orthogonal log-stable uncertainty assumption implies that the risk neutral probability distribution of $\log S_T$ is simply a convolution[13] of max-negatively skewed stable distribution and exponentially tiled positively skewed stable distribution:

$$\log S_T \quad = \quad z \sim S(\alpha,-1,c_A T^{1/\alpha},\delta) * TS_+(\alpha,c_N T^{1/\alpha},0,1)$$

where $S(\cdot)$ is a stable distribution, and $TS_+(\cdot)$ is an exponentially tilted positively skewed stable distribution, $\alpha \in (0,2]$ is the peakedness parameter, $c_A, c_N \in (0,\infty)$ are the scale parameters for the asset and numeraire, respectively, and δ is the location parameter.

The risk neutral density function for the $\log S_T$ is given by:

$$\begin{aligned} q(z) \quad &= \quad s\left(z_1;\alpha,-1,c_A T^{1/\alpha},\delta\right) * ts_+\left(z_2;\alpha,c_N T^{1/\alpha},0,1\right) \\ &= \quad e^{\delta+c_N^\alpha \sec\left(\frac{\pi\alpha}{2}\right)T}\, s\left(z_1;\alpha,-1,c_A T^{1/\alpha},\delta\right) * e^{-z_2} s\left(z_2;\alpha,+1,c_N T^{1/\alpha},0\right), \end{aligned} \tag{3.13}$$

[12]The option pricing model with stable distribution was first proposed by McCulloch (1978, 1987, 1996) using a utility maximization setting under the assumption that the marginal utilities of numeraire and asset follow a log-stable distribution with maximum negative skewness, respectively, and are also independently distributed.

[13]The convolution of f and g is written $f * g$. If X and Y are two independent random variables with probability distributions f and g, respectively, then the probability distribution of the sum $z = X + Y$ is given by the convolution:

$$(f * g)(z) \quad = \quad \int f(\tau) g(z-\tau) d\tau.$$

where $s(\cdot)$ is a stable density function, and $ts_+(\cdot)$ is an exponentially tilted positively skewed stable density.

Under the risk neutral density (3.13), the characteristic function of the log price $z \equiv \log S_T$ is given by:

$$\begin{aligned} cf_q(u) &= \exp\left[iu\left(\log S_0 + (r_f - d)T - ({c_N}^\alpha - {c_A}^\alpha)\sec\left(\frac{\pi\alpha}{2}\right)T\right)\right. \\ &\quad \left. -{c_A}^\alpha \sec\left(\frac{\pi\alpha}{2}\right)(iu)^\alpha T + {c_N}^\alpha \sec\left(\frac{\pi\alpha}{2}\right)(1-(1-iu)^\alpha)\,T\right]. \end{aligned}$$

Using the mean-forward price equality condition (3.2):

$$E^Q(S_T) = e^{\delta + ({c_N}^\alpha - {c_A}^\alpha)\sec\left(\frac{\pi\alpha}{2}\right)T} = S_0 e^{(r_f - d)T},$$

we have:

$$\delta = \log S_0 + (r_f - d)T - ({c_N}^\alpha - {c_A}^\alpha)\sec\left(\frac{\pi\alpha}{2}\right)T,$$

so that the orthogonal log-stable (OS) model has three free parameters—the peakedness parameter α and the scale parameters c_A and c_N:

$$q(z) = os(z; \alpha, c_A, c_N),$$

where $os(\cdot)$ denotes the risk neutral density of the OS model.[14]

d. Generalized Two-Factor Log-Stable Model (GS)

McCulloch and Lee (2008) estimate the RNM using the generalized two-factor log-stable option pricing model which allows the interdependency between the marginal utili-

[14] Alternatively, the RNM of the OS model may be expressed using a different parameterization:

$$q(z) = os(z; \alpha, \beta, c),$$

where $\beta = (c_N^\alpha - c_A^\alpha)/c^\alpha$ and $c = (c_N^\alpha + c_A^\alpha)^{1/\alpha}$.

ties of numeraire and asset.[15] The generalized two-factor log-stable model also provides a flexible RNM probability distribution function as a convolution of two exponentially tilted stable distributions:

$$\log S_T \quad = \quad z \sim *_{j=1}^{2} TS_{\mathrm{sgn}(c_{Nj}-c_{Aj})}\left(\alpha, |c_{Nj}-c_{Aj}|T^{1/\alpha}, \delta_j, \left|\frac{c_{Nj}}{c_{Nj}-c_{Aj}}\right|\right),$$

where $*_{j=1}^{2} TS$ is the convolution of the two tilted maximally skewed stable distributions, $\alpha \in (0, 2]$ is the peakedness parameter, $c_{ij} > 0$, $i = A, N$, $j = 1, 2$, are the elements of the scale matrix, and δ_1, δ_2 are the elements of location vector with $\delta_2 = 0$. The risk neutral density function for $\log S_T$ is given by:

$$q(z) \quad = \quad *_{j=1}^{2} ts_{\mathrm{sgn}(c_{Nj}-c_{Aj})}\left(z_j; \alpha, |c_{Nj}-c_{Aj}|T^{1/\alpha}, \delta_j, \left|\frac{c_{Nj}}{c_{Nj}-c_{Aj}}\right|\right), \tag{3.14}$$

where $ts(\cdot)$ is an exponentially tilted positively skewed stable density if $\mathrm{sgn}(c_{Nj} - c_{Aj}) = 1$ or an exponentailly tilted negatively skewed stable density if $\mathrm{sgn}(c_{Nj} - c_{Aj}) = -1$.

Under the risk neutral density (3.14), the characteristic function of $\log S_T$ is given by:

$$\begin{aligned} cf_q(u) \quad &= \quad \exp\left\{iu\left(\log S_0 + (r_f - d)T - \sum_{j=1}^{2}(c_{Nj}{}^{\alpha} - c_{Aj}{}^{\alpha})\sec\left(\frac{\pi\alpha}{2}\right)T\right)\right. \\ &+ \quad \left.\sum_{j=1}^{2}|c_{Nj}-c_{Aj}|^{\alpha}\sec\left(\frac{\pi\alpha}{2}\right)\left[\left|\frac{c_{Nj}}{c_{Nj}-c_{Aj}}\right|^{\alpha} - \left(\left|\frac{c_{Nj}}{c_{Nj}-c_{Aj}}\right| - \mathrm{sgn}(c_{Nj}-c_{Aj})iu\right)^{\alpha}\right]T\right\}. \end{aligned}$$

Using the mean-forward price equality condition (3.2):

$$E^{Q}(S_T) \quad = \quad e^{\delta_1 + \left(\sum_{j=1}^{2}(c_{Nj}{}^{\alpha} - c_{Aj}{}^{\alpha})\right)\sec\left(\frac{\pi\alpha}{2}\right)T} \quad = \quad S_0 e^{(r_f-d)T},$$

we have:

$$\delta_1 \quad = \quad logS_0 + (r_f - d)T - \left(\sum_{j=1}^{2}(c_{Nj}{}^{\alpha} - c_{Aj}{}^{\alpha})\right)\sec\left(\frac{\pi\alpha}{2}\right)T,$$

[15]The orthogonal assumption can be generalized by introducing two factors which are independent max-negatively skewed standard stable variates and contribute to both the log marginal utilities of numeraire and asset.

so that the generalized two-factor log-stable (GS) model has five free parameters—the peakedness parameter α and the scale parameters c_{ij}, $i = A, N$, $j = 1, 2$:

$$q(z) \quad = \quad gs(z; \alpha, c_{A1}, c_{A2}, c_{N1}, c_{N2}),$$

where $gs(\cdot)$ denotes the risk neutral density of the GS model.

3.3.4 Jump Diffusion Risk Neutral Processes

a. Variance-Gamma Model (VG)

Madan and Milne (1991), and Madan, Carr, and Chang (1998) assume that the log price obeys the variance-gamma (VG) process, under which the log price follows a pure jump Lévy process. The VG process is obtained by evaluating arithmetic Brownian motion with drift β and volatility σ at a random time given by a gamma process having a mean rate per unit time of 1 and a variance rate of α. The resulting risk-neutral process for S_T is:

$$S_t \quad = \quad S_0 e^{(r_f - d)t + \mu t + X_t(\sigma, \beta, \alpha)}, \quad t > 0,$$

where

$$\begin{aligned} X_t(\sigma, \beta, \nu) &= b\left(\gamma(t; 1, \nu); \beta, \sigma\right) \quad \text{(Variance Gamma Process)}, \\ b(t; \beta, \sigma) &= \beta t + \sigma W(t) \quad \text{(Brownian Motion with drift), and} \\ \gamma(t; 1, \alpha) &\qquad \text{(Gamma process with unit mean rate).} \end{aligned}$$

Accordingly, the risk neutral process of $\log S_T$ is given by

$$\log S_T \equiv z \quad = \quad \log S_0 + (r_f - d + \mu)T + X(T; \sigma, \beta, \alpha).$$

Madan, Carr, and Chang (1998) provide a closed form risk neutral density for $\log S_T$:[16]

$$q(z) = \int_0^\infty \frac{1}{\sigma\sqrt{2\pi g}} e^{-\frac{(z-\log S_0-(r_f-d+\mu)T-\beta g)^2}{2\sigma^2 g}} \frac{g^{t/\alpha-1}e^{-g/\alpha}}{\alpha^{t/\nu}\Gamma(t/\alpha)} dg, \tag{3.15}$$

where $g = \gamma(t+h;\mu,\alpha) - \gamma(t;\mu,\alpha)$. The additional two parameters α and β relative to the geometric Brownian motion control over skewness and kurtosis respectively.

Under the risk neutral density (3.15), the characteristic function of the log price $z \equiv \log S_T$ is given by:

$$cf_q(u) = e^{iu\left(\log S_0+(r_f-d+\mu)T\right)}\left[1-\left(i\beta u - \frac{1}{2}\sigma^2 u^2\right)\alpha\right]^{-T/\alpha}$$

Using the mean-forward price equality condition (3.2):

$$E^Q(S_T) = S_0 e^{(r_f-d)T+\mu T}\left[1-\left(\beta+\frac{1}{2}\sigma^2\right)\alpha\right]^{-T/\alpha} = S_0 e^{(r_f-d)T},$$

we have:

$$\mu = \frac{1}{\alpha}\log\left[1-\left(\beta+\frac{1}{2}\sigma^2\right)\alpha\right],$$

so that the variance-gamma (VG) model has three free parameters—the peakedness parameter α, the skewness parameter β, and the scale parameter σ:

$$q(z) = vg(z;\alpha,\beta,\sigma),$$

where $vg(\cdot)$ denotes the risk neutral density of the VG model.

b. Poisson Jump Diffusion (JD) Model

Option pricing models with jumps have been developed by Merton (1976), Naik and Lee (1990), and Bates (1991). The jump processes are Poisson jump processes in which the

[16] Madan, Carr, and Chang (1998) derive the closed form solution, but it is slow because it requires computation of modified Bessel functions. Therefore, the characteristic function approach is computationally more efficient for the VG model than the closed form distribution approach.

occurrence of a jump is determined by a Poisson process, and if a jump occurs, the size of the jump for the log of the underlying asset price is assumed to have a normal distribution.

The resulting risk-neutral process for S_T is:

$$\frac{dS_t}{S_t} = \Big((r_f - d) - \lambda\mu_J\Big)dt + \sigma dW_t^s + J_t dq_t, \tag{3.16}$$

where W_t^s is a standard Brownian motion; J_t is the percentage jump size (conditional on no jump occuring) with $\log(1+J_t) \sim N(\log(1+\mu_J) - 1/2\sigma_J^2, \sigma_J^2)$; q_t is a Poisson jump counter with intensity λ, i.e., $\Pr[dq_t = 1] = \lambda dt$, $\Pr[dq_t = 0] = 1 - \lambda dt$. Skewness in the terminal risk-neutral distribution is controlled by the mean jump μ_J, whereas the amount of kurtosis is regulated by the magnitude (μ_J and λ) and variability (σ_J) of the jump component.

Under the risk neutral process (3.16), the characteristic function of $\log S_T$ is given by:

$$\begin{aligned} cf_q(u) = \exp\Bigg[& iu\left(\log S_0 + (r_f - d)T - \lambda\mu_J T - \frac{1}{2}\sigma^2\right) \\ & -\frac{1}{2}u^2\sigma^2 T + \lambda\left(e^{iu\left(\log(1+\mu_J) - 1/2\sigma_J^2\right) - 1/2u^2\sigma_J^2} - 1\right)T\Bigg]. \end{aligned}$$

The risk neutral procss (3.16) implies that the JD model has four free parameters—the volatility parameter σ, the mean jump parameter μ_J, the jump volatility parameter σ_J, and the jump intensity parameter λ:

$$q(z) = jd(z; \sigma, \lambda, \mu_J, \sigma_J),$$

where $jd(\cdot)$ is the risk neutral density of the JD model.

c. Jump Diffusion Model with Stochastic Volatilities (JS)

Bates (1996), Scott (1997), Bakshi, Cao, and Chen (1997) develop closed form solutions for a jump-diffusion model with stochastic volatilities by using the Fourier inversion formula. Under the risk neutral measure, the price of the underlying asset S_t follows a geometric jump diffusion process with the instantaneous conditional variance V_t, following

a mean reverting square root process. The resulting risk-neutral process for S_T is:

$$\frac{dS_t}{S_t} = ((r_f - d) - \lambda\mu_J)dt + \sqrt{V_t}dW_t^s + J_t dq_t \tag{3.17}$$

$$dV_t = \kappa(\vartheta - V_t)dt + \sigma_v\sqrt{V_t}dW_t^v, \tag{3.18}$$

where V_t is the diffusion component of return variance(conditional on no jump occurring); W_t^s and W_t^v are a standard Brownian motion, respectively, with $Cov_t[dW_t^s, dW_t^v] = \rho dt$; J_t is the percentage jump size (conditional on no jump occuring) with $\log(1+J_t) \sim N(\log(1+\mu_J) - 1/2\sigma_J^2, \sigma_J^2)$; q_t is a Poisson jump counter with intensity λ, i.e., $\Pr[dq_t = 1] = \lambda dt$, $\Pr[dq_t = 0] = 1 - \lambda dt$; κ, ϑ, and σ_v are respectively the speed of adjustment, long-run mean and variation coefficient of the diffusion volatility V_t. These parametric assumptions offer a sufficiently versatile RNM structure that can accommodate most of the desired features. For instance, skewness in the distribution is controlled by either the correlation ρ or the mean jump μ_J, whereas the amount of kurtosis is regulated by either the volatility diffusion parameter σ_v or the magnitude and variability of the jump component.

Under the risk neutral process (3.17) and (3.18), the characteristic function of the log price $z \equiv \log S_T$ is given by:

$$\begin{aligned} cf_q(u) = \exp\Big\{iu\Big(\log S_0 + (r_f - d)T - \lambda\mu_J T\Big) \\ +\lambda\Big[e^{iu\left(\log(1+\mu_J) - 1/2\sigma_J^2\right) - 1/2u^2\sigma_J^2} - 1\Big]T - C(u)V_t - D(u)\Big\}, \end{aligned}$$

where

$$\begin{aligned} C(u) &= \frac{\xi(1 - e^{-\eta T})}{2\eta - (\eta - \kappa^*)(1 - e^{-\eta T})} \\ D(u) &= \frac{\kappa\vartheta}{\sigma_v^2}\left[2\log\left(1 - \frac{(\eta - \kappa^*)(1 - e^{-\eta T})}{2\eta}\right) + (\eta - \kappa^*)T\right] \\ \eta &= \sqrt{(\kappa^*)^2 + \sigma_v^2\xi} \\ \kappa^* &= \kappa - iu\sigma_v\rho \\ \xi &= iu + u^2. \end{aligned}$$

The jump diffusion model with stochastic volatilities (JS) has eight free parameters—the mean jump μ_J, the jump variance σ_J, the volatility diffusion parameter σ_v, the correlation ρ, intensity λ, the speed of adjustment κ, the long-run mean ϑ, and the instantaneous variance V_t:[17]

$$q(z) \quad = \quad js(z; \lambda, \mu_J, \sigma_J, \sigma_v, \rho, \kappa, \vartheta, V_t),$$

where $js(\cdot)$ denotes the risk neutral density of the JS model.

3.3.5 RNM Distribution Tree

In this section, we discuss interrelationships between the 12 alternative RNM models. Some RNM models can be seen as a special case or limiting case of other models.

(1) The GS model nests the OS, FS, BS models:

$$\begin{aligned}
&gs\Big(z; \alpha, c_{A1}, c_{A2} = 0, c_{N1} = 0, c_{N2}\Big) \\
&= \; os\Big(z; \alpha, \beta = (c_{N2}^{\alpha} - c_{A1}^{\alpha})/c^{\alpha}, c = (c_{N2}^{\alpha} + c_{A1}^{\alpha})^{1/\alpha}\Big); \\
&os\Big(z; \alpha, \beta = -1, c, \delta\Big) \; = \; fs\Big(z; \alpha, c\Big); \text{ and} \\
&fs\Big(z; \alpha = 2, c = \sqrt{\sigma^2/2}, \delta\Big) \; = \; bs\Big(z; \sigma\Big)
\end{aligned}$$

(2) The GB model nests the GG, WB, BS models:[18]

$$\begin{aligned}
&\lim_{q\to\infty} gb\Big(x; \tilde{\alpha} = \alpha q^{1/\beta}, \beta, p, q\Big) \; = \; gg\Big(x; \alpha, \beta, p\Big); \\
&\lim_{\substack{q\to\infty \\ \beta\to 0}} gg\Big(x; \alpha = (\sigma^2\beta^2)^{1/\beta} q^{-1/\beta}, \beta, p = (\beta\mu + 1)/\sigma^2\beta^2\Big) \; = \; bs\Big(\log x; \mu, \sigma\Big); \text{ and} \\
&gg\Big(x; \alpha, \beta, p = 1\Big) \; = \; wb\Big(x; \alpha, \beta\Big)
\end{aligned}$$

[17] The level of the instantaneous variance V_t is a state variable. However, since V_t is unobservable, we treat V_t as another free parameter in the RNM estimation.

[18] The scale parameter α can be fixed by mean-forward price equality condition.

(3) The VG model nests the BS models:

$$\lim_{\substack{\alpha\to 0\\ \beta\to 0}} vg\Big(z;\alpha,\beta,\sigma\Big) = bs\Big(z;\sigma\Big)$$

(4) The DS model nests the DN, FS, BS models:

$$\begin{aligned}
&ds\Big(z;\alpha_1=2,\alpha_2=2,c_1=\sqrt{\sigma_1^2/2},c_2=\sqrt{\sigma_2^2/2},\omega,\delta_1=\alpha+c_1^{\alpha}\sec(\pi\alpha_1/2)+\sigma_1^2/2\Big)\\
&=\ dn\Big(z;\sigma_1=(2c_1^2)^{1/2},\sigma_2=(2c_2^2)^{1/2},\omega,\alpha\Big)\\
&ds\Big(z;\alpha_1,\alpha_2,c_1,c_2,\omega=1,\delta_1=\log F+c_1^{\alpha}\sec(\pi\alpha/2)\Big)\ =\ fs\Big(z;\alpha_1,c_1\Big)\\
&dn\Big(z;\sigma_1,\sigma_2,\omega=1,\alpha_1=\log F-\sigma_1^2/2\Big)=bs\Big(z;\sigma\Big)
\end{aligned}$$

(5) The JS model nests the JD, BS models:

$$\begin{aligned}
&js\Big(z;\lambda,\mu_J,\sigma_J,\vartheta=0,\kappa=0,\sigma_v=0,\rho=0,V_t=\sigma^2\Big)\ =\ jd\Big(z;\lambda,\mu_J,\sigma_J,\sigma\Big);\ \textit{and}\\
&jd\Big(z;\lambda=0,\mu_J=0,\sigma_J=0,\sigma\Big)\ =\ bs\Big(z;\sigma\Big).
\end{aligned}$$

Figure 3.1 illustrates a visual summary of some limiting and special cases of the RNM models and their interrelationships. Greater flexibility for fitting observed option prices can be obtained as we introduce additional parameters and move up the RNM distributional tree. The computation involved in estimating additional parameters can generally be accommodated by recent advances in computational capability and numerical procedures. However, it is necessary to test whether the extra computations significantly improve the fitting performance. The hypothesis that there are no additional improvements involving nested distributions can be tested by using likelihood ratio (LR) tests based on asymptotic chi-square distributions as in Vuong (1989).

3.4 Estimation of the Parametric RNM

Since the OTM options are generally more liquid than the in-the-money (ITM) options, we estimate the RNM parameter vector $\boldsymbol{\theta}$ from each cross-section of the OTM option prices with the different strike prices K_i and the same time to maturity T. The theoretical OTM option prices are defined as in (3.10):

$$V(K_i;\boldsymbol{\theta}) = \begin{cases} P(K_i;\boldsymbol{\theta}) & \text{for } K < F, \quad i = 1,\ldots,N \\ \\ C(K_i;\boldsymbol{\theta}) & \text{for } K \geq F, \end{cases}$$

where

$$\begin{aligned} C(K_i;\boldsymbol{\theta}) &= e^{r_f T}\int_{K_i}^{\infty}(x-K_i)\,\mathrm{r}(x;\boldsymbol{\theta})dx, \quad \text{and} \\ P(K_i;\boldsymbol{\theta}) &= e^{r_f T}\int_{0}^{K_i}(K_i-x)\,\mathrm{r}(x;\boldsymbol{\theta})dx, \end{aligned}$$

and $\boldsymbol{\theta}$ is the RNM parameter vector.

The put price function $P(K;\boldsymbol{\theta})$ is monotone increasing, the call price function $C(K;\boldsymbol{\theta})$ is monotone decreasing, and $P(F;\boldsymbol{\theta}) = C(F;\boldsymbol{\theta})$ for any RNM by put-call parity, so that OTM option prices can be defined alternatively as:

$$V(K_i;\boldsymbol{\theta}) = \min\left[C(K_i;\boldsymbol{\theta}), P(K_i,\boldsymbol{\theta})\right], \quad i = 1,\ldots,N.$$

For each cross-section of options with the same time to maturity T, parametric option pricing models may be expressed as a non-linear regression with unknown RNM parameters:

$$V_i = V(K_i;\boldsymbol{\theta}) + \epsilon_i, \quad i = 1,\ldots,N, \tag{3.19}$$

where V_i is the OTM option market price associated with the strike price K_i, ϵ_i is the pricing error associated with the OTM option whose strike price is K_i. Consequently, we can apply non-linear regression techniques to the model (3.19) for estimating the vector of RNM pa-

rameters $\boldsymbol{\theta}$. The RNM parameters may be estimated by using a nonlinear generalized least squares (NL-GLS) methodology developed by Engle and Mustafa (1992) to take into account the heteroskedasticity of the OTM prices across strike prices. However, it is difficult to estimate the structure of the heteroskedasticity with small cross-section sample data. Therefore, the vector of RNM parameters has been estimated by the nonlinear ordinary least squares (NL-OLS) in many researches—Bakshi, Cao, and Chen (1997), Bondarenko (2003), Carr and Wu (2003), Tunaru and Albota (2005), and Bu and Hadri (2007):[19]

$$\begin{aligned} \min_{\boldsymbol{\theta}\in\boldsymbol{\Theta}} \quad L(SSE) &= \sum_{i=1}^{N} (V_i - V(K_i;\boldsymbol{\theta}))^2 \\ &= \epsilon^\top \epsilon, \end{aligned}$$

where ϵ is the vector of pricing errors.

Under the assumption that the pricing errors are i.i.d. normally distributed with variance σ^2, the NL-OLS estimates are equivalent to maximum likelihood estimates (MLE):

$$\begin{aligned} \max_{\boldsymbol{\theta}\in\boldsymbol{\Theta}} \quad \mathcal{L}(\epsilon;\boldsymbol{\theta}) &= \sum_{i=1}^{N} \log f(\epsilon_i;\boldsymbol{\theta}) \\ &= -\frac{N}{2}\left[1 + \log(2\pi) + \log\left(\frac{\epsilon^\top\epsilon}{N}\right)\right], \end{aligned}$$

where f is the normal density ($=\frac{1}{\sqrt{2\pi}\sigma} e^{-\epsilon_i^2/2\sigma^2}$) and the maximum likelihood estimate for σ^2 is the mean squared pricing error, mse $= \epsilon^\top\epsilon/N$.

[19]The NL-OLS criterion with the bid-ask average prices does not fully exploit the information contained in the bid and ask price quotes because it can not utilize the bid-ask price range. McCulloch and Lee (2008) modified the NL-OLS criterion by setting the loss function which increases only when the theoretical prices fall outside of the bid-ask price range. Also this modified NL-OLS criterion contains an arbitrary small OLS term to guarantee a unique solution:

$$\min_{\boldsymbol{\theta}\in\boldsymbol{\Theta}} \quad L = \sum_{i=1}^{N} \left[\left(V_i^B - V_i(\boldsymbol{\theta})\right)_+^2 \left(V_i(\boldsymbol{\theta}) - V_i^A\right)_+^2 + \lambda \left(V_i - V(_i(\boldsymbol{\theta}))^2 \right],$$

where V_i^B and V_i^A are bid and ask OTM option price quotes respectively, λ is an arbitrary small number, and $X_+ = \max(0, X)$. However, in this paper we use the simple NL-OLS criterion since the modified NL-OLS criterion can not be applied to the model specification tests such as a likelihood ratio test.

3.5 Empirical Results

3.5.1 Data

We have estimated the parametric risk-neutral density using the cross-section data on the S&P 500 index options traded at the Chicago Board of Options Exchange (CBOE). The transaction prices are recorded with substantial measurement errors due to non-synchronous trading so that we use daily closing bid and ask price quotes. We have obtained 100 sets of cross-section data on the S&P 500 index options which are transacted with 2 months to maturity in 2006. We have filtered the data using the arbitrage violation conditions since the existence of arbitrage possibilities can lead to negative risk-neutral probabilities. By checking the monotonicity and convexity of the option pricing functions, we may eliminate option prices which violate the arbitrage-free condition. After eliminating the violated data, we have 8,468 option price quotes.

3.5.2 Goodness of Fit

The goodness-of-fit of the parametric RNM estimation methods are compared by examining the pricing errors associated with each model on the basis of the Root Mean Squared Errors (RMSE):

$$\text{RMSE} \quad = \quad \left(\frac{1}{N} \sum_{i=1}^{N} (V_i - V(K_i; \boldsymbol{\theta}))^2 \right)^{1/2}.$$

To take the number of free parameters into account, we may also compare the adjusted RMSE:

$$\text{Adj. RMSE} \quad = \quad \left(\frac{1}{N-k} \sum_{i=1}^{N} (V_i - V(K_i; \boldsymbol{\theta}))^2 \right)^{1/2}.$$

Table 3.1 reports the RMSE and the adjusted RMSE for each model. Among the 12 alternative parametric models, the JS model shows the smallest RMSE. The JS model seems

to perform slightly better than the GS model, but the JS model has so many free-parameters that it may suffer from over-fitting problems in the RNM estimation. The over-fitting problems may be detected by Monte-Carlo experiments.

3.5.3 Likelihood Ratio Test

Using the Kullback-Leibler Information Criterion (KLIC), Vuong (1989) proposed simple likelihood-ratio tests for the model selection among the competing models, which are non-nested or nested. We assume that the pricing errors are i.i.d normally distributed with variance σ^2 as in Carr and Wu (2003). Under such assumptions, minimizing the sum of squared pricing errors is equivalent to maximizing the log likelihood function. The NL-OLS estimates can therefore be regarded as maximum likelihood estimates.

Consider two competing models **F** and **G** whose log density function are given by, respectively:

$$\begin{aligned} \log f(e_{\theta i};\boldsymbol{\theta}) &= -\frac{1}{2}\log\left(2\pi\sigma_f^2\right) - \frac{e_{\theta i}^2}{2\sigma_f^2} \quad \text{and} \\ \log g(e_{\gamma i};\boldsymbol{\gamma}) &= -\frac{1}{2}\log\left(2\pi\sigma_g^2\right) - \frac{e_{\gamma i}^2}{2\sigma_g^2}, \end{aligned}$$

where $e_{\theta i}$ and $e_{\gamma i}$ denote the pricing error on the ith option under the model **F** and **G**, respectively, and $\boldsymbol{\theta}$ and $\boldsymbol{\gamma}$ are the parameter vectors of **F** and **G**, respectively. Since the maximum likelihood estimate for σ^2 is simply the mean squared pricing error: mse $= \mathbf{e}^\top\mathbf{e}/N$, the log likelihood functions are given by, respectively:

$$\begin{aligned} \mathcal{L}_f(\mathbf{e}_\theta;\boldsymbol{\theta}) &= \sum_{i=1}^{N}\log f(e_{\theta i};\boldsymbol{\theta}) = -\frac{N}{2}\left[1+\log(2\pi)+\log\left(\frac{\mathbf{e}_\theta^\top\mathbf{e}_\theta}{N}\right)\right] \quad \text{and} \\ \mathcal{L}_g(\mathbf{e}_\gamma;\boldsymbol{\gamma}) &= \sum_{i=1}^{N}\log g(e_{\gamma i};\boldsymbol{\gamma}) = -\frac{N}{2}\left[1+\log(2\pi)+\log\left(\frac{\mathbf{e}_\gamma^\top\mathbf{e}_\gamma}{N}\right)\right], \end{aligned}$$

where $\mathbf{e}_\theta$ and $\mathbf{e}_\gamma$ are the pricing error vectors for each model. Furthermore, the likelihood

ratio between the two models (**F** and **G**) is given by:

$$\begin{aligned} LR\left(\hat{\boldsymbol{\theta}}, \hat{\boldsymbol{\gamma}}\right) &= \mathcal{L}_f(\hat{\mathbf{e}}_\theta; \hat{\boldsymbol{\theta}}) - \mathcal{L}_g(\hat{\mathbf{e}}_\gamma; \hat{\boldsymbol{\gamma}}) \\ &= -\frac{N}{2}\left[\log\left(\frac{\hat{\mathbf{e}}_\theta^\top \hat{\mathbf{e}}_\theta}{N}\right) - \log\left(\frac{\hat{\mathbf{e}}_\gamma^\top \hat{\mathbf{e}}_\gamma}{N}\right)\right] \\ &= -\frac{N}{2}\left[\log\left(\frac{\hat{\mathbf{e}}_\theta^\top \hat{\mathbf{e}}_\theta}{\hat{\mathbf{e}}_\gamma^\top \hat{\mathbf{e}}_\gamma}\right)\right]. \end{aligned}$$

Using the likelihood ratio, we can conduct a test on the model selection between alternative models which are nested or non-nested. We set the hypotheses by letting model **F** be the GS model and letting model **G** be the 11 alternative models: BS, WB, FS, DN, DL, GG, GB, OS, VG, JD, and JS.

a. Test for Non-nested Models

Given the competing non-nested models **F** and **G**, the Vuong's likelihood ratio test selects the model that is closest to the true model. Based on the KLIC, we consider the following hypotheses and definitions:

$$\begin{aligned} H_0 &: E\left[\log \frac{f(e_{\theta i}; \boldsymbol{\theta})}{g(e_{\gamma i}; \boldsymbol{\gamma})}\right] = 0 : \mathbf{F} \text{ and } \mathbf{G} \text{ are equivalent} \\ H_f &: E\left[\log \frac{f(e_{\theta i}; \boldsymbol{\theta})}{g(e_{\gamma i}; \boldsymbol{\gamma})}\right] > 0 : \mathbf{F} \text{ is better than } \mathbf{G} \\ H_g &: E\left[\log \frac{f(e_{\theta i}; \boldsymbol{\theta})}{g(e_{\gamma i}; \boldsymbol{\gamma})}\right] < 0 : \mathbf{F} \text{ is worse than } \mathbf{G}. \end{aligned}$$

The test statistic for non-nested model selection can be constructed based on the likelihood ratio:

$$\hat{\ell} = N^{-1/2} LR(\hat{\boldsymbol{\theta}}, \hat{\boldsymbol{\gamma}})/\hat{\omega},$$

where $\hat{\omega}$ is the variance estimate of $(\log f - \log g)$:

$$\hat{\omega}^2 = \frac{1}{N}\sum_{i=1}^{N}\left[\log \frac{f(\hat{e}_\theta; \hat{\boldsymbol{\theta}})}{g(\hat{e}_\gamma; \hat{\boldsymbol{\gamma}})}\right]^2 - \left[\frac{1}{N}\sum_{i=1}^{N} \log \frac{f(\hat{e}_\theta; \hat{\boldsymbol{\theta}})}{g(\hat{e}_\gamma; \hat{\boldsymbol{\gamma}})}\right]^2$$

with

$$\log \frac{f(\hat{e}_{\theta i}; \hat{\boldsymbol{\theta}})}{g(\hat{e}_{\gamma i}; \hat{\boldsymbol{\gamma}})} = -\frac{1}{2} \log \left(\frac{\hat{\mathbf{e}}_{\theta}^{\top} \hat{\mathbf{e}}_{\theta}}{\hat{\mathbf{e}}_{\gamma}^{\top} \hat{\mathbf{e}}_{\gamma}} \right) - N \left[\frac{\hat{e}_{\theta i}^2}{2 \hat{\mathbf{e}}_{\theta}^{\top} \hat{\mathbf{e}}_{\theta}} - \frac{\hat{e}_{\gamma i}^2}{2 \hat{\mathbf{e}}_{\gamma}^{\top} \hat{\mathbf{e}}_{\gamma}} \right].$$

If **F** and **G** are non-nested and $f(e_{\theta i}; \boldsymbol{\theta}) \neq g(e_{\gamma i}; \boldsymbol{\gamma})$, then

$$\begin{aligned} \text{under } H_0 &: \hat{\ell} \xrightarrow{D} N(0,1), \\ \text{under } H_f &: \hat{\ell} \xrightarrow{a.s} +\infty, \\ \text{under } H_g &: \hat{\ell} \xrightarrow{a.s} -\infty. \end{aligned}$$

The likelihood ratio *LR* can be adjusted for differences in number of free parameters in each model:

$$LR_A = LR - (p - q), \quad or \quad LR_S = LR - \frac{1}{2}(p - q) \log N,$$

where p and q are the number of parameters in models **F** and **G**, respectively. These adjustments correspond to Akaike (1973) and Schwarz (1978) information criteria, respectively, and the resulting statistics $\hat{\ell}_A$ and $\hat{\ell}_S$ have the same asymptotic properties as $\hat{\ell}$ since both $N^{-1/2}(p - q)$ and $N^{-1/2} \frac{1}{2}(p - q) \log N$ are $o_p(1)$.

As depicted in Figure 3.1, the GS model does not nest the WB, VG, DN, DS, GG, GB, JD, and JS models, so the LR test for non-nested models can be applied to the model selection between the GS model and other non-nested models. We compute the the statistics $\hat{\ell}$, $\hat{\ell}_A$, and $\hat{\ell}_S$ by letting model **F** be the GS model and letting model **G** be the WB, VG, DN, DS, GG, GB, JD, and JS models, which are reported in Table 3.2. Similarly to the RMSE criterion, the model selection tests show that the GS model significantly outperforms other non-nested models except for the JS model. The three LR test statistics between the GS model and JS model indicate that neither model significantly outperforms the other.

b. Test for Nested Models

If the model **G** is nested in the model **F**, any conditional density $g(\cdot;\gamma)$ is also a conditional density $f(\cdot;\boldsymbol{\theta})$ for some $\boldsymbol{\theta}$ in $\boldsymbol{\Theta}$. The null hypothesis in the nested model selection is the same as H_0 in the non-nested model selection. However, the alternative hypothesis H_A is H_f since H_g can never occur becasue **G** can never be better than **F**:

$$\begin{aligned} H_0 &: E\left[\log \frac{f(e_{\theta i};\boldsymbol{\theta})}{g(e_{\gamma i};\boldsymbol{\gamma})}\right] = 0 : \mathbf{F} \text{ and } \mathbf{G} \text{ are equivalent} \\ H_A &: E\left[\log \frac{f(e_{\theta i};\boldsymbol{\theta})}{g(e_{\gamma i};\boldsymbol{\gamma})}\right] > 0 : \mathbf{F} \text{ is better than } \mathbf{G}. \end{aligned}$$

If **G** is nested in **F** and **F** is correctly specified, then

$$\begin{aligned} \text{under } H_0^\theta &: 2LR(\hat{\boldsymbol{\theta}},\hat{\boldsymbol{\gamma}}) \xrightarrow{D} \chi^2_{p-q}, \\ \text{under } H_A^\theta &: 2LR(\hat{\boldsymbol{\theta}},\hat{\boldsymbol{\gamma}}) \xrightarrow{a.s.} +\infty. \end{aligned}$$

As illustrated in Figure 3.1, the three stable type models (BS, FS, and OS) are nested in the GS model. The LR test statistics P-values between the GS model and other nested models are reported in Table 3.3. The test results indicate that the GS model is significantly better the BS, FS, and OS models.

3.5.4 Monte-Carlo Experiments

We perform Monte-Carlo experiments to compare the capability to recover the simulated actual RNM and to detect the over-fitting problem due to a large number of parameters. The accuracy and stability of RNM estimators can be also measured by means of the Monte-Carlo experiment under the root mean integrated squared errors (RMISE) criterion as in Bondarenko (2003). If $\hat{\mathrm{r}}(x)$ is an estimator of risk neutral density $\mathrm{r}(x)$, then the

(normalized) RMISE for the density estimator is defined as:[20]

$$\begin{aligned}\text{RMISE}(\hat{\text{r}}) &= \frac{1}{||\text{r}(x)||}\left(E[||\hat{\text{r}}(x)-\text{r}(x)||^2]\right)^{1/2} \\ &= \frac{1}{||\text{r}(x)||}\left(E\left[\int_0^\infty (\hat{\text{r}}(x)-\text{r}(x))^2\,\text{d}x\right]\right)^{1/2}.\end{aligned}$$

Similarly to the MSE for the point estimator, the RMISE may be decomposed as:

$$\text{RMISE}^2(\hat{\text{r}}) = \text{RISB}^2(\hat{\text{r}}) + \text{RIV}^2(\hat{\text{r}}),$$

where

$$\begin{aligned}\text{RISB}(\hat{r}) &= \frac{1}{||\text{r}(x)||}\left(\int_0^\infty (E[\hat{\text{r}}(x)]-\text{r}(x))^2\,\text{d}x\right)^{1/2}, \\ \text{RIV}(\hat{r}) &= \frac{1}{||\text{r}(x)||}\left(\int_0^\infty E\left[(\hat{\text{r}}(x)-E[\hat{\text{r}}(x)])^2\right]\text{d}x\right)^{1/2},\end{aligned}$$

$||\cdot||$ is the L_2 norm, RISB is the (normalized) root integrated squared bias, and RIV is the (normalized) root integrated variance. Intuitively, RMISE is a measure of the overall quality of the estimator, RISB is a measure of the accuracy, and RIV is a measure of the stability. This decomposition allows us to study the relative contributions of the bias (RISB) and variability (RIV) to RMISE of different models.[21]

[20] In view of Fubini's Theorem, RMISE is the same as RIMSE. If the expectation integration can be interchanged with the outer integration, then the root integrated mean squared error:

$$\begin{aligned}\text{RIMSE}[\hat{\text{r}}] &= \frac{1}{||\text{r}(x)||}\left(\int_0^\infty E\left[(\hat{\text{r}}(x)-\text{r}(x))^2\,\text{d}x\right]\right)^{1/2} \\ &= \frac{1}{||\text{r}(x)||}\left(E\left[\int_0^\infty (\hat{r}(x)-\text{r}(x))^2\,\text{d}x\right]\right)^{1/2} \\ &= \text{RMISE}[\hat{\text{r}}(x)]\end{aligned}$$

is nothing but the root mean integrated squared error.

[21] Alternatively, we can apply some of the most useful distance measures include: (i) The L_1 norm or the Integrated Absolute Error (IAE): $\text{IAE}[\hat{f}] = \int_0^\infty |\hat{r}(x)-\text{r}(x)|\text{d}x$; (ii) the L_2 norm or the Integrated Squared Error (ISE): $\text{ISE}[\hat{r}] = \int_0^\infty (\hat{r}(x)-\text{r}(x))^2\,\text{d}x$; (iii) The L_∞ norm or Sup Absolute Error (SAE): $\text{SAE}[\hat{r}] = \sup_{x\in[0,\infty]}|\hat{r}(x)-\text{r}(x)|$; (iv) the Kullback-Leibler measure (KL): $\text{KL}[\hat{r}] = \int_0^\infty \text{r}(x)\log\left(\frac{\text{r}(x)}{\hat{r}(x)}\right)\text{d}x$; and (v) the Hellinger distance (H): $\text{H}[\hat{r}] = \left(\int_0^\infty \left(\hat{r}^{1/p}(x)-r^{1/p}(x)\right)^p\,\text{d}x\right)^{1/p}$.

Monte-Carlo experiments are conducted based on the following 12 scenarios:

Scenario i: i model is true RNM model,

where i=BS, WB, FS, DN, DS, GG, GB, OS, GS, VG, JD, and JS. For each scenario, we calibrate the actual RNM based on assumed true parametric RNM estimation method using the closing prices on April 17, 2006 of the S&P 500 options with the maturity date on Jun 17, 2006. The resulting actual RNM density r(x) for each scenario is depicted as a dotted line in Figure 3.2 through 3.13, respectively. To generate 200 simulated cross-sections of OTM option prices V_i for each scenario, the theoretical prices computed from the actual r(x) are perturbed independently by random noises uniformly distributed on the maximum bid-ask range permitted by the CBOE. For each simulated cross-section, the RNM density is estimated with the 12 different parametric estimation methods. The estimated RNMs with the 12 parametric models for each scenario are depicted in Figure 3.2 through 3.13 and the associated RMISE statistics are also reported in Table 3.5 through 3.16. Under the scenarios that fat-tailed distributions–such as FS, OS, and GS models are true RNMs, the estimated JS RNMs reveal the over-fitting problems, which create spurious oscillations due to sampling noise. The over-fitting problem of the JS model can be found in Figure 3.3, 3.4, 3.7, 3.9, 3.10, and 3.13. Panel A of Table 3.4 reports the average RMISE statistics for all scenarios. Since the RMISE tend to be small under the scenario that the nested model is true RNM model, we also compute the average RMISE of the scenarios for non-nested models, which reported in Panel B of Table 3.4. Panel A of Table 3.4 indicates that the GS model outperforms other alternative models on the basis of RMISE criterion. Further, Panel B of Table 3.4 implies that even if our comparison is restricted to the non-nested models, the GS model shows the best performance among alternative models.

3.6 Concluding Remarks

The risk-neutral measure of the future asset prices can be estimated from the currently observed cross-section of option prices with the same time-to-maturity. The estimated RNM of the asset prices provides valuable information about the market's expectations on the future movement of asset prices.

We have implemented 12 parametric RNM estimation methods by means of the closed form of RNM distributions or RNM characteristic functions. We then compared the empirical performance of the 12 parametric RNM estimation methods under three criteria—the root mean squared error (RMSE) for the goodness-of-fit, likelihood ratio (LR) for the model selection, and the root mean integrated squared error (RMISE) for the accuracy and stability of the estimated RNMs.

The empirical results show that the two-factor generalized log-stable model outperforms other alternative parametric RNM estimation methods. The RMSEs and the LR tests indicate that the two-factor generalized log-stable model and the jump diffusion model with stochastic volatilities dominates other models. However, the jump diffusion model with stochastic volatilities is vulnerable to over-fitting problems due to a large number of parameters. Our Monte-Carlo experiments reveal that the jump diffusion model with stochastic volatilities suffers from the serious over-fitting problems and also show that the generalized two-factor log-stable model outperforms the alternatives.

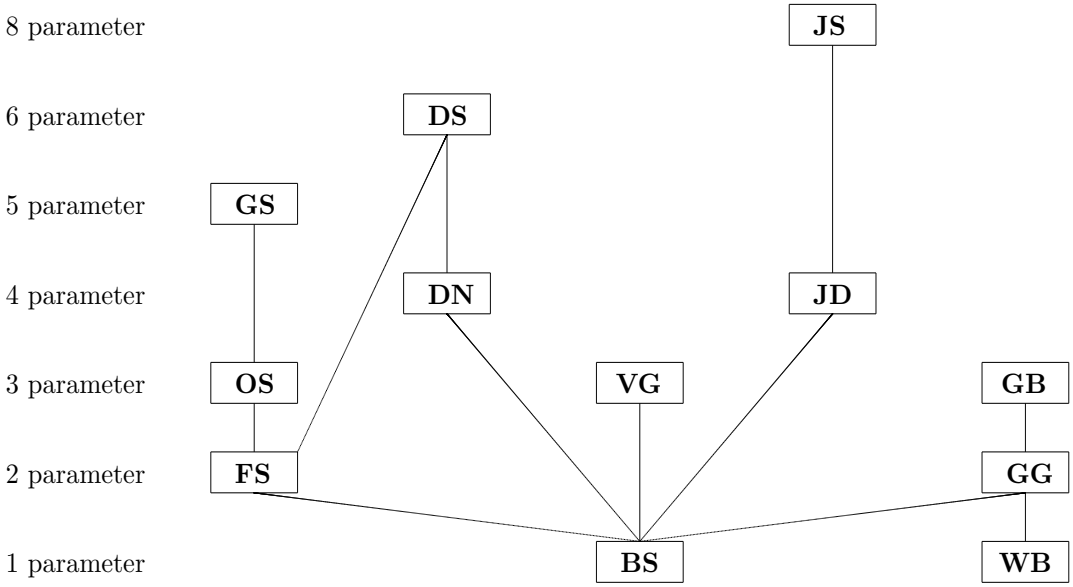

Figure 3.1: RNM Distribution Tree.

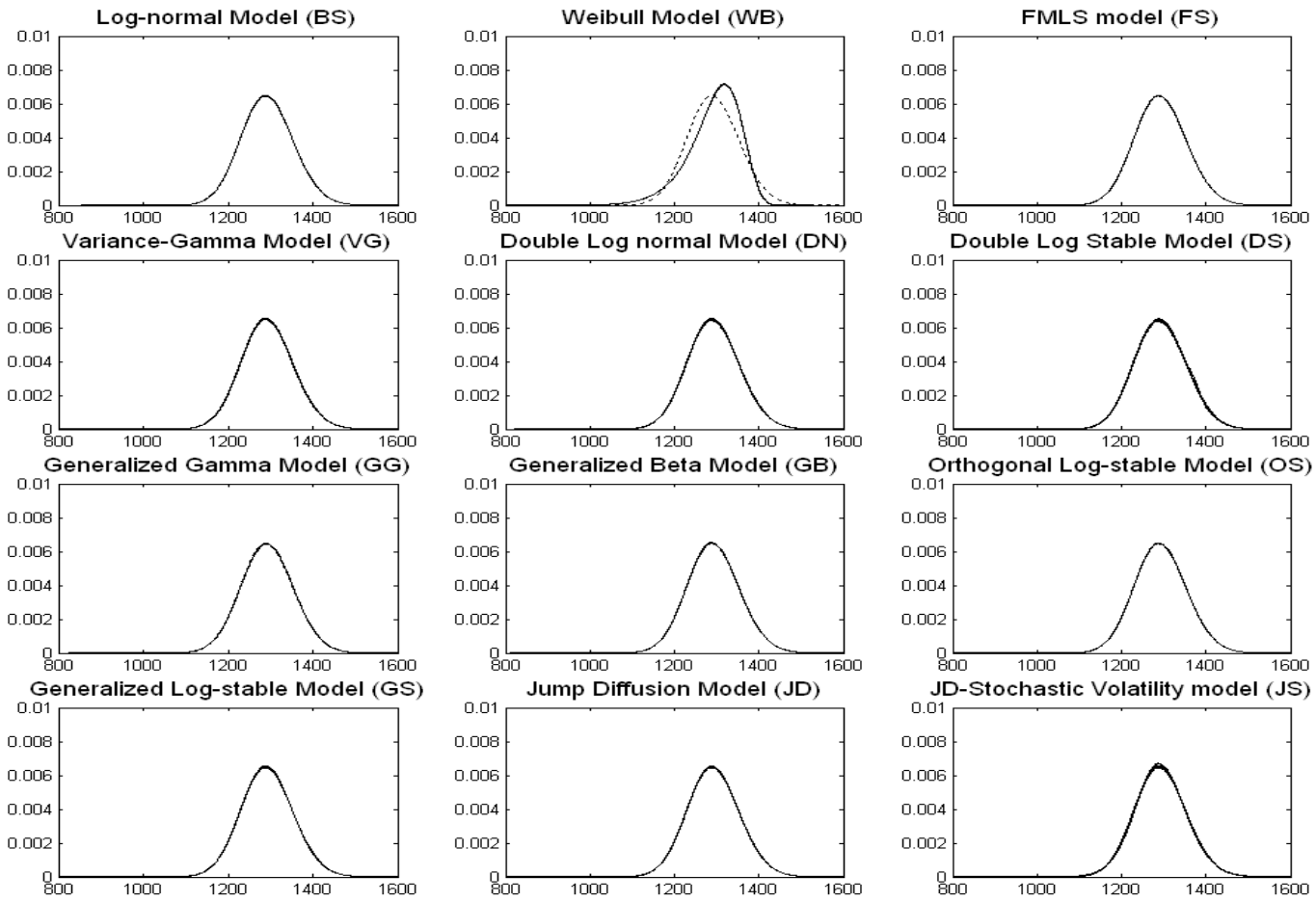

Figure 3.2: Monte-Carlo Simulation Results under the Scenario that the True RNM (dotted line) is the Black Scholes Log-Normal (BS) Model

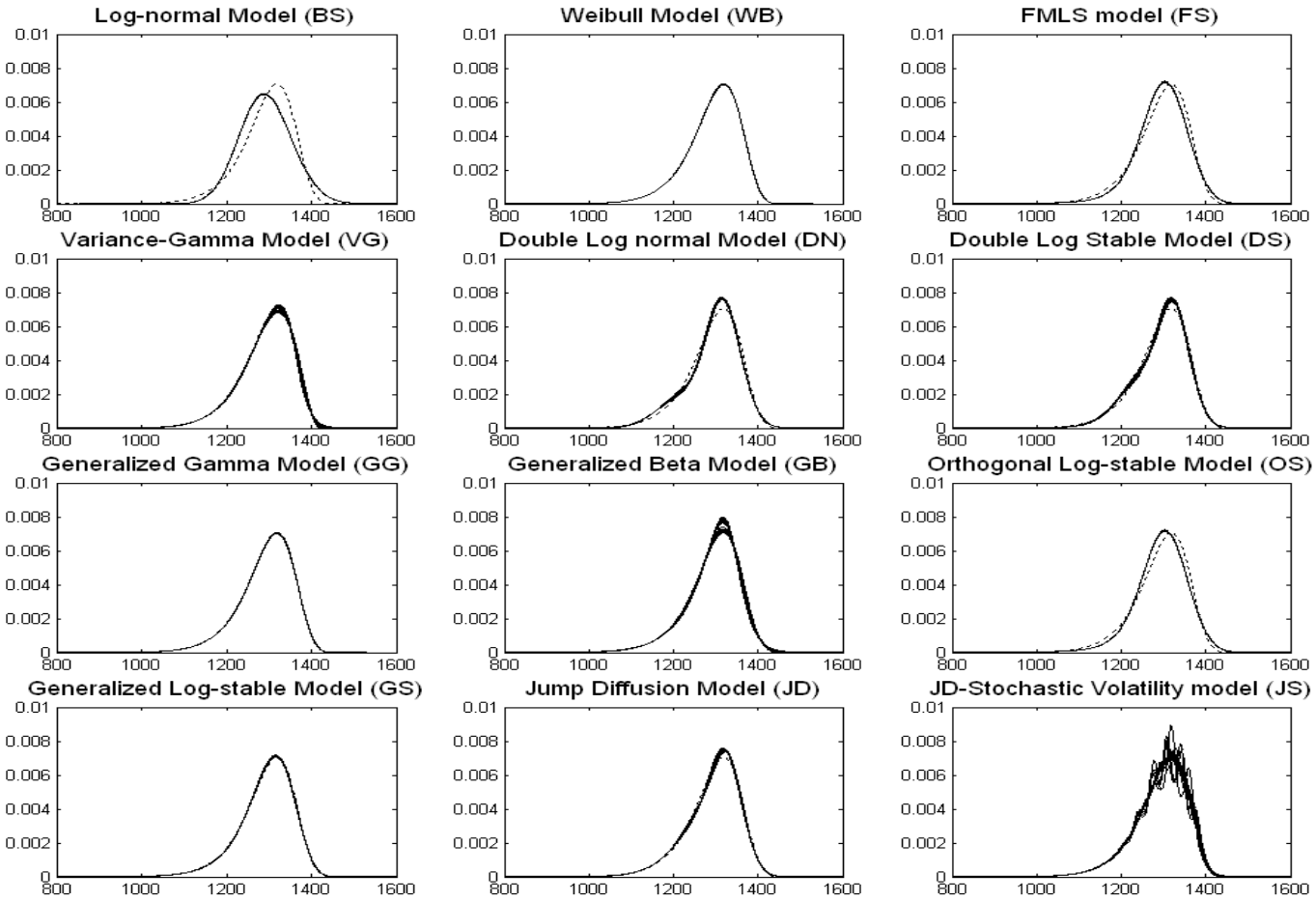

Figure 3.3: Monte-Carlo Simulation Results under the Scenario that the True RNM (dotted line) is the Weibull (WB) Model

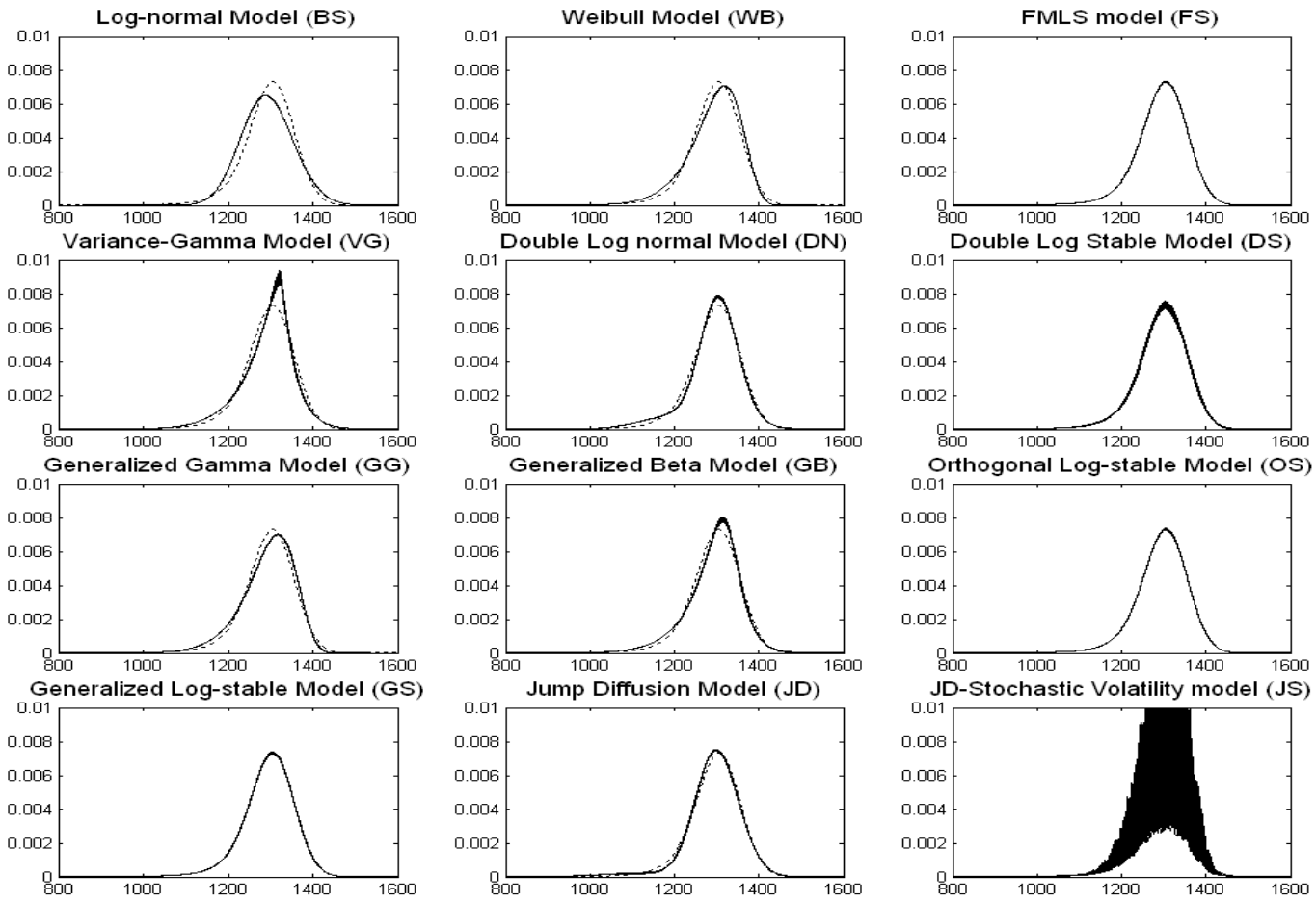

Figure 3.4: Monte-Carlo Simulation Results under the Scenario that the True RNM (dotted line) is the Finite Moment Log-Stable (FS) Model

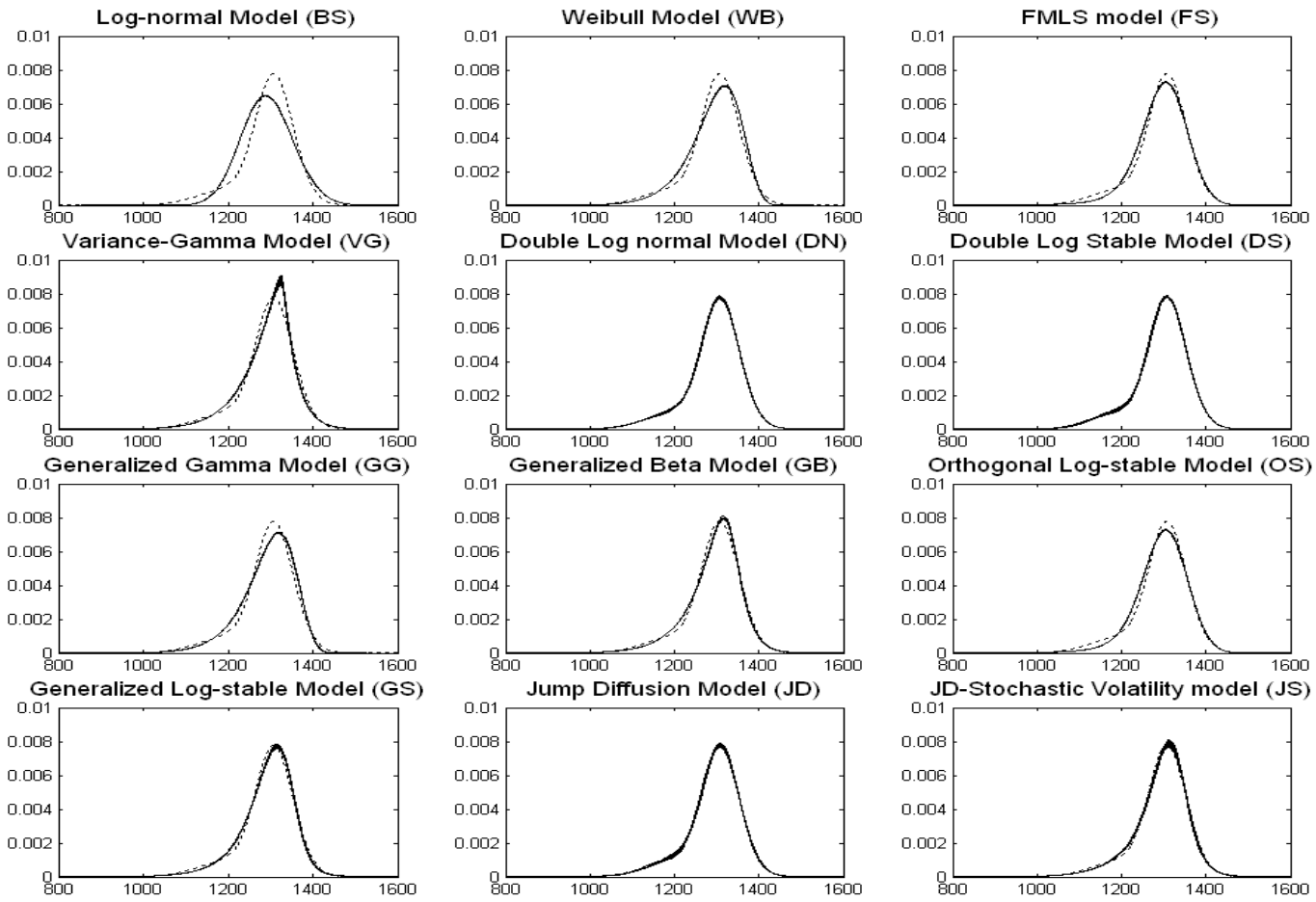

Figure 3.5: Monte-Carlo Simulation Results under the Scenario that the True RNM (dotted line) is the Mixture of Log-Normal (DN) Model

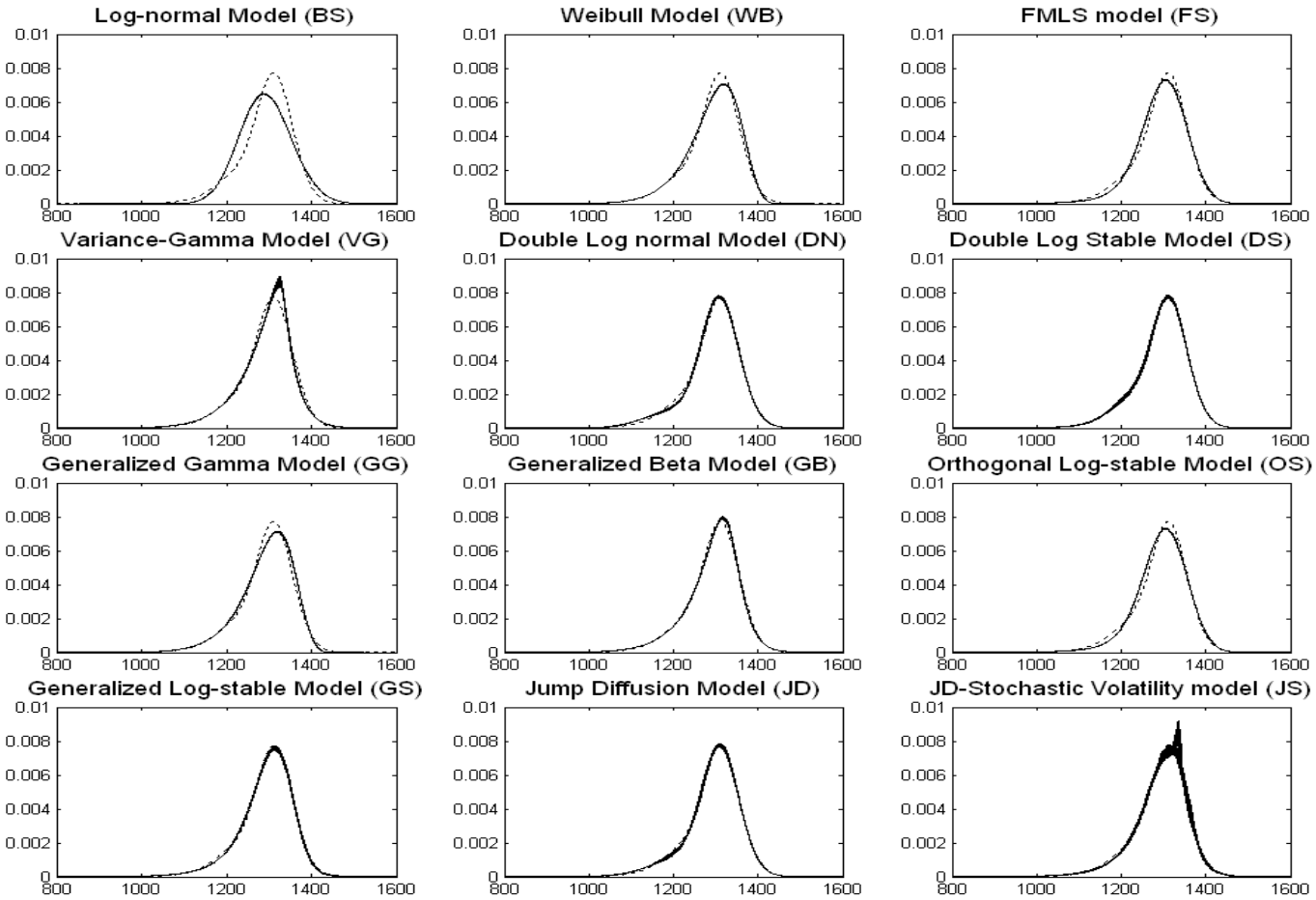

Figure 3.6: Monte-Carlo Simulation Results under the Scenario that the True RNM (dotted line) is the Mixture of Log-Stable (DS) Model

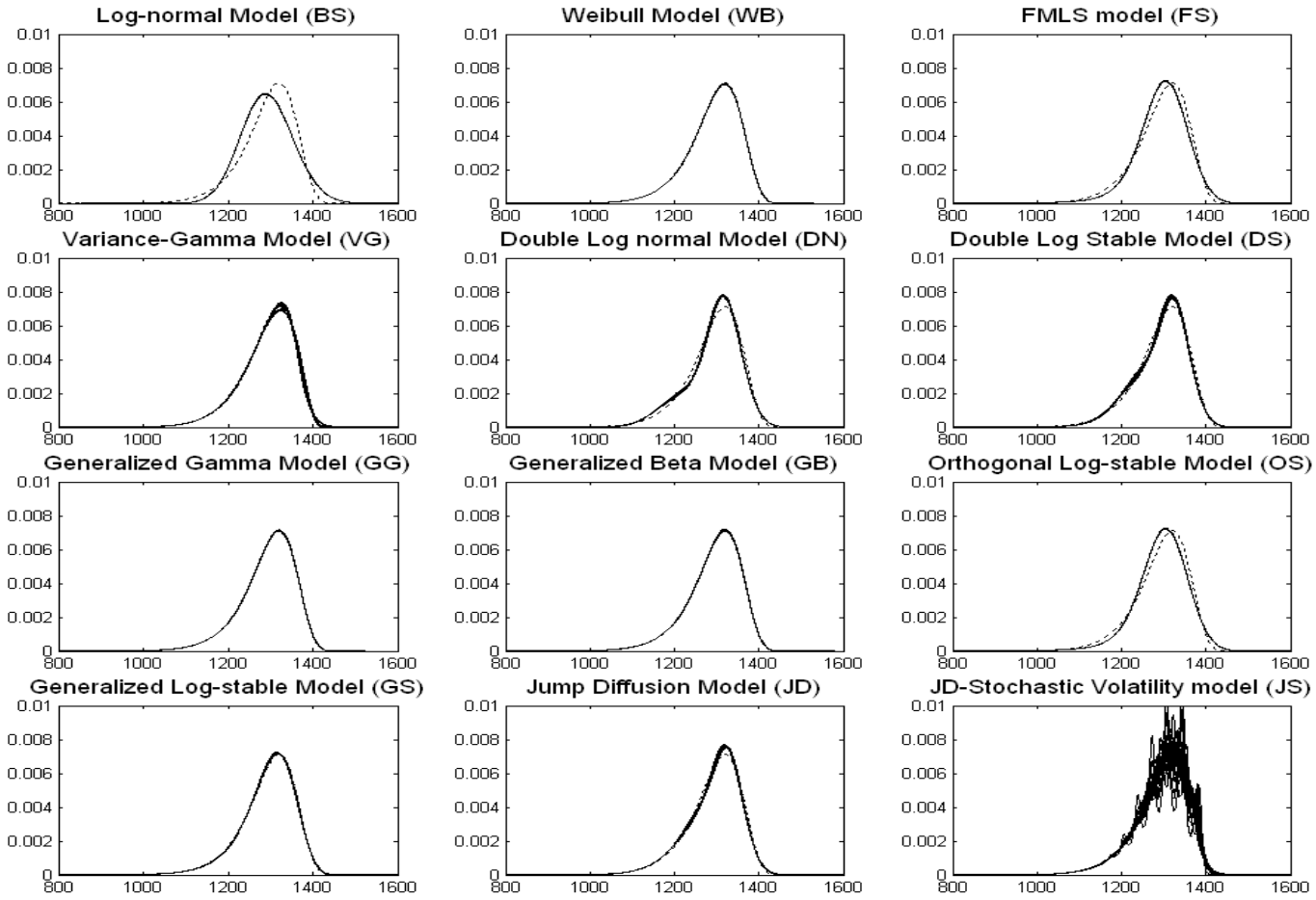

Figure 3.7: Monte-Carlo Simulation Results under the Scenario that the True RNM (dotted line) is the Generalized Gamma (GG) Model

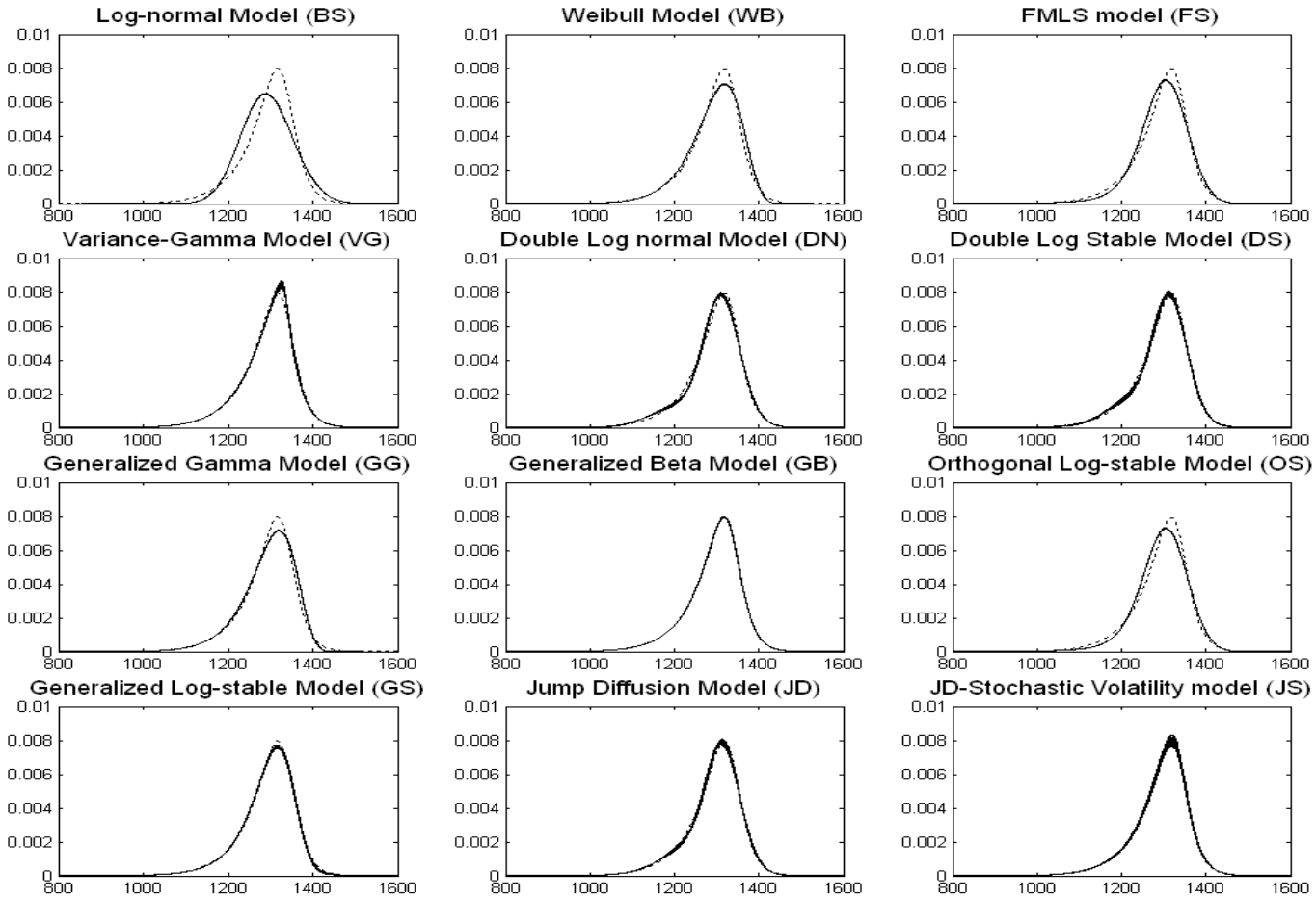

Figure 3.8: Monte-Carlo Simulation Results under the Scenario that the True RNM (dotted line) is the Generalized Beta (GB) Model

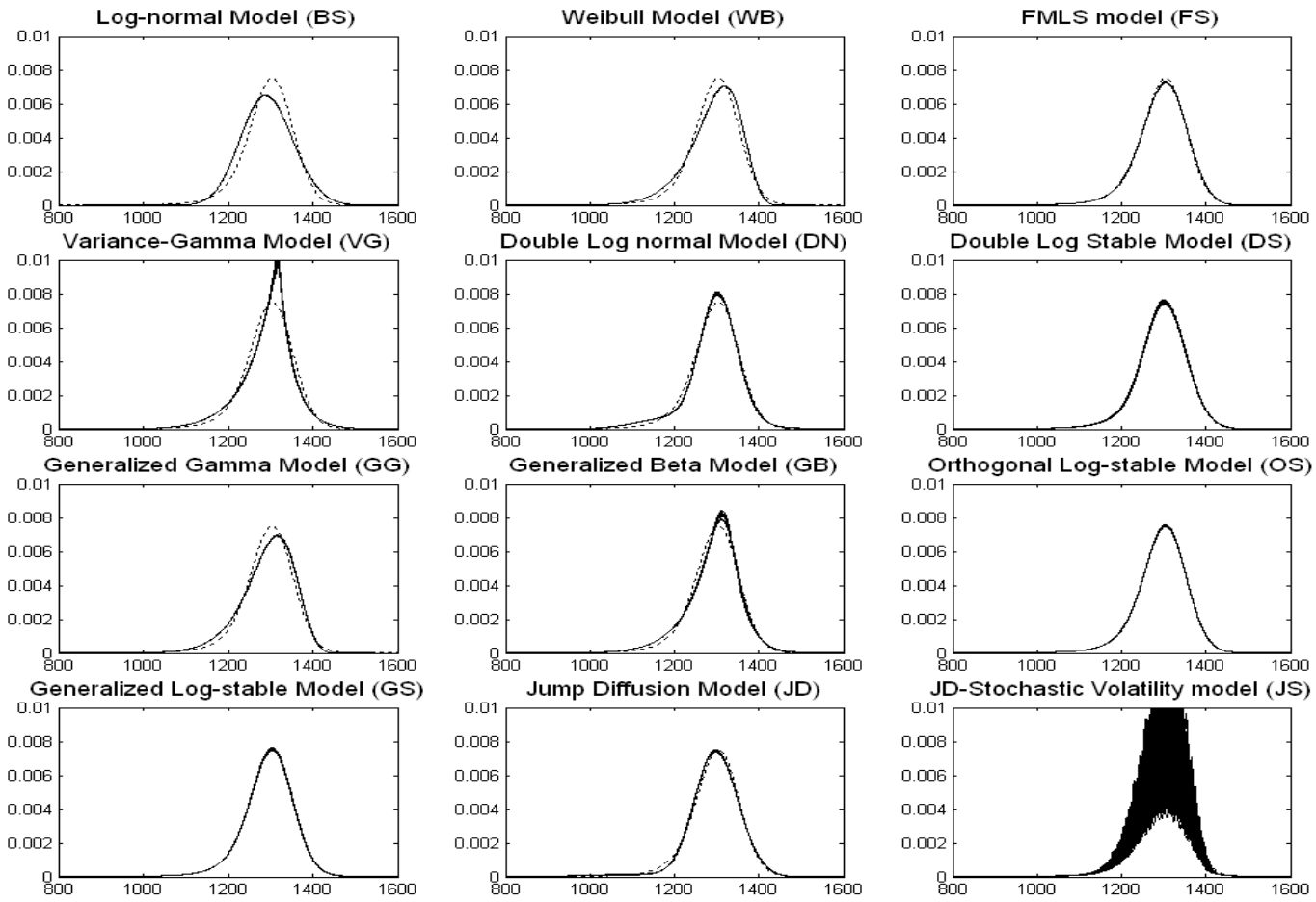

Figure 3.9: Monte-Carlo Simulation Results under the Scenario that the True RNM (dotted line) is the Orthogonal Log-Stable (OS) Model

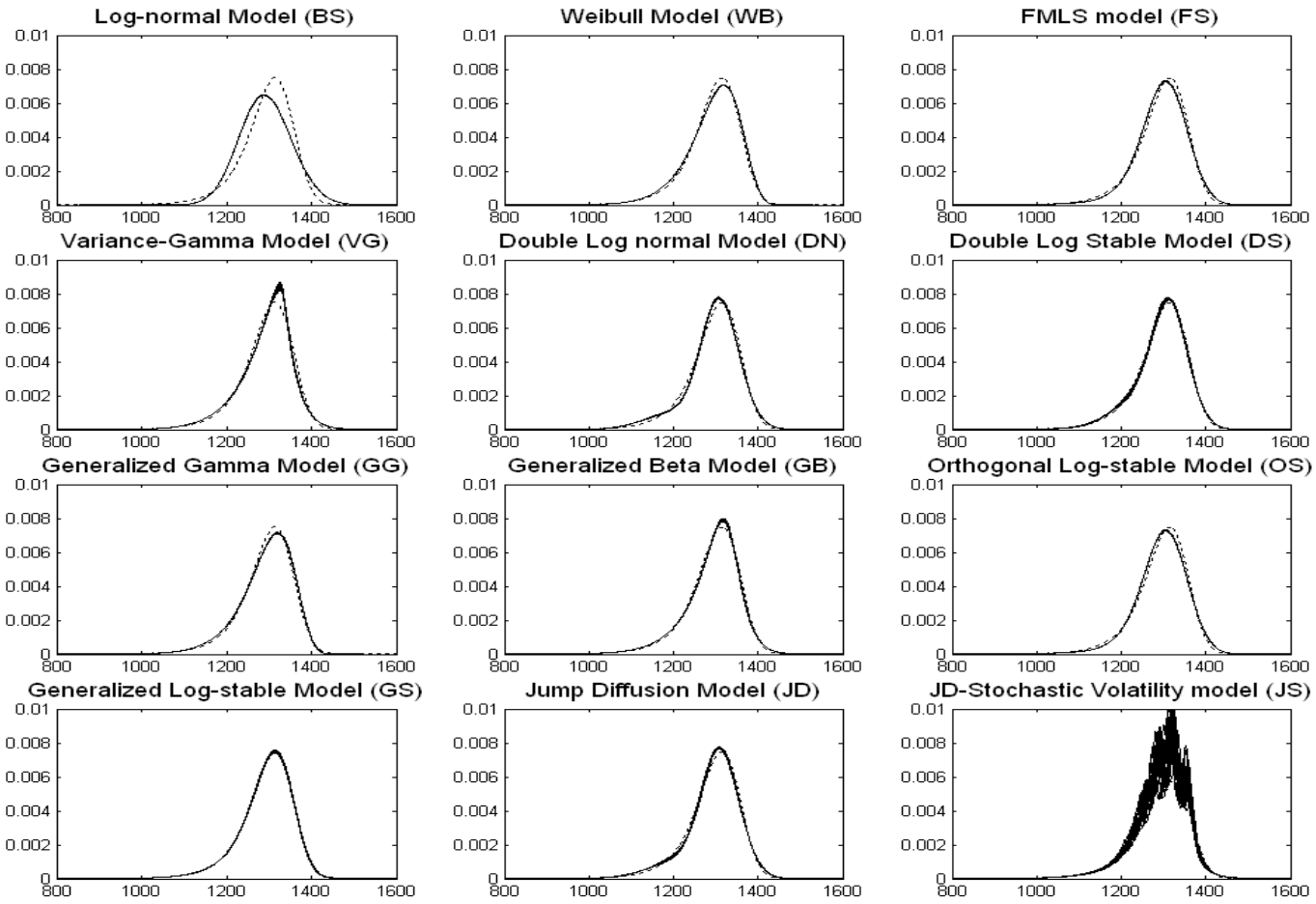

Figure 3.10: Monte-Carlo Simulation Results under the Scenario that the True RNM (dotted line) is the Two-Factor Generalized Log-Stable (GS) Model

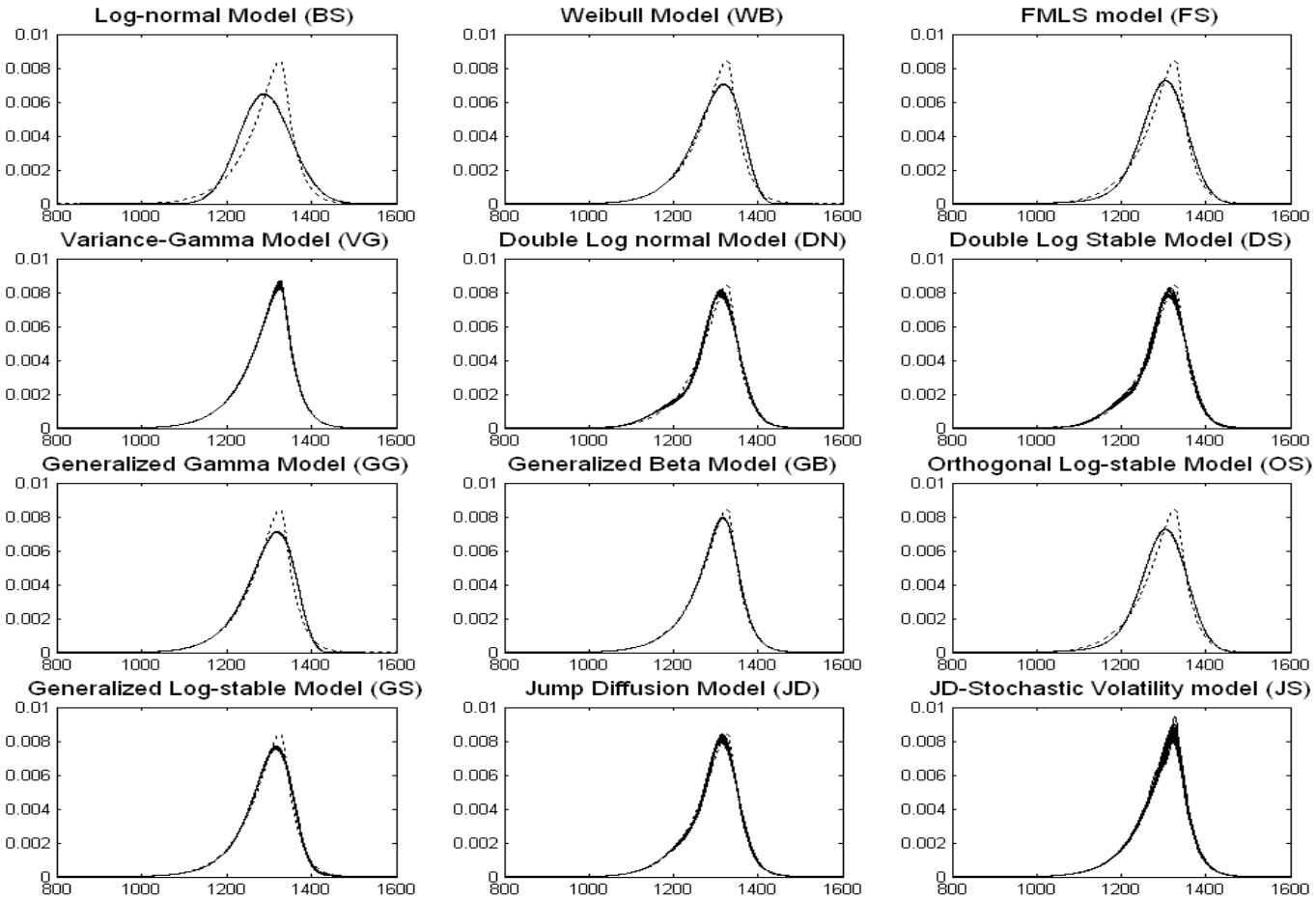

Figure 3.11: Monte-Carlo Simulation Results under the Scenario that the True RNM (dotted line) is the Variance-Gamma (VG) Model

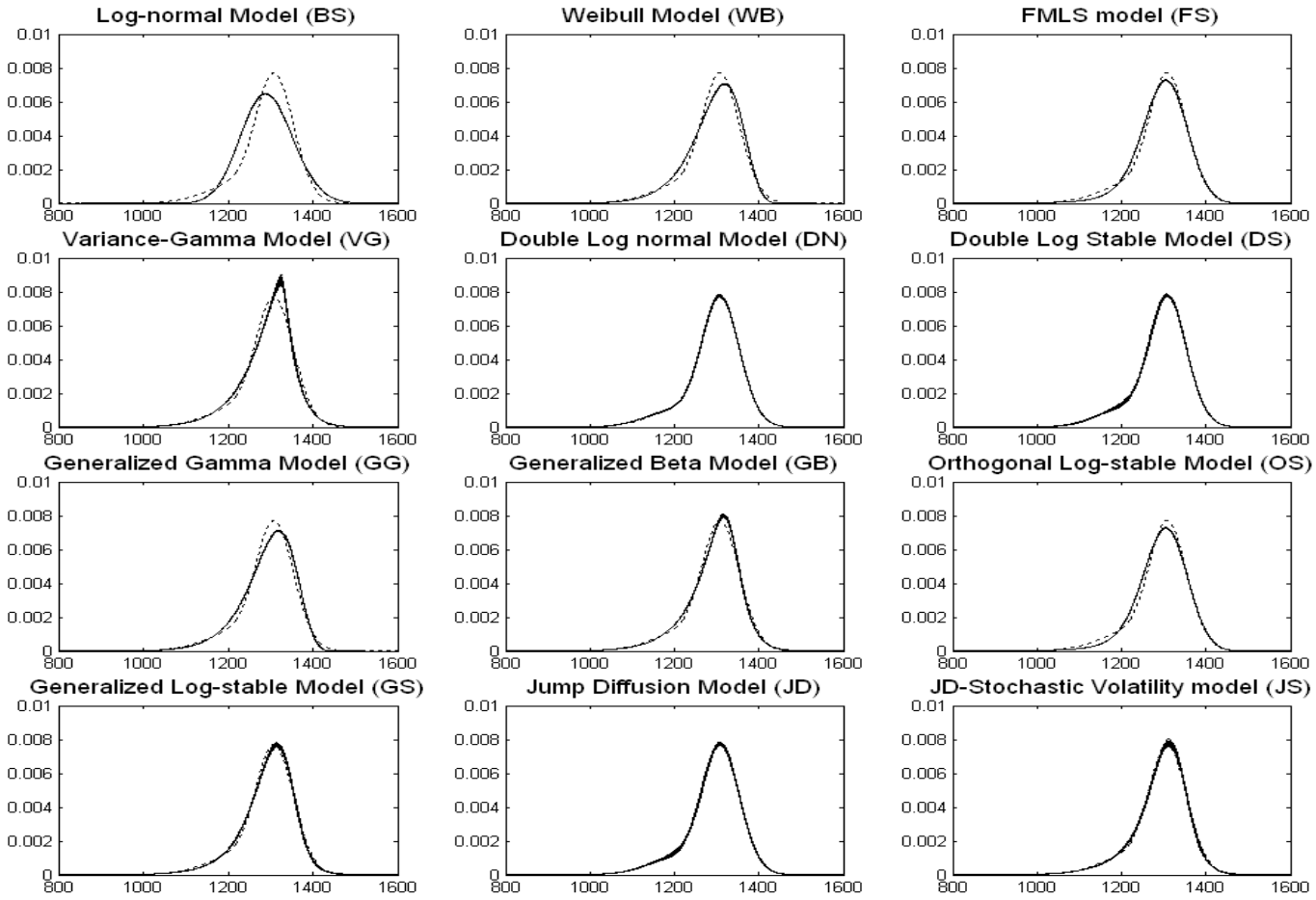

Figure 3.12: Monte-Carlo Simulation Results under the Scenario that the True RNM (dotted line) is the Jump Diffusion (JD) Model

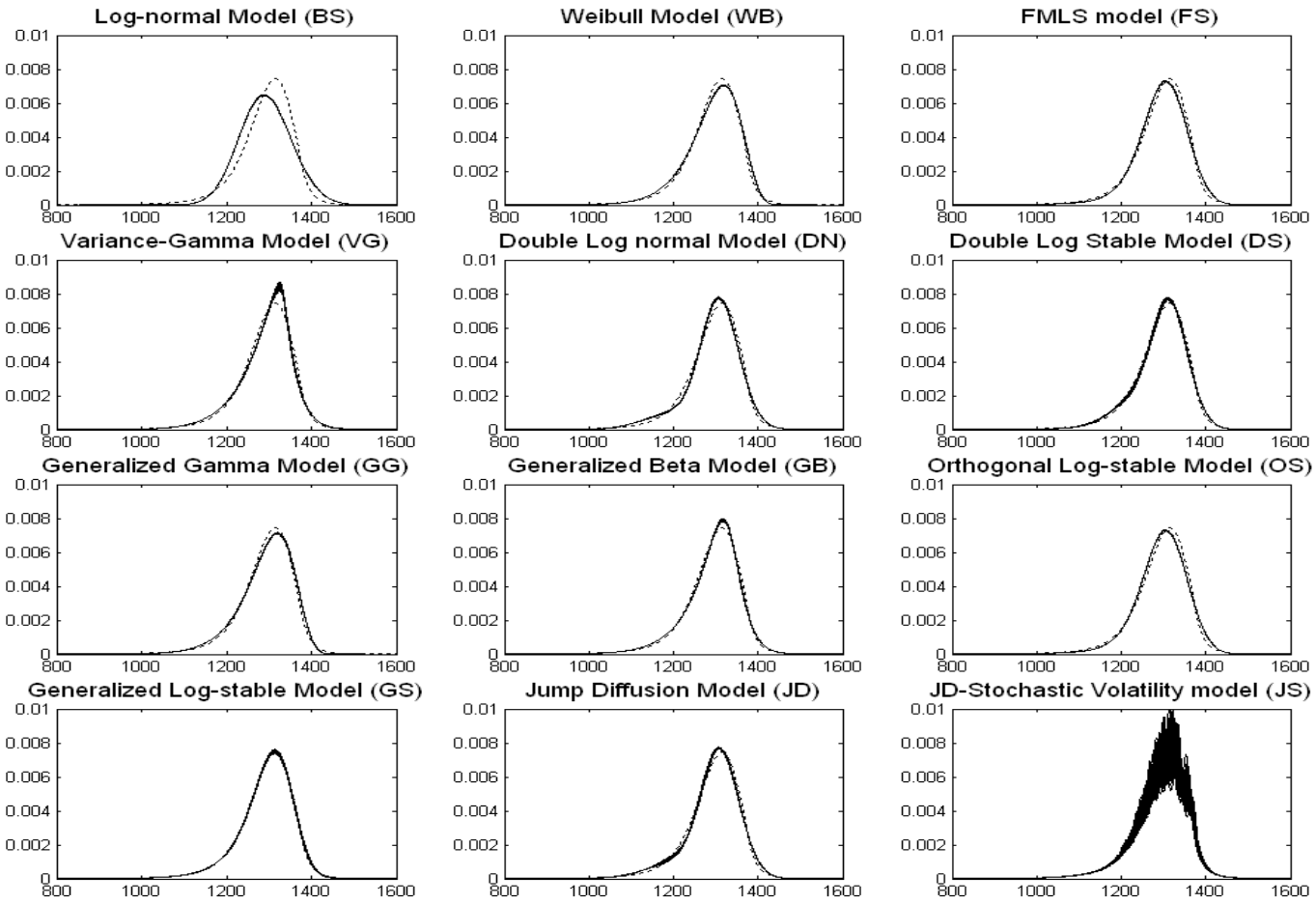

Figure 3.13: Monte-Carlo Simulation Results under the Scenario that the True RNM (dotted line) is the Jump Diffusion Model with Stochastic Volatility (JS)

	BS	WB	FS	VG	DN	DS
RMSE	2.135	0.687	0.513	0.276	0.305	0.120
Adj.	2.188	0.704	0.532	0.290	0.325	0.132
	GG	GB	OS	GS	JD	JS
RMSE	0.380	0.342	0.513	0.098	0.246	0.076
Adj.	0.395	0.360	0.539	0.106	0.263	0.086

Note: RMSEs are computed for each set of cross-section data on S&P 500 index options by minimizing the sum of squared pricing errors. The entries report the sample average of the RMSEs and adjusted RMSEs. The sample contains 100 sets of cross-section data on S&P 500 index options with 2 months to maturity, which are traded in 2006.

Table 3.1: Root Mean Squared Errors (RMSE)

Models	LR Statistics			P-values		
	$\hat{\ell}$	$\hat{\ell}_A$	$\hat{\ell}_S$	$\hat{\ell}$	$\hat{\ell}_A$	$\hat{\ell}_S$
WB	12.5	11.9	11.3	0.000	0.000	0.000
VG	6.9	6.6	6.3	0.000	0.000	0.000
DN	7.6	7.4	7.3	0.000	0.000	0.000
DS	1.9	2.1	2.3	0.026	0.017	0.011
GG	9.6	9.1	8.7	0.000	0.000	0.000
GB	8.5	8.1	7.9	0.000	0.000	0.000
JD	6.5	6.3	6.2	0.000	0.000	0.000
JS	-1.2	-0.4	0.3	0.881	0.654	0.391

Note: Three likelihood ratio statistics ($\hat{\ell}$, $\hat{\ell}_A$, and $\hat{\ell}_S$) are computed by letting model **F** be the GS model and letting model **G** be the WB, VG, DN, DS, GG, GB, JD, and JS models. All three tests are asymptotically normally distributed with zero mean and unit variance. The entries report the sample average of the test statistics and the corresponding P-values. The sample contains 100 sets of cross-section data on S&P 500 index options with 2 months to maturity, which are traded in 2006.

Table 3.2: Likelihood Ratio Tests for Non-Nested Models

BS		FS		OS	
2LR	P-value	2LR	P-value	2LR	P-value
266.3	0.000	144.5	0.000	144.5	0.000

Note: The likelihood ratio statistics ($2LR$) are computed by letting model **F** be the GS model and letting model **G** be the BS, FS, and OS models. The test statistic is asymptotically chi-square distributed with $p - q$ degree of freedom. The entries report the sample average of the test statistics and the corresponding P-values. The sample contains 100 sets of cross-section data on S&P 500 index options with 2 months to maturity, which are traded in 2006.

Table 3.3: Likelihood Ratio Tests for Nested Models

A. Average RMISE of all scenarios

	BS	WB	FS	VG	DN	DS
RMISE	0.2187	0.1004	0.0812	0.0856	0.0598	0.0379
RISB	0.2186	0.1002	0.0809	0.0832	0.0588	0.0354
RIV	0.0012	0.0014	0.0020	0.0108	0.0063	0.0095
	GG	GB	OS	GS	JD	JS
RMISE	0.0793	0.0530	0.0791	0.0314	0.0451	0.1045
RISB	0.0788	0.0514	0.0785	0.0299	0.0434	0.0358
RIV	0.0027	0.0080	0.0022	0.0061	0.0086	0.0927

B. Average RMISE of scenarios for non-nested models

	BS	WB	FS	VG	DN	DS
RMISE	0.2385	0.1093	0.0971	0.1014	0.0707	0.0518
RISB	0.2385	0.1093	0.0970	0.0995	0.0704	0.0507
RIV	0.0012	0.0014	0.0020	0.0118	0.0065	0.0101
	GG	GB	OS	GS	JD	JS
RMISE	0.1031	0.0678	0.1045	0.0448	0.0529	0.1218
RISB	0.1031	0.0675	0.1045	0.0441	0.0518	0.0384
RIV	0.0028	0.0060	0.0020	0.0069	0.0092	0.1105

Note: Panel A reports the average RMISE statistics for all 12 scenarios, and Panel B reports the average RMISE of the scenarios for non-nested models. The 12 scenarios are that i model is true RNM model, i=BS, WB, FS, DN, DS, GG, GB, OS, GS, VG, JD, and JS.

Table 3.4: Root Mean Integrated Squared Errors (RMISE)

	BS	WB	FS	VG	DN	DS
RMISE	0.0012	0.2462	0.0015	0.0046	0.0041	0.0076
RISB	0.0001	0.2462	0.0007	0.0030	0.0005	0.0042
RIV	0.0011	0.0014	0.0014	0.0035	0.0040	0.0064
	GG	GB	OS	GS	JD	JS
RMISE	0.0175	0.0043	0.0019	0.0032	0.0037	0.0072
RISB	0.0175	0.0036	0.0008	0.0011	0.0016	0.0029
RIV	0.0012	0.0023	0.0018	0.0030	0.0034	0.0065

Table 3.5: Root Mean Integrated Squared Errors (RMISE) under the Scenario that the True RNM is the Black Scholes Log-Normal (BS) Model

	BS	WB	FS	VG	DN	DS
RMISE	0.2367	0.0016	0.1206	0.0367	0.0876	0.0691
RISB	0.2367	0.0001	0.1206	0.0272	0.0872	0.0680
RIV	0.0013	0.0016	0.0022	0.0246	0.0090	0.0124
	GG	GB	OS	GS	JD	JS
RMISE	0.0029	0.0814	0.1206	0.0234	0.0529	0.0318
RISB	0.0001	0.0714	0.1205	0.0231	0.0516	0.0079
RIV	0.0029	0.0390	0.0022	0.0039	0.0116	0.0308

Table 3.6: Root Mean Integrated Squared Errors (RMISE) under the Scenario that the True RNM is the Weibull (WB) Model

	BS	WB	FS	VG	DN	DS
RMISE	0.1789	0.1113	0.0022	0.1563	0.0797	0.0133
RISB	0.1789	0.1113	0.0001	0.1559	0.0796	0.0041
RIV	0.0012	0.0015	0.0022	0.0102	0.0043	0.0127
	GG	GB	OS	GS	JD	JS
RMISE	0.1049	0.0921	0.0029	0.0042	0.0635	0.4265
RISB	0.1049	0.0917	0.0008	0.0016	0.0633	0.1044
RIV	0.0029	0.0084	0.0028	0.0039	0.0048	0.4136

Table 3.7: Root Mean Integrated Squared Errors (RMISE) under the Scenario that the True RNM is the Finite Moment Log-Stable (FS) Model

	BS	WB	FS	VG	DN	DS
RMISE	0.2510	0.1248	0.0897	0.1272	0.0065	0.0127
RISB	0.2510	0.1248	0.0897	0.1269	0.0016	0.0102
RIV	0.0011	0.0014	0.0021	0.0090	0.0063	0.0075
	GG	GB	OS	GS	JD	JS
RMISE	0.1262	0.0755	0.0897	0.0714	0.0160	0.0506
RISB	0.1261	0.0754	0.0897	0.0711	0.0133	0.0497
RIV	0.0029	0.0033	0.0021	0.0067	0.0089	0.0091

Table 3.8: Root Mean Integrated Squared Errors (RMISE) under the Scenario that the True RNM is the Mixture of Log-Normal (DN) Model

	BS	WB	FS	VG	DN	DS
RMISE	0.2453	0.0935	0.0854	0.1007	0.0491	0.0067
RISB	0.2453	0.0935	0.0853	0.1002	0.0488	0.0008
RIV	0.0011	0.0013	0.0019	0.0090	0.0054	0.0066
	GG	GB	OS	GS	JD	JS
RMISE	0.0953	0.0464	0.0853	0.0351	0.0343	0.0539
RISB	0.0953	0.0463	0.0853	0.0341	0.0332	0.0432
RIV	0.0026	0.0034	0.0019	0.0079	0.0086	0.0323

Table 3.9: Root Mean Integrated Squared Errors (RMISE) under the Scenario that the True RNM is the Mixture of Log-Stable (DS) Model

	BS	WB	FS	VG	DN	DS
RMISE	0.2476	0.0126	0.1257	0.0385	0.0930	0.0732
RISB	0.2476	0.0126	0.1257	0.0318	0.0926	0.0723
RIV	0.0012	0.0015	0.0021	0.0217	0.0090	0.0116
	GG	GB	OS	GS	JD	JS
RMISE	0.0029	0.0050	0.1257	0.0250	0.0577	0.0707
RISB	0.0003	0.0024	0.1257	0.0240	0.0565	0.0120
RIV	0.0029	0.0044	0.0021	0.0070	0.0116	0.0697

Table 3.10: Root Mean Integrated Squared Errors (RMISE) under the Scenario that the True RNM is the Generalized Gamma (GG) Model

	BS	WB	FS	VG	DN	DS
RMISE	0.2672	0.1000	0.1179	0.0538	0.0643	0.0470
RISB	0.2672	0.1000	0.1179	0.0532	0.0638	0.0458
RIV	0.0011	0.0014	0.0018	0.0076	0.0082	0.0108
	GG	GB	OS	GS	JD	JS
RMISE	0.0982	0.0025	0.1179	0.0381	0.0442	0.0149
RISB	0.0982	0.0000	0.1179	0.0375	0.0426	0.0031
RIV	0.0026	0.0025	0.0018	0.0071	0.0118	0.0146

Table 3.11: Root Mean Integrated Squared Errors (RMISE) under the Scenario that the True RNM is the Generalized Beta (GB) Model

	BS	WB	FS	VG	DN	DS
RMISE	0.1859	0.1318	0.0302	0.1785	0.0746	0.0219
RISB	0.1859	0.1318	0.0302	0.1782	0.0745	0.0210
RIV	0.0012	0.0014	0.0020	0.0101	0.0044	0.0062
	GG	GB	OS	GS	JD	JS
RMISE	0.1196	0.0931	0.0036	0.0054	0.0604	0.3282
RISB	0.1196	0.0916	0.0005	0.0027	0.0603	0.0656
RIV	0.0027	0.0163	0.0036	0.0047	0.0042	0.3215

Table 3.12: Root Mean Integrated Squared Errors (RMISE) under the Scenario that the True RNM is the Orthogonal Log-Stable (OS) Model

	BS	WB	FS	VG	DN	DS
RMISE	0.2368	0.0655	0.0772	0.1000	0.0717	0.0404
RISB	0.2368	0.0655	0.0772	0.0997	0.0716	0.0394
RIV	0.0012	0.0014	0.0020	0.0080	0.0043	0.0089
	GG	GB	OS	GS	JD	JS
RMISE	0.0671	0.0508	0.0772	0.0063	0.0609	0.0855
RISB	0.0670	0.0505	0.0771	0.0003	0.0604	0.0397
RIV	0.0028	0.0050	0.0021	0.0063	0.0073	0.0757

Table 3.13: Root Mean Integrated Squared Errors (RMISE) under the Scenario that the True RNM is the Two-Factor Generalized Log-Stable (GS) Model

	BS	WB	FS	VG	DN	DS
RMISE	0.2891	0.1342	0.1575	0.0082	0.0926	0.0919
RISB	0.2891	0.1342	0.1574	0.0011	0.0919	0.0909
RIV	0.0013	0.0015	0.0021	0.0081	0.0115	0.0137
	GG	GB	OS	GS	JD	JS
RMISE	0.1320	0.0537	0.1574	0.0799	0.0657	0.0338
RISB	0.1320	0.0536	0.1574	0.0796	0.0640	0.0196
RIV	0.0029	0.0028	0.0021	0.0077	0.0150	0.0275

Table 3.14: Root Mean Integrated Squared Errors (RMISE) under the Scenario that the True RNM is the Variance-Gamma (VG) Model

	BS	WB	FS	VG	DN	DS
RMISE	0.2461	0.1143	0.0825	0.1210	0.0127	0.0170
RISB	0.2461	0.1143	0.0825	0.1207	0.0117	0.0149
RIV	0.0012	0.0014	0.0020	0.0091	0.0049	0.0082
	GG	GB	OS	GS	JD	JS
RMISE	0.1162	0.0722	0.0825	0.0619	0.0089	0.0404
RISB	0.1162	0.0720	0.0825	0.0615	0.0010	0.0395
RIV	0.0027	0.0053	0.0020	0.0073	0.0088	0.0086

Table 3.15: Root Mean Integrated Squared Errors (RMISE) under the Scenario that the True RNM is the Jump Diffusion (JD) Model

	BS	WB	FS	VG	DN	DS
RMISE	0.2387	0.0684	0.0840	0.1013	0.0821	0.0538
RISB	0.2387	0.0684	0.0840	0.1009	0.0820	0.0530
RIV	0.0012	0.0015	0.0020	0.0083	0.0044	0.0092
	GG	GB	OS	GS	JD	JS
RMISE	0.0686	0.0588	0.0840	0.0233	0.0735	0.1108
RISB	0.0686	0.0587	0.0840	0.0221	0.0730	0.0419
RIV	0.0028	0.0031	0.0020	0.0072	0.0078	0.1026

Table 3.16: Root Mean Integrated Squared Errors (RMISE) under the Scenario that the True RNM is the Jump Diffusion Model with Stochastic Volatility (JS)

CHAPTER 4

NONPARAMETRIC ESTIMATION OF RISK NEUTRAL MEASURES USING QUARTIC B-SPLINE CDFs WITH POWER TAILS

4.1 Introduction

Investors and researchers have long used option prices to infer market expectations about the volatilities and correlations of the underlying assets by recovering risk neutral distributions from observed option prices. Option prices are computed as a present value of its expected payoffs under the risk neutral (probability) measure (RNM). The RNM can be estimated from a set of European option prices using the relationship proposed in Ross (1976) and Breeden and Litzenberger (1978). Since the RNM embodies important information about market participants' sentiments concerning prices of the underlying asset in the future, a number of methods have been developed to estimate the RNM from the observed option prices. Generally, these methods are divided into two broad groups of parametric and nonparametric methods.

The parametric methods make particular assumptions on the form or family of the RNM and then typically use a non-linear regression technique to estimate the parameters of the RNM which minimizes sum of squared pricing errors. On the other hand, the nonparametric methods make no strong assumptions about the RNM since they are flexible data-driven methods. However, the nonparametric approaches are so data-intensive that they usually lead to over-fitting problems and are not effective in small samples.

The nonparametric methods can be again divided in three groups: kernel methods

[Aït-Sahalia and Lo (1998), Aït-Sahalia and Duarte (2000)], maximum-entropy methods [Buchen and Kelly (1996), Stutzer (1996)], and curve fitting methods [Shimko (1993), Bliss and Panigirtzoglou (2002)]. The kernel methods construct a kernel estimator of the option pricing function without specifying a parametric form. Second, the maximum-entropy methods find a non-parametric probability distribution that matches the information content, while at the same time satisfying certain constraints, such as pricing observed options correctly. Finally, the curve fitting methods fit the implied volatilities or the risk neutral density with some flexible function such as spline functions or polynomial functions.

The most widely used nonparametric technique for estimating RNMs is the smoothed implied volatility smile (SML) method which has been discerned as a standard method by users such as central banks and market participants. The SML method was originally developed by Shimko (1993), and it explicitly utilizes the results of Breeden and Litzenberger (1978) on the call option pricing function. Shimko (1993) proposes that the observed option prices first be converted to implied volatilities using the Black-Scholes option pricing formula. A continuous smoothing function is then fitted to implied volatilities against the strike prices. The implied volatility function could then be fitted and the continuum of fitted implied volatilities converted back to a continuum of fitted option prices. The RNM probability density function (PDF) can be obtained by applying the results of Breeden and Litzenberger (1978) on the call option pricing function. The advantage of this method is that the implied volatilities are much more similar in magnitude across strike prices than option prices are. Bliss and Panigirtzoglou (2002) follow Malz (1997) in smoothing in implied volatility/delta space and Campa, Chang and Reider (1998) in using a natural cubic spline to approximate the function. Recently, Bu and Hadry (2007) improve the SML method by providing an analytic expression for the RNM estimator.

The SML method has some problems in estimating the RNM. First, the natural spline is restricted to become linear outside the range of observed option prices. As Bliss and Panigirtzoglou (2002) point out, this restriction can lead to negative tail probabilities if the

slope of the polynomial is negative at the extreme knot points.[1] Further, the estimated tail probabilities have no information about true ones since they are not estimated by observed option prices. Second, the SML method cannot guarantee the resulting RNM PDF to be integrated to unity. The negative probabilities or probabilities not integrating to unity seriously violate no-arbitrage constraints. Lastly, problems with the SML method include the difficulty of selecting the optimal tradeoff between smoothness and fit since the shape of RNM PDFs is very sensitive to the smoothing parameter. The SML method is typically unable to avoid both overfitting and oversmoothing. To effectively eliminate noise in data, this method requires substantial smoothing, which considerably distorts the genuine features of the estimated function.

This chapter proposes a new nonparametric approach which overcomes the drawbacks of the SML method. First, we model the probability distribution outside the traded strike range using power tails, which may be estimated from the far-from-the-money option prices. With the power tails, the RNM has nonnegative tail probabilities and also reflects information about true tail probabilities. Second, the RNM cumulative distribution function (CDF) is constructed by using quartic B-spline functions with power tails so that the resulting RNM PDF has continuity C^2. The use of B-splines also improves computational efficiency and reduces the number of spline parameters since every spline function can be represented as a linear combination of B-splines. The advantage of constructing the RNM CDF with power tails is that the integral of RNM probabilities is guaranteed to be unity. Lastly, by choosing an optimum number of knots, our method can avoid both overfitting and oversmoothing. A small number of knots may result in a function space which is not flexible enough to capture the true RNM CDF, but one the other hand a large number may

[1] To ensure the non-negativity of the estimated PDF, Monterio, Tütüncü, and Vicente (2005) estimate the cubic spline RNM PDF using the semi-definite programming (SDP) formulation, but they just truncate the tails of PDF without estimating them from option prices. Fengler (2005) propose an algorithm for estimating the implied volatility smile under suitable linear inequality constraints, ensuring non-negativity of the RNM pdf, but this algorithm does not guarantee the resulting RNM PDF to be integrated to unity.

lead to serious overfitting. To select optimal tradeoff between smoothness and fit, we use the minimum number of knots which attains zero bid-ask pricing errors in constructing the B-spline RNM CDF. The method is termed the B-spline RNM CDF with power tails (BSP), which is nonparametric because any probability distribution is a possible solution.

Our nonparametric method involves solving a highly nonlinear optimization problem with a number of constraints due to the power tails. It is computationally difficult and inaccurate to estimate the B-spline part of the CDF and the power tails simultaneously. To improve computational efficiency and accuracy we develop a 3-step RNM estimation technique: (i) estimating the power tail parameters; (ii) selecting the optimum number of the knots; and (iii) estimating the B-spline control points. The 3-step estimation procedure transforms a nonlinear optimization problem into a convex quadratic program which is efficiently solved by numerical optimization software.

To compare the performance of the BSP method with the SML method for estimating option implied RNMs, we evaluate the two methods on the basis of the flexibility of the estimated RNM and conduct Monte-Carlo experiments based on 12 hypothetical true distributions. We find that the BSP method dominates the SML method as a technique for estimating the option-implied RNM. The SML method violates the no-arbitrage constrains, and it is significantly biased, particularly under the scenarios that the true RNM is a fat-tailed distribution. In contrast, the BSP method always produces arbitrage-free RNM estimators, and it almost perfectly recovers the actual RNM PDFs for all hypothetical distributional assumptions.

The rest of the chapter is organized as follows. Section 4.2 briefly reviews the smoothed implied volatility smile (SML) method. Section 4.3 constructs the quartic B-spline RNM CDF with power tails. Section 4.4 introduces the 3-step RNM estimation procedure with the quartic B-spline RNM CDF with power tails. In Section 4.5, we compare the flexibility of BSP and SML and conduct Monte-Carlo experiments. Section 4.6 concludes.

4.2 Smoothed Implied Volatility Smile (SML) method

The smoothed implied volatility smile method explicitly utilizes the results of Breeden and Litzenberger (1978) on the call option pricing function. Breeden and Litzenberger showed that the RNM PDF of the price of underlying asset at maturity date is related to call (or put) prices through

$$R'(S_T) = e^{r_f T} \left. \frac{\partial^2 C(K)}{\partial K^2} \right|_{K=S_T},$$

where $R(x)$ is the RNM CDF, S_T is the underlying asset price at maturity date, r_f is the risk free interest rate, T is the time to maturity, K is the strike price, and $C(K)$ is the call pricing function. Thus, if we observed the call pricing function we could differentiate twice to obtain the RNM PDF. However, we only observe option prices for relatively few discretely spaced strikes.

Shimko (1993) proposes interpolating in the implied volatility domain instead of the call price domain since it is technically difficult to fit accurately the shape of the latter and small fitted price errors tend to have large effects on the resulting RNM PDFs, particularly in the tails. Shimko chooses to use a simple quadratic polynomial smoothing function within the span of available strikes and with lognormal tails outside the span of available strikes. Malz (1997) modifies Shimko's technique by fitting the implied volatility against the Black-Scholes option delta ($\delta = \partial C / \partial S$) rather than the strike price, but follows Shimko in using a low-order polynomial as the smoothing function. Campa, Chang and Reider (1998) introduce the use of a smoothing spline[2] for fitting implied volatility curves. They apply this to smoothing the implied volatility/strike function. Use of a natural spline, rather than a low-order polynomial, permits the user to control the smoothness of the fitted function.

[2]The curve fitting method based on spline functions was first used by McCulloch (1971, 1975) in financial economics for modeling the term structure of interest rates.

In this paper we use the smoothed implied volatility smile (SML) method developed by Bliss and Panigirtzoglou (2002). This method follows Malz (1997) in smoothing in implied volatility/delta space and Campa et al. (1998) in using a smoothing cubic spline to approximate the function. The RNM PDF can be obtained by a five-step estimation procedure.

Step 1 Converting call option prices $C(K_i)$ into implied volatilities σ_{K_i} using the inverse Black-Scholes formula[3]

$$\sigma_{K_i} = BS^{-1}(C(K_i); K_i, S_0, r_f, d, T)$$

where $BS^{-1}(\cdot)$ is the inverse Black-Scholes formula; σ_{K_i} and $C(K_i)$ are the implied volatility and the price of European call option, respectively, associated with the strike price K_i; S_0 is the underlying asset price at time 0; r is the risk-free interest rate; d is the dividend rate; and T is the maturity date.

Step 2 Converting implied volatility/strike space into implied volatility/delta space

$$\begin{aligned} \delta_i &= e^{-dT}\Phi\left(\frac{\ln S_0 - \ln K_i + \left(r - d + \sigma_A^2/2\right)T}{\sigma_A\sqrt{T}}\right) \\ IV(\delta_i) &= \sigma_{K_i} \end{aligned}$$

where δ_i is the delta associated with the strike price K_i[4]; σ_A is the at-the-money volatility[5]; $IV(\delta_i)$ is the implied volatility associated with δ_i; and $\Phi(\cdot)$ is the standard

[3]The use of the Black-Scholes formula to transfer between the call price and implied volatility domains does not require that the Black-Scholes model is ture. Black-Scholes formula is used as a translation device that allows us to interpolate implied volatilities rather than the observed option prices themselves for a computational convenience.

[4]It should be recalled that $0 \leq \delta_i \leq e^{dT}$, where d is the dividend rate of the underlying asset.

[5]Transforming each strike into a delta using the at-the-money implied volatility has the advantage that the ordering of deltas is always the same as that of the strikes. Panigirtzoglou and Skiadopoulos (2004) pointed out that using the implied volatilities that corresponds to each strike could change the ordering in the delta

normal CDF.

Step 3 Approximating the implied volatility smile using smoothing cubic spline functions

$$\min_{\Theta} \quad \sum_{i=1}^{N} w_i \left(IV(\delta_i) - f(\delta_i; \Theta)\right)^2 + \omega \int_0^{e^{-dT}} f''(\delta; \Theta)^2 d\delta,$$

where Θ is the matrix of polynomial parameters of the cubic spline; $f(\Theta)$ is the cubic spline function; $f(\delta_i, \Theta)$ is the fitted implied volatility at δ_i given the spline parameters Θ; w_i is the relative weights to each observation[6]; ω is the smoothing parameter, which multiplies a measure of the degree of curvature in the function–the integral of the squared second derivative of the function over its range.[7]

Step 4 Converting the implied volatility smile into a option pricing function in price/strike space

$$\begin{aligned}
\delta(K) &= e^{-dT}\Phi\left(\frac{\ln S_0 - \ln K + \left(r - d + \sigma_A^2/2\right)T}{\sigma_A\sqrt{T}}\right) \\
\sigma(K) &= f(\delta(K); \Theta) \\
C(K) &= BS\left(K; \sigma(K), S_0, r, d, , T\right)
\end{aligned}$$

where $\sigma(K)$ is the fitted implied volatility smile; $C(K)$ is the fitted call pricing function; and $BS(\cdot)$ is the Black-Scholes formula.

space, in cases where steep volatility skews are observed. This would result in generating volatility smiles with artificially created kinks.

[6]Bliss and Panigirtzoglou (2002) discussed different types of weighting schemes and how the weighting can account for different sources of pricing errors.

[7]The objective function suggests that the degree of freedom for the estimation is also related to the smoothing parameter. In particular, the maximum degree of freedom is achieved when $\omega = 1$, which amounts to fitting a straight line to the data; whereas, when $\omega = 0$, the cubic spline provides an exact fit to the data. Fisher et al. (1995) gives a rigorous definition of the effective number of parameter of the regression.

Step 5 Computing the RNM PDF using numerical methods

$$R'(x) = e^{rT} \frac{\partial^2 C(x)}{\partial x^2},$$

where $R'(x)$ is the RNM PDF.

4.3 Quartic B-Spline RNM CDF with Power Tails

4.3.1 Uniform Quartic B-Spline

A spline is a piecewise polynomial function. A spline $S : [a, b] \to R$ consists of polynomical pieces $P_i : [x_i, x_{i+1}) \to R$, where

$$a = x_1 < \cdots < x_n = b.$$

The given n points x_i are called knots. The vector $x = (x_1, \cdots, x_n)$ is called knot vector for the spline. A spline on $[a, b]$ is of degree m if its first $m-1$ derivatives exist on each interior knot and the highest degree of the polynomials defining the spline function is m.

A B-spline is a spline function that has minimal support with respect to a given order, smoothness, and domain partition. Every spline function of a given degree, smoothness and domain partition, can be represented as a linear combination of B-splines of which same order and smoothness, and over that same partition. A B-spline basis function of degree m is a piecewise polynomial whose pieces are defined over the spans between knots. Each piece is a polynomial of degree m. The pieces meet with continuity of all derivatives below the m^{th} and with (possible) discontinuities of the m^{th} derivative. The function is identically zero outside a range of $m + 1$ spans, and positive within its non-zero domain.

The i^{th} B-spline basis of degree m for n knots x_i with $x_1 < x_2 < \ldots < x_n$ can be constructed using the Cox-de Boor recursion formula:

$$B_{i,0}(x) = I_{[x_i,x_{i+1})}(x), \tag{4.1}$$

$$B_{i,m}(x) = \frac{x - x_i}{x_{i+m} - x_i} B_{i,m-1}(x) + \frac{x_{i+m+1} - x}{x_{i+m+1} - x_{i+1}} B_{i+1,m-1}(x) \tag{4.2}$$

where $I_{[x_i,x_{i+1})}(x) = 1$ for $x \in [x_i, x_{i+1})$, $I_{[x_i,x_{i+1})}(x) = 0$ for $x \notin [x_i, x_{i+1})$, $B_{i,m}(x) > 0$ for $x \in [x_i, x_{i+m+1}]$, and $B_{i,m}(x) = 0$ for $x \notin [x_i, x_{i+m+1}]$. When the knots are equidistant, we say the B-spline is uniform otherwise we call it non-uniform. In our study, we use a uniform quartic B-spline basis to construct the risk-neutral CDF.

A quartic spline is a spline of degree 4 with C^3 continuity. The quartic spline can be constructed as a linear combination of 4^{th} degree B-spline basis functions:

$$f(x) = \sum_{i=1}^{n-5} c_i B_{i,4}(x), \quad x \in [x_5, x_{n-4}].$$

The coefficients c_i are called the control points.[8] The uniform quartic B-spline basis function is illustrated in Figure 4.1.

Consider a uniform knot vector $x = (x_1, \cdots, x_n)$ with $(x_{i+1} - x_i) = h$ for all $i = 1, \ldots, n-1$. Since knots are equidistant,

$$\frac{x_{i+j} - x_i}{h} = j. \tag{4.3}$$

In order to simplify notations, let

$$z_i \equiv \frac{x - x_i}{h}, \tag{4.4}$$

$$z_{i+j} \equiv \frac{x - x_{i+j}}{h}. \tag{4.5}$$

[8]The control points form a sequence which is known as the control polygon which is often visualized by joining them in sequence by straight lines. This set of straight lines is in fact the B-spline curve of order 1-defined by that set of control points.

By combining (4.3) and (4.5),

$$z_{i+j} = z_i - j. \tag{4.6}$$

By means of (4.4) and (4.2), we can rewrite the Cox-de Boor formula (4.1) and (4.2):

$$B_{i,0}(x) = I_{[x_i, x_{i+1})}(x), \tag{4.7}$$

$$B_{i,m}(x) = \frac{z_i}{m} B_{i,m-1}(x) + \frac{m+1-z_i}{m} B_{i+1,m-1}(x). \tag{4.8}$$

Finally, we may construct the basis of a uniform quartic B-spline recursively by using (4.7) and (4.8):

$$\begin{aligned} B_{i,4}(x) = & \left(\frac{z_i^4}{24}\right) I_{[x_i, x_{i+1})}(x) \\ & + \left(\frac{-4z_i^4 + 20z_i^3 - 30z_i^2 + 20z_i - 5}{24}\right) I_{[x_{i+1}, x_{i+2})}(x) \\ & + \left(\frac{6z_i^4 - 60z_i^3 + 210z_i^2 - 300z_i + 155}{24}\right) I_{[x_{i+2}, x_{i+3})}(x) \\ & + \left(\frac{-4z_i^4 + 60z_i^3 - 330z_i^2 + 780z_i - 655}{24}\right) I_{[x_{i+3}, x_{i+4})}(x) \\ & + \left(\frac{(5-z_i)^4}{24}\right) I_{[x_{i+4}, x_{i+5})}(x). \end{aligned}$$

where $z_i = \frac{x - x_i}{h}$, and $h = x_{i+1} - x_i$.

4.3.2 Constructing a Quartic B-spline RNM CDF with Power Tails

Consider N traded strike price sequence $K_1 < K_2 < \cdots < K_N$. We construct a RNM CDF by means of the quartic B-spline for the traded strike range $[K_1,\ K_N]$, and then extrapolate beyond the traded strike range by grafting power tails onto each of the endpoints of the RNM CDF. To ensure a smooth transition from the traded strike range of the distribution to the tails, we impose end point constraints for continuity up to the second derivative. To guarantee non-negativity of the RNM PDF, we also restrict the slope of the RNM CDF

to be non-negative at all the knots within the traded strike range $[K_1,\ K_N]$. Thus, the quartic B-spline CDF with power tails is described as:

$$\begin{aligned} R(x) &= R(x; c_1, \ldots, c_{n-5}, \rho_1, \rho_2, \lambda_1, \lambda_2) \\ &= \rho_1 x^{\lambda_1} I_{[0,K_1)}(x) + \sum_{i=1}^{n-5} c_i B_{i,4}(x)\, I_{[K_1,K_N]}(x) + \left(1 - \rho_2 x^{-\lambda_2}\right) I_{(K_N,\infty]}(x) \end{aligned} \tag{4.9}$$

s.t.

(i) Level continuity constraints

$$\rho_1 K_1^{\lambda_1} = \sum_{i=1}^{n-5} c_i B_{i,4}(K_1) \qquad \text{(left end)} \tag{4.10}$$

$$1 - \rho_2 K_N^{-\lambda_2} = \sum_{i=1}^{n-5} c_i B_{i,4}(K_N) \qquad \text{(right end)} \tag{4.11}$$

(ii) 1st derivative continuity constraints

$$\rho_1 \lambda_1 K_1^{\lambda_1 - 1} = \sum_{i=1}^{n-5} c_i B_{i,4}^{(1)}(K_1) \qquad \text{(left end)} \tag{4.12}$$

$$\rho_2 \lambda_2 K_N^{-\lambda_2 - 1} = \sum_{i=1}^{n-5} c_i B_{i,4}^{(1)}(K_N) \qquad \text{(right end)} \tag{4.13}$$

(iii) 2nd derivative continuity constraints

$$\rho_1 \lambda_1 (\lambda_1 - 1) K_1^{\lambda_1 - 2} = \sum_{i=1}^{n-5} c_i B_{i,4}^{(2)}(K_1) \qquad \text{(left end)} \tag{4.14}$$

$$-\rho_2 \lambda_2 (\lambda_2 + 1) K_N^{-\lambda_2 - 2} = \sum_{i=1}^{n-5} c_i B_{i,4}^{(2)}(K_N) \qquad \text{(right end)} \tag{4.15}$$

(iv) Non-negative probability constraints

$$\sum_{i=1}^{n-5} c_i B_{i,4}^{(1)}(x_j) \geq 0, \quad j = 6, \ldots, n-5. \tag{4.16}$$

where $x = (x_1, \cdots, x_n)$ is a uniform knot vector with $x_5 = K_1$ and $x_{n-4} = K_N$, and $B^{(j)}$ denotes the j^{th} derivative of the B-spline basis.

Once we have the Quartic B-spline RNM CDF with power tails $R(x)$, the RNM PDF can be derived as a first derivative of $R(x)$:

$$R'(x) = \rho_1 \lambda_1 x^{\lambda_1 - 1} I_{[0,K_1)}(x) + \sum_{i=1}^{n-5} c_i B_{i,4}^{(1)}(x) I_{[K_1,K_N]}(x) + \rho_2 \lambda_2 x^{-\lambda_2 - 1} I_{(K_N,\infty]}(x) \tag{4.17}$$

where

$$\begin{aligned} B_{i,4}^{(1)}(x) &= \left(\frac{z_i^3}{6h}\right) I_{[x_i,x_{i+1})}(x) \\ &+ \left(\frac{-4z_i^3 + 15z_i^2 - 15z_i + 5}{6h}\right) I_{[x_{i+1},x_{i+2})}(x) \\ &+ \left(\frac{6z_i^3 - 45z_i^2 + 105z_i - 75}{6h}\right) I_{[x_{i+2},x_{i+3})}(x) \\ &+ \left(\frac{-4z_i^3 + 45z_i^2 - 165z_i + 195}{6h}\right) I_{[x_{i+3},x_{i+4})}(x) \\ &+ \left(\frac{z_i^3 - 15z_i^2 + 75z_i - 125}{6h}\right) I_{[x_{i+4},x_{i+5})}(x) \end{aligned}$$

with $z_i = \frac{x - x_i}{h}$, $h = x_{i+1} - x_i$. The quartic B-spline RNM CDF and PDF with power tails are illustrated in Figure 4.2.

4.4 Option pricing with a B-Spline RNM CDF

By ruling out arbitrage possibilities, Cox and Ross (1976) showed that options can be priced as if investors' were risk neutral, regardless of investors risk preferences. Consider a European call option whose terminal payoff is $max(0, S_T - K)$, where S_T is the underlying asset price at maturity, T is the time to maturity, and K is the strike price. In a complete arbitrage-free market, the price of a European call option $C(K)$ can then be computed as

the discounted value of the option's expected payoff under the RNM. Formally,

$$\begin{aligned} C(K) &= e^{-r_f T} \int_K^\infty (x - K)\, R'(x)\, dx \\ &= e^{-r_f T} \left[\int_K^\infty x\, R'(x)\, dx + KR(K) - K \right], \end{aligned} \tag{4.18}$$

where r_f is the risk free rate, $R'(x)$ is the risk-neutral density of the underlying asset price at maturity.

In a similar manner the price of a European put option $P(K)$ can be calculated as:

$$\begin{aligned} P(K) &= e^{-r_f T} \int_0^K (K - x)\, R'(x)\, dx \\ &= e^{-r_f T} \left[- \int_0^K x\, R'(x)\, dx + KR(K) \right] \end{aligned} \tag{4.19}$$

In the arbitrage-free market, the expected price at maturity under the RNM should equal the forward price of the underlying asset with the same time to maturity, i.e. the RNM must satisfy the so-called the mean-forward price equality condition:

$$E^Q(x) = \int_0^\infty x\, R'(x) dx = S_0 e^{(r_f - d)T}, \tag{4.20}$$

where S_0 is the underlying asset price at time 0; d is the annual dividend rate of the underlying asset; $S_0 e^{(r_f - d)T}$ is the implicit forward price; and E^Q is the conditional expectation on time 0 information under the RNM.

By applying the B-spline RNM (4.9) and (4.17) to call and put price functions (4.18) and (4.19), call and put option prices under the B-Spline RNM CDF with power tails are

written as:

$$
\begin{aligned}
& C(K;\mathbf{c},\boldsymbol{\theta}) \\
= \;& e^{-r_f T}\left[\sum_{i=1}^{n-5} c_i \int_K^{K_N} x B_{i,4}^{(1)}(x)dx + \frac{\rho_1\lambda_1}{\lambda_1+1}K_1^{\lambda_1+1} + \frac{\rho_2\lambda_2}{\lambda_2-1}K_N^{-\lambda_2+1} + \frac{\rho_1}{\lambda_1+1}K^{\lambda_1+1} - K\right] I_{[0,K_1)}(K) \\
+ \;& e^{-r_f T}\left[\sum_{i=1}^{n-5} c_i \left(K B_{i,4}(K) + \int_K^{K_N} x\, B_{i,4}^{(1)}(x)\, dx\right) + \frac{\rho_2\lambda_2}{\lambda_2-1}K_N^{-\lambda_2+1} - K\right] I_{[K_1,K_N]}(K) \qquad (4.21) \\
+ \;& e^{-r_f T}\frac{\rho_2}{\lambda_2-1}K^{-\lambda_2+1}\, I_{(K_N,\infty]}(K)
\end{aligned}
$$

$$
\begin{aligned}
& P(K;\mathbf{c},\boldsymbol{\theta}) \\
= \;& e^{-r_f T}\,\frac{\rho_1\lambda_1}{\lambda_1+1}K^{\lambda_1+1}\, I_{[0,K_1)}(K) \\
+ \;& e^{-r_f T}\left[\sum_{i=1}^{n-5} c_i \left(K B_{i,4}(K) - \int_{K_1}^{K} x\, B_{i,4}^{(1)}(x)\, dx\right) + \frac{\rho_1\lambda_1}{\lambda_1+1}K_1^{\lambda_1+1}\right] I_{[K_1,K_N]}(K) \qquad (4.22) \\
+ \;& e^{-r_f T}\left[-\sum_{i=1}^{n-5} c_i K B_{i,4}(K) - \frac{\rho_1\lambda_1}{\lambda_1+1}K_1^{\lambda_1+1} - \frac{\rho_2\lambda_2}{\lambda_2-1}K_N^{-\lambda_2+1} + \frac{\rho_2}{\lambda_2-1}K^{-\lambda_2+1} + K\right] I_{(K_N,\infty]}(K)
\end{aligned}
$$

where $\mathbf{c} = [c_1 \ldots c_{n-5}]'$ and $\boldsymbol{\theta} = [\rho_1\ \rho_2\ \lambda_1\ \lambda_2]'$. The derivation of the call and put pricing functions (4.22) and (4.22) is given in Appendix B.

4.5 Estimation of the RNM CDF

4.5.1 Optimization Problem

Since out-of-the-money (OTM) options are generally more liquid than in-the-money (ITM) options, we estimate the RNM CDF $R(x)$ from each cross-section of the OTM option prices with the different strike prices K_i and the same time to maturity T. The OTM option prices are defined as:

$$
V(K_i) \;=\; \begin{cases} P(K_i) & \text{for } K_i < F, \quad i = 1,\ldots,N \\ \\ C(K_i) & \text{for } K_i \geq F, \end{cases}
$$

where $P(K_i)$ and $C(K_i)$ are the traded put and call option prices, respectively, associated with strike price K_i. By put-call parity, the OTM option prices can be alternatively defined as:

$$V(K_i) = min\big[C(K_i), P(K_i)\big], \quad i = 1, \ldots, N.$$

Similarly, under the quartic B-spline RNM CDF with power tails $R(x; \boldsymbol{\theta}, \mathbf{c})$, the OTM option model prices are defined as:

$$V(K_i; \mathbf{c}, \boldsymbol{\theta}) = min\big[C(K_i; \mathbf{c}, \boldsymbol{\theta}), P(K_i; \mathbf{c}, \boldsymbol{\theta})\big], \quad i = 1, \ldots, N.$$

The vector of tail parameters $\boldsymbol{\theta}$ and control points $\mathbf{c}$ can be simply estimated by the least squares criterion, i.e., minimizing the sum of squared pricing errors (SSE) given a number of knots n:

$$\min_{\mathbf{c},\boldsymbol{\theta}} \quad L(SSE) \quad = \quad \sum_{i=1}^{N} \left(V(K_i) - V(K_i; \mathbf{c}, \boldsymbol{\theta})\right)^2 .$$

However, since the least squares criterion can not reduce rapid local variations of the estimated RNM PDF, a roughness penalty is introduced in the loss function to prevent wiggly RNM PDFs. The roughness penalty for the RNM PDF is defined as the integrated squared third derivative of the RNM CDF:

$$\int_{K_1}^{K_N} \left[R'''(x; \mathbf{c}, \boldsymbol{\theta})\right]^2 dx.$$

The resulting optimization problem is solved by minimizing the penalized SSE subject to the constraints of satisfying the quartic B-spline RNM CDF conditions (4.10)-(4.16) and mean-forward price equality condition (4.20):

$$\min_{\mathbf{c},\boldsymbol{\theta}} \quad L_\omega \quad = \quad \sum_{i=1}^{N} \left(V(K_i) - V(K_i; \mathbf{c}, \boldsymbol{\theta})\right)^2 + \omega \int_{K_1}^{K_N} \left[R'''(x; \mathbf{c}, \boldsymbol{\theta})\right]^2 dx \tag{4.23}$$

s.t. (4.10)-(4.16) and (4.20)

where ω denotes a smoothing parameter.[9] The smoothing parameter represents the rate of exchange between pricing error and roughness of the RNM PDF.

The optimization problem (4.23) has two computational difficulties in estimating the RNM. The loss function in (4.23) is highly nonlinear due to the tail parameters $\boldsymbol{\theta}$. It is computationally inefficient and inaccurate to estimate $\boldsymbol{\theta}$ and $\mathbf{c}$ simultaneously with a number of constraints. Another problem is the choice of the optimum number of the knots. A small number of knots may result in a function space which is not flexible enough to capture the true RNM CDF. A large number may lead to serious overfitting. In order to avoid these problems, we develop a 3-step estimation procedure:

Step 1 : Estimating the tail parameters $\boldsymbol{\theta}$.

Step 2 : Selecting the optimum number of the knots n.

Step 3 : Estimating the control points $\mathbf{c}$.

4.5.2 3-Step Estimation Procedure

a. Estimation of Power tail parameters

Since deep out-of-the-money option prices are almost determined by the shape of the RNM CDF tails, the power tail parameters can be pinned down by the observed deep OTM option prices. The left power tail parameters are estimated from the deep OTM put option prices. Under the left power tail of RNM CDF, $\rho_1 x^{\lambda_1}$, the deep OTM put prices can be expressed as:

$$\begin{aligned} P(K) &= e^{-r_f T} \int_0^K (K-x)\,\rho_1 \lambda_1 x^{\lambda_1 - 1}\, dx \\ &= e^{-r_f T} \frac{\rho_1}{\lambda_1 + 1} K^{\lambda_1 + 1} \end{aligned}$$

[9] We set the smoothness penalty parameter ω equal to 10^{-3} which minimizes the RMISE of SML under the log-normal RNM PDF.

Consider two deep observed OTM put option prices P_1 and P_2 with strikes K_1 and K_2:

$$P_1 = e^{-r_f T} \frac{\rho_1}{\lambda_1 + 1} K_1^{\lambda_1 + 1} \tag{4.24}$$

$$P_2 = e^{-r_f T} \frac{\rho_1}{\lambda_1 + 1} K_2^{\lambda_1 + 1} \tag{4.25}$$

Solving (4.24) and (4.25) for λ_1 and ρ_1 then gives

$$\begin{aligned} \lambda_1^* &= \frac{\log(P_2/P_1)}{\log(K_2/K_1)} - 1 \\ \rho_1^* &= e^{r_f T} \frac{(\lambda_1^* + 1) P_1}{K_1^{\lambda_1^* + 1}}. \end{aligned}$$

Similarly, the left tail of the RNM CDF, $1 - \rho_2 x^{-\lambda_2}$, can be estimated by deep OTM call option prices. The deep OTM call option prices are expressed as a function of right tail parameters:

$$\begin{aligned} C(K) &= e^{-r_f T} \int_K^\infty (x - K) \rho_2 \lambda_2 x^{-\lambda_2 - 1} \, dx \\ &= e^{-r_f T} \frac{\rho_2}{\lambda_2 - 1} K^{-\lambda_2 + 1} \end{aligned}$$

Consider two deep observed OTM call option prices C_{N-1} and C_N with strikes K_{N-1} and K_N:

$$C_{N-1} = e^{-r_f T} \frac{\rho_2}{\lambda_2 - 1} K_{N-1}^{-\lambda_2 + 1} \tag{4.26}$$

$$C_N = e^{-r_f T} \frac{\rho_2}{\lambda_2 - 1} K_N^{-\lambda_2 + 1} \tag{4.27}$$

Solving (4.26) and (4.27) for λ_2 and ρ_2 then gives

$$\begin{aligned} \lambda_2^* &= 1 - \frac{\log(C_N/C_{N-1})}{\log(K_N/K_{N-1})} \\ \rho_2^* &= e^{r_f T} \frac{(\lambda_2^* - 1) C_N}{K_N^{-\lambda_2^* + 1}}. \end{aligned}$$

b. Selection of the Number of Knots

With the estimated tail parameter vector $\boldsymbol{\theta}^*$, the OTM option pricing function can be described only by the control points vector, $\mathbf{c}$:

$$V(K_i; \mathbf{c}|\boldsymbol{\theta}^*) = min[C(K_i; \mathbf{c}|\boldsymbol{\theta}^*), P(K_i; \mathbf{c}|\boldsymbol{\theta}^*)], \quad i = 1, \ldots, N,$$

where $\boldsymbol{\theta}^* = [\rho_1^* \; \rho_2^* \; \lambda_1^* \; \lambda_2^*]^\top$ is the RNM tail parameter vector which are pinned down in the first step. In order to estimate the control points vector, the number of knots, n, must be selected. A small number of knots may result in underfitting, but one the other hand a large number may lead to serious overfitting. To select optimal tradeoff between smoothness and fit, we choose the minimum number of knots, which attains zero bid-ask pricing errors, in constructing the B-spline RNM CDF.

Define the bid-ask pricing errors as:

$$\mathrm{e}_i = \left(V_i^B - V(K_i; \mathbf{c}|\boldsymbol{\theta}^*)\right)_+ + \left(V(K_i; \mathbf{c}|\boldsymbol{\theta}^*) - V_i^A\right)_+,$$

where V_i^B is the bid-quote OTM option price; V_i^A is the ask-quote OTM option price associated with the strike price K_i; and $x_+ = \max(0, x)$. If all the estimated OTM prices fell within the bid-ask price range, the sum of squared bid-ask pricing errors would be zero:

$$\min_{\mathbf{c} \in \mathbb{R}^{n-5}} \mathbf{e}^\top \mathbf{e} = 0, \tag{4.28}$$

where $\mathbf{e} = [\mathrm{e}_1, \cdots, \mathrm{e}_N]^\top$ is the bid-ask pricing error vector. To construct the B-spline RNM CDF, we choose the minimum number of knots n^* satisfying the zero bid-ask pricing error condition (4.28):

$$n^* = arg \min_{n \in \mathbb{Z}} \quad n$$

s.t. (4.28) with (4.10)-(4.16), and (4.20).

c. Estimation of the control points of B-Splines

Once the tail parameter vector $\boldsymbol{\theta}^*$ and the optimum number of knots n^* are determined by the step 1 and 2, the nonlinear optimization problem (4.23) is expressed as a convex quadratic program which is efficiently solved by numerical optimization software. The optimization problem

$$\begin{aligned} \min_{\mathbf{c}\in\mathbb{R}^{n^*-5}} \quad & L_\omega \;=\; \sum_{i=1}^{N} \left(V(K_i) - V(K_i;\mathbf{c}|\boldsymbol{\theta}^*)\right)^2 \;+\; \omega \int_{K_1}^{K_N} \left[R'''(x;\mathbf{c}|\boldsymbol{\theta}^*)\right]^2 dx \qquad (4.29) \\ \text{s.t.} \quad & \text{(4.10)-(4.16) and (4.20)} \end{aligned}$$

is equivalent to the following quadratic program:

$$\min_{\mathbf{c}\in\mathbb{R}^{n^*-5}} \quad \frac{1}{2}\mathbf{c}'\mathbf{Q}\mathbf{c} + \mathbf{F}'\mathbf{c} \qquad (4.30)$$

s.t

(i) End points conditions

$$\begin{bmatrix} 1 & 11 & 11 & 1 & 0 & \dots & 0 & 0 & 0 & 0 & 0 \\ -1 & -3 & 3 & 1 & 0 & \dots & 0 & 0 & 0 & 0 & 0 \\ 1 & -1 & -1 & 1 & 0 & \dots & 0 & 0 & 0 & 0 & 0 \\ 0 & 0 & 0 & 0 & 0 & \dots & 0 & 1 & 11 & 11 & 1 \\ 0 & 0 & 0 & 0 & 0 & \dots & 0 & -1 & -3 & 3 & 1 \\ 0 & 0 & 0 & 0 & 0 & \dots & 0 & 1 & -1 & -1 & 1 \end{bmatrix} \mathbf{c} \;=\; \begin{bmatrix} 24\rho_1^* K_1^{\lambda_1^*} \\ 6h\rho_1^*\lambda_1^* K_1^{\lambda_1^*-1} \\ 2h^2\rho_1^*\lambda_1^*(\lambda_1^*-1)K_1^{\lambda_1^*-2} \\ 24(1-\rho_2^* K_N^{-\lambda_2^*}) \\ 6h\rho_2^*\lambda_2^* K_N^{-\lambda_2^*-1} \\ -2h^2\rho_2^*\lambda_2^*(\lambda_2^*+1)K_N^{-\lambda_2^*-2} \end{bmatrix}$$

(ii) Mean-forward price equality condition

$$\left[\int_{K_1}^{K_N} x\, B_{1,4}^{(1)}(x)\,dx \dots \int_{K_1}^{K_N} x\, B_{n-5,4}^{(1)}(x)\,dx\right]\mathbf{c} = S_0 e^{r_f T} - \frac{\rho_1^*\lambda_1^*}{\lambda_1^*+1}K_1^{\lambda_1^*+1} - \frac{\rho_2^*\lambda_2^*}{\lambda_2^*-1}K_N^{-\lambda_2^*+1}$$

(iii) Non-negativity conditions

$$\begin{bmatrix} 0 & -1 & -3 & 3 & 1 & 0 & 0 & 0 & \dots & 0 \\ 0 & 0 & -1 & -3 & 3 & 1 & 0 & 0 & \dots & 0 \\ \vdots & \vdots & & \ddots & \ddots & \ddots & \ddots & \vdots & \vdots & \vdots \\ 0 & \dots & 0 & 0 & -1 & -3 & 3 & 1 & 0 & 0 \\ 0 & \dots & 0 & 0 & 0 & -1 & -3 & 3 & 1 & 0 \end{bmatrix} \mathbf{c} \geq \mathbf{0}.$$

where

$$\begin{aligned} \mathbf{Q} &= \mathbf{G}^\top \mathbf{G} + \omega \mathbf{D}^\top \mathbf{R} \mathbf{D} \\ \mathbf{F} &= -\mathbf{G}^\top \mathbf{W}, \end{aligned}$$

with

$$\mathbf{W} = \begin{bmatrix} P(K_1) + e^{-r_f T} \frac{\rho_1^* \lambda_1^*}{\lambda_1^* + 1} K_1^{\lambda_1^* + 1} \\ \vdots \\ P(K_p) + e^{-r_f T} \frac{\rho_1^* \lambda_1^*}{\lambda_1^* + 1} K_1^{\lambda_1^* + 1} \\ \\ C(K_{p+1}) - e^{-r_f T} \left(\frac{\rho_2^* \lambda_2^*}{\lambda_2^* - 1} K_N^{-\lambda_2^* + 1} - K_{p+1} \right) \\ \vdots \\ C(K_N) - e^{-r_f T} \left(\frac{\rho_2^* \lambda_2^*}{\lambda_2^* - 1} K_N^{-\lambda_2^* + 1} - K_N \right) \end{bmatrix},$$

$$\mathbf{G} = \begin{bmatrix} \mathbf{M_1'} \\ \vdots \\ \mathbf{M_p'} \\ \mathbf{H_{p+1}'} \\ \vdots \\ \mathbf{H_N'} \end{bmatrix},$$

$$\mathbf{H_i} = e^{-r_f T} \begin{bmatrix} K_i B_{1,4}(K_i) + \int_{K_i}^{K_N} x\, B_{1,4}^{(1)}(x)\, dx \\ \vdots \\ K_i B_{n-5,4}(K_i) + \int_{K_i}^{K_N} x\, B_{n-5,4}^{(1)}(x)\, dx \end{bmatrix},$$

$$\mathbf{M_i} = e^{-r_f T} \begin{bmatrix} K_i B_{1,4}(K_i) - \int_{K_1}^{K_i} x\, B_{1,4}^{(1)}(x)\, dx \\ \vdots \\ K_i B_{n-5,4}(K_i) - \int_{K_1}^{K_i} x\, B_{n-5,4}^{(1)}(x)\, dx \end{bmatrix},$$

$$\mathbf{R} = \begin{bmatrix} \frac{h}{3} & \frac{h}{6} & 0 & 0 & \dots & 0 \\ \frac{h}{6} & \frac{2h}{3} & \frac{h}{6} & 0 & \dots & 0 \\ 0 & \frac{h}{6} & \ddots & \ddots & \ddots & \vdots \\ 0 & 0 & \ddots & \ddots & \frac{h}{6} & 0 \\ \vdots & \vdots & \ddots & \frac{h}{6} & \frac{2h}{3} & \frac{h}{6} \\ 0 & 0 & \dots & 0 & \frac{h}{6} & \frac{h}{3} \end{bmatrix},$$

$$\mathbf{D} = \begin{bmatrix} B_{1,4}^{(3)}(x_5) & \cdots & B_{n-5,4}^{(3)}(x_5) \\ \vdots & \vdots & \vdots \\ B_{1,4}^{(3)}(x_{(n-4)}) & \cdots & B_{n-5,4}^{(3)}(x_{n-4}) \end{bmatrix},$$

$$
\begin{aligned}
B_{i,4}^{(3)}(x) &= \left(\frac{z_i}{h^3}\right) I_{[x_i, x_{i+1})}(x) \\
&+ \left(\frac{-4z_i + 5}{h^3}\right) I_{[x_{i+1}, x_{i+2})}(x) \\
&+ \left(\frac{6z_i - 15}{h^3}\right) I_{[x_{i+2}, x_{i+3})}(x) \\
&+ \left(\frac{-4z_i + 15}{h^3}\right) I_{[x_{i+3}, x_{i+4})}(x) \\
&+ \left(\frac{z_i - 5}{h^3}\right) I_{[x_{i+4}, x_{i+5})}(x),
\end{aligned}
$$

$z_i = \frac{x - x_i}{h}$, and $h = x_{i+1} - x_i$. The derivation of the quadratic program (4.30) is given in Appendix C.

4.6 Results

4.6.1 Recovering the RNM PDF

In this section we compare our Quartic B-spline RNM CDF (BSP) method and the SML method with respect to their flexibility in recovering hypothetical actual RNM PDFs. A good RNM estimation technique should be able to recover the true RNMs whatever the complexity of their shape. Therefore, to compare the ability to recover a wide range of different shape of PDFs, the following 12 parametric PDFs are assumed to be a actual RNM PDF.

1. Log-Normal Distribution (LN)
2. Log-Stable Distribution (LS)
3. Double Log-Normal Distribution (DN)
4. Double Log-Stable Distribution (DS)

5. Generalized Two-Factor Log-stable Distribution (GS)

6. Weibull Distribution (WB)

7. Generalized Gamma Distribution (GG)

8. Generalized Beta Distribution (GB)

9. Finite Moment Log-stable Distribution (FS)

10. Variance Gamma Distribution (VG)

11. Poisson Jump Diffusion Process (JD)

12. Jump Diffusion Process with Stochastic Volatility (VG)

The closed form PDFs (or characteristic functions) for the 12 distributions are given in Chapter 3.

First, 12 cross-sections of OTM option prices are generated from each hypothetical actual RNM PDF. The OTM option prices $V(K_i),\ i = 1, 2, \ldots, N$ are calculated at equally spaced strike prices $K_1 < \ldots < K_N$ with $K_{i+1} - K_i = \Delta K$[10] for each hypothetical actual RNM PDF by using the call and put option price functions:

$$\begin{aligned} C(K_i) &= e^{-r_f T} \int_{K_i}^{\infty} (x - K_i)\, p(x)\, dx, \\ P(K_i) &= e^{-r_f T} \int_{0}^{K_i} (K_i - x)\, p(x)\, dx, \quad \text{and} \\ V(K_i) &= \min\left[C(K_i), P(K_i)\right], \end{aligned}$$

where r_f is the risk-free interest rate, T is the time to maturity, and $p(x)$ is the actual RNM PDF. The parameters of the hypothetical actual distributions are chosen to approximate

[10] In our experiment we generate the OTM option prices $V(K_i)$ for 25 strikes K_i in interval $[1100, 1800]$.

a typical cross-section of OTM option prices on the S&P 500 index with 2 months to maturity.

With the generated OTM option prices, we then recover the actual RNM PDF using the BSP method and SML method, respectively. Finally, we measure the closeness between the actual distribution P and the recovered distribution Q by means of Kullback-Leibler Information Criterion (KLIC) divergence:[11]

$$D_{KL}(P\|Q) = \int_0^\infty p(x) \log \frac{p(x)}{q(x)} dx$$

where $p(x)$ and $q(x)$ denotes the PDFs of the actual distribution P and the recovered distribution Q, respectively.

The recovered RNM PDFs are plotted against each actual RNM PDFs for the BSP method in Figure 4.3, and for the SML method in Figure 4.4. These figures suggest that the BSP method is more flexible than the SML method in recovering the actual distributions. The BSP method almost perfectly recovers the actual RNM PDFs for all hypothetical distributional assumptions. In contrast, the SML method is significantly biased and gives negative probability, particularly for some fat-tailed distributions such as stable distributions: LS, DS, and GS. The KLIC divergence between the actual and recovered RNM PDFs for each method are reported in Table 4.1. The KLIC divergence of the BSP method is much less than those of the SML method except for the cases in which the actual RNM PDF is log-normal or double log-normal. The SML method recovers the log-normal distributions relatively well since the biases due to the linear extrapolation property of the natural spline are very small for thin-tailed distributions such as LN and DN.

[11]The Kullback-Leibler divergence is a measure of the difference between two probability distributions: from a "true" probability distribution to an arbitrary probability distribution. Although it is often intuited as a distance metric, the KL divergence is not a true metric since it is not symmetric (hence 'divergence' rather than 'distance').

4.6.2 Monte Carlo Experiments

In the previous section we only compare the accuracy of the two methods using the theoretical OTM option prices which are generated with no pricing errors from the 12 different hypothetical actual RNM PDFs. However, stability to pricing errors is also desirable properties of a good RNM estimation method. Therefore, in this section we perform Monte-Carlo experiments to compare both accuracy and stability of the two methods in the RNM estimation. To test the robustness of alternative methods to pricing errors embedded in OTM option prices, we add noise ϵ_i to the theoretical prices computed in the previous section. Pricing errors ϵ_i are introduced to model observational errors that arise from market imperfections such as non-synchronicity, bid-ask spread, and discreteness, etc.

As pointed out by Andersson and Lomakka (2005), the option pricing errors exhibit dependence and heteroskedasticity over the range of strike prices. To take into account the dependency and heteroskedastic characteristics in the pricing error structures, we specify the pricing errors as a random walk process bounded by the maximum bid-ask spread permitted by the exchange, which is a function of the option prices:

$$\epsilon_i = \max\left[\min\left(\epsilon_{i-1} + \xi_i, 0.5s_i\right), -0.5s_i\right], \quad i = 1, \ldots, N, \ \epsilon_0 = 0,$$

where ξ_i is independently and uniformly distributed on $[-.5s_i, 0.5s_i]$, and s_i is the maximum bid-ask spread which depends on the strike K_i.[12] In the experiment, the actual RNM PDFs are modeled by the 12 parametric distributions as in the previous section. Parameters of these distributions are chosen to fit a randomly selected cross-section from the S&P 500

[12]The maximum bid-ask spread permitted by the exchange is linked to the option quotes. For instance, the CBOE rules state that the maximum bid-ask spread is 1/4 for options with bid quote below \$2, 3/8 for bid quotes between \$2 and \$5, 1/2 for bid quotes between \$5 and \$10, . . . ,and so on.

$$s_i = M(K_i)$$

The function $M(\cdot)$ is constructed to represent such rules. See Bondarenko (2003) for details on the construction of $M(\cdot)$.

index options dataset. For given an actual RNM PDF, we simulate 500 cross-sections of OTM option prices with pricing errors for each scenario and apply the two methods to estimate the corresponding RNM PDFs.

We measure accuracy and stability of RNM estimators by means of the root mean integrated squared errors (RMISE) criterion as in Bondarenko (2003). Let $\hat{\mathrm{p}}(x)$ be the estimator of risk neutral density $\mathrm{p}(x)$, then the (normalized) RMISE for the density estimator is defined as:

$$\begin{aligned}\mathrm{RMISE}(\hat{\mathrm{p}}) &= \frac{1}{||\mathrm{p}(x)||}\left(E[||\hat{\mathrm{p}}(x)-\mathrm{p}(x)||^2]\right)^{1/2} \\ &= \frac{1}{||\mathrm{p}(x)||}\left(E\left[\int_0^\infty (\hat{\mathrm{p}}(x)-\mathrm{p}(x))^2\,\mathrm{d}x\right]\right)^{1/2}.\end{aligned}$$

Simliarly to the MSE for the point estimator, the RMISE may be decomposed as:

$$\mathrm{RMISE}^2(\hat{\mathrm{p}}) = \mathrm{RISB}^2(\hat{\mathrm{p}}) + \mathrm{RIV}^2(\hat{\mathrm{p}}),$$

where

$$\begin{aligned}\mathrm{RISB}(\hat{p}) &= \frac{1}{||\mathrm{p}(x)||}\left(\int_0^\infty (E[\hat{\mathrm{p}}(x)]-\mathrm{p}(x))^2\,\mathrm{d}x\right)^{1/2}, \\ \mathrm{RIV}(\hat{p}) &= \frac{1}{||\mathrm{p}(x)||}\left(\int_0^\infty E\left[(\hat{\mathrm{p}}(x)-E[\hat{\mathrm{p}}(x)])^2\right]\mathrm{d}x\right)^{1/2},\end{aligned}$$

$||\cdot||$ is the L_2 norm, RISB is the (normalized) root integrated squared bias, and RIV is the (normalized) root integrated variance. Intuitively, RMISE is a measure of the overall quality of the estimator, RISB is a measure of the accuracy, and RIV is a measure of the stability. This decomposition allows us to study the relative contributions of the bias (RISB) and the variability (RIV) to RMISE of different models.

Monte-Carlo experiments are conducted based on the following 12 scenarios:

Scenario *i*: *i* distribution is the true RNM PDF,

where i=LN, LS, DN, DS, DS, GS, WB, GG, GB, FS, JD, and JS. The resulting true RNM PDFs p(x) for each scenario are depicted by the dashed lines in Figure 4.5 and Figure 4.6, respectively. For each scenario, the estimated 500 RNM PDFs from the two method are plotted against the true RNM PDFs in Figure 4.5 and Figure 4.6, respectively. It can be seen that the SML is significantly biased, particularly on the left tail of the distribution. The associated RMISE statistics for the 12 scenarios are also presented in Table 4.2. The results for the BSP method are displayed on the left panel. Examining the RMISE statistics from the two methods, we find that the BSP provides lower RMISE than the SML does in most scenarios except for LN and DN. Particularly, under the scenarios that the true RNM is fat-tailed distribution such as LS, DS, FS, and GS, the SML method reveals large biases from the true RNM PDFs. This result indicates better overall quality of the BSP as a RNM estimator. Examining the RISB and the RIV reveals that the large bias from the true RNM PDF is the main cause of the relatively poor performance of the SML method.

4.7 Concluding Remarks

In this chapter, we propose a new nonparametric RNM estimation method which overcomes the problems with the smoothed implied volatility smile (SML) method. In our new approach, we model a RNM CDF using quartic B-splines with power tails. With the power tails, the estimated RNM has nonnegative tail probabilities and also reflects information about true tail probabilities. Since the RNM CDFs are constructed using quartic B-spline functions, the resulting RNM PDFs have continuity C^2. The use of B-spline also improves computational efficiency and reduces the number of spline parameters. The advantage of constructing the RNM CDF with power tails is that the sum of RNM probabilities is guaranteed to be unity. We also choose the optimum number of knots so that our method avoids both overfitting and oversmoothing.

Our nonparametric approach involves solving a highly nonlinear optimization problem with a number of constraints due to the power tails. It is computationally difficult and inaccurate to estimate the B-spline part of the CDF and the power tails simultaneously. To improve computational efficiency and accuracy we develop a 3-step RNM estimation technique: (i) estimate the power tail parameters; (ii) select the optimum number of the knots; and (iii) estimate the B-spline control points. The 3-step estimation procedure transforms a nonlinear optimization problem into a convex quadratic programming which is efficiently solved by numerical optimization software.

The Monte-Carlo experiments suggest that the BSP method performs considerably better than the SML method as a technique for estimating option implied RNM. The SML method violates the no-arbitrage constrains, and is also significantly biased, particularly under the scenarios that the ture RNM is a fat-tailed distribution. In contrast, the BSP method always produces arbitrage-free RNM estimators, and almost perfectly recovers the actual RNM PDFs for all hypothetical distributional assumptions.

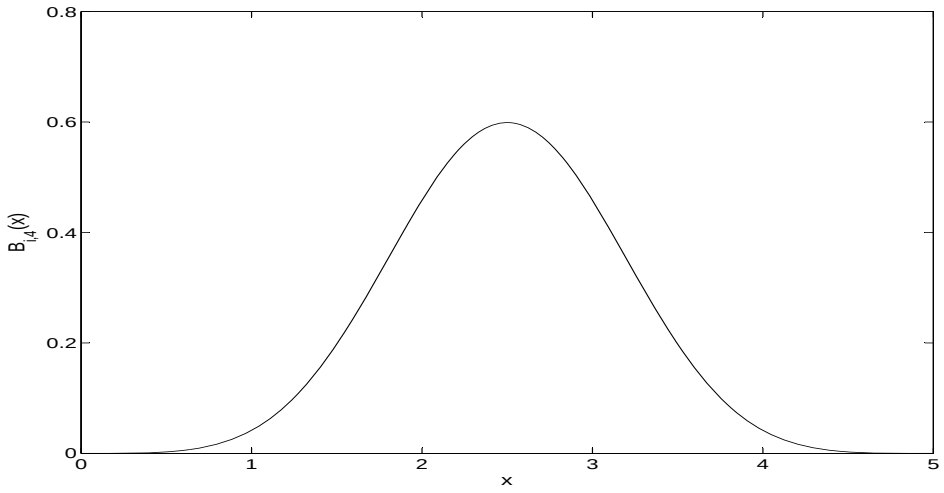

Figure 4.1: Uniform Quartic B-Spline Basis Function, where $x_i = 0$ and $\Delta x = 1$

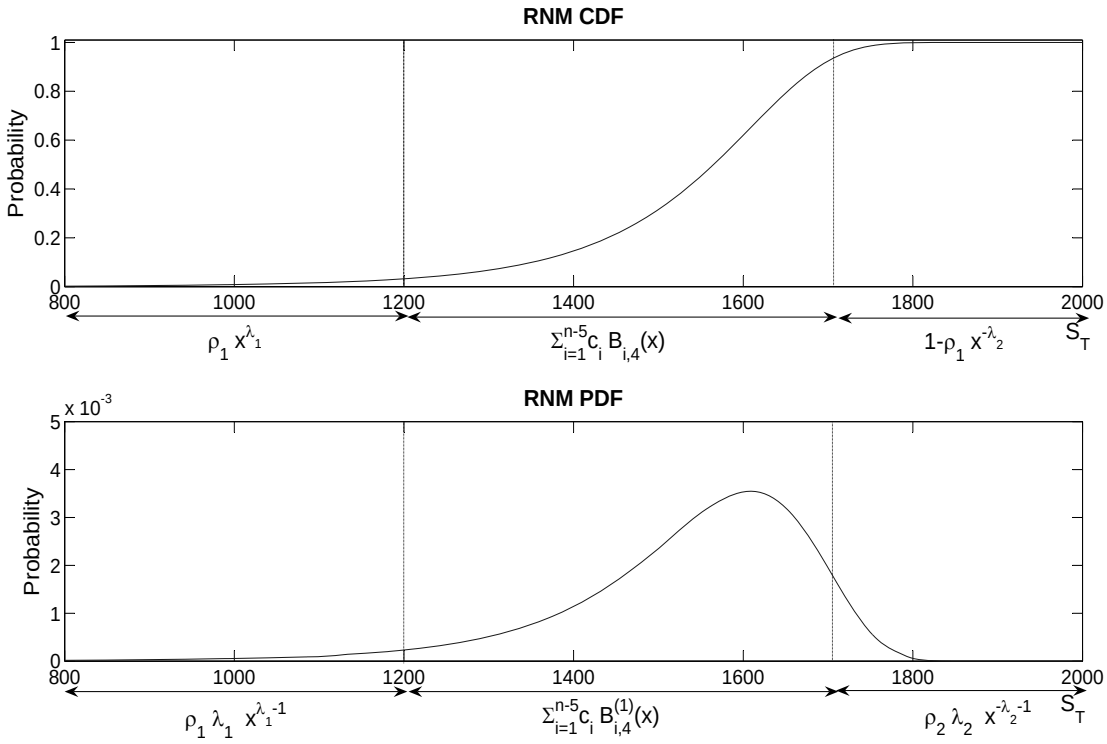

Figure 4.2: Quartic B-Spline RNM CDF and PDF with Powr Tails

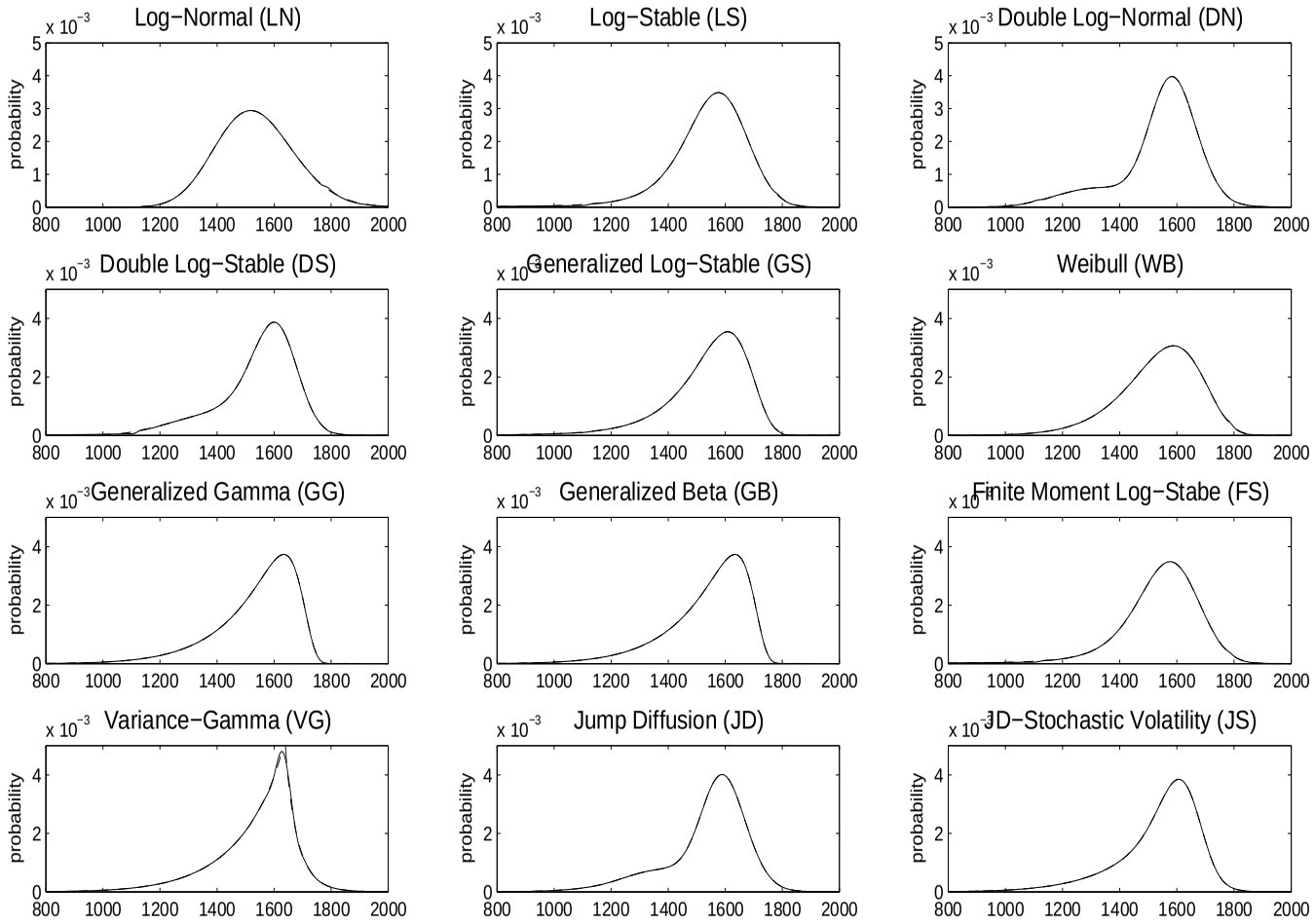

Figure 4.3: BSP method: Recovering the hypothetical actual RNM PDF. The dashed lines are actual RNM PDFs and the solid lines are recovered RNM PDFs by the BSP method.

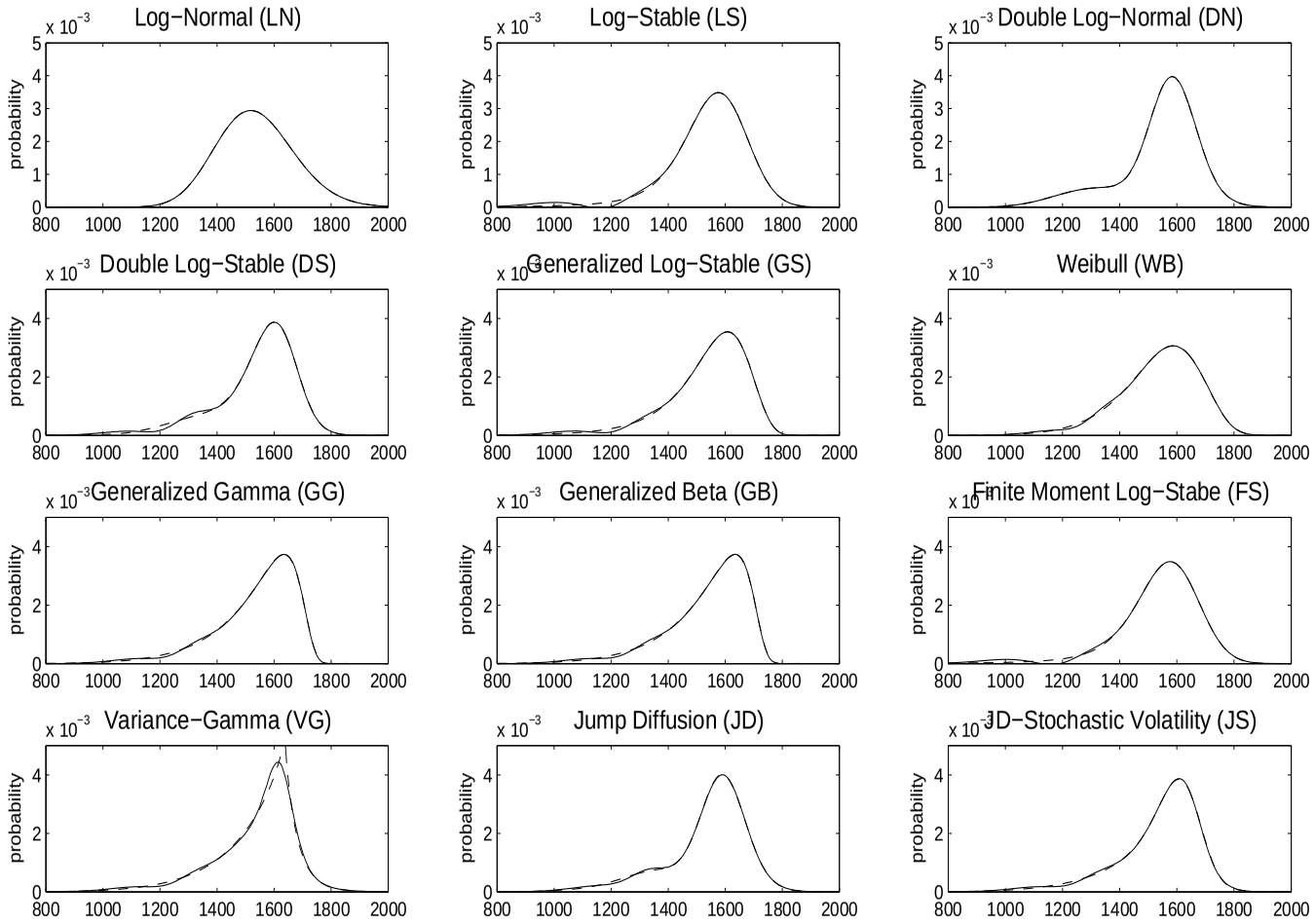

Figure 4.4: SML method: Recovering the hypothetical actual RNM PDF. The dashed lines are actual RNM PDFs and the solid lines are recovered RNM PDFs by the SML method.

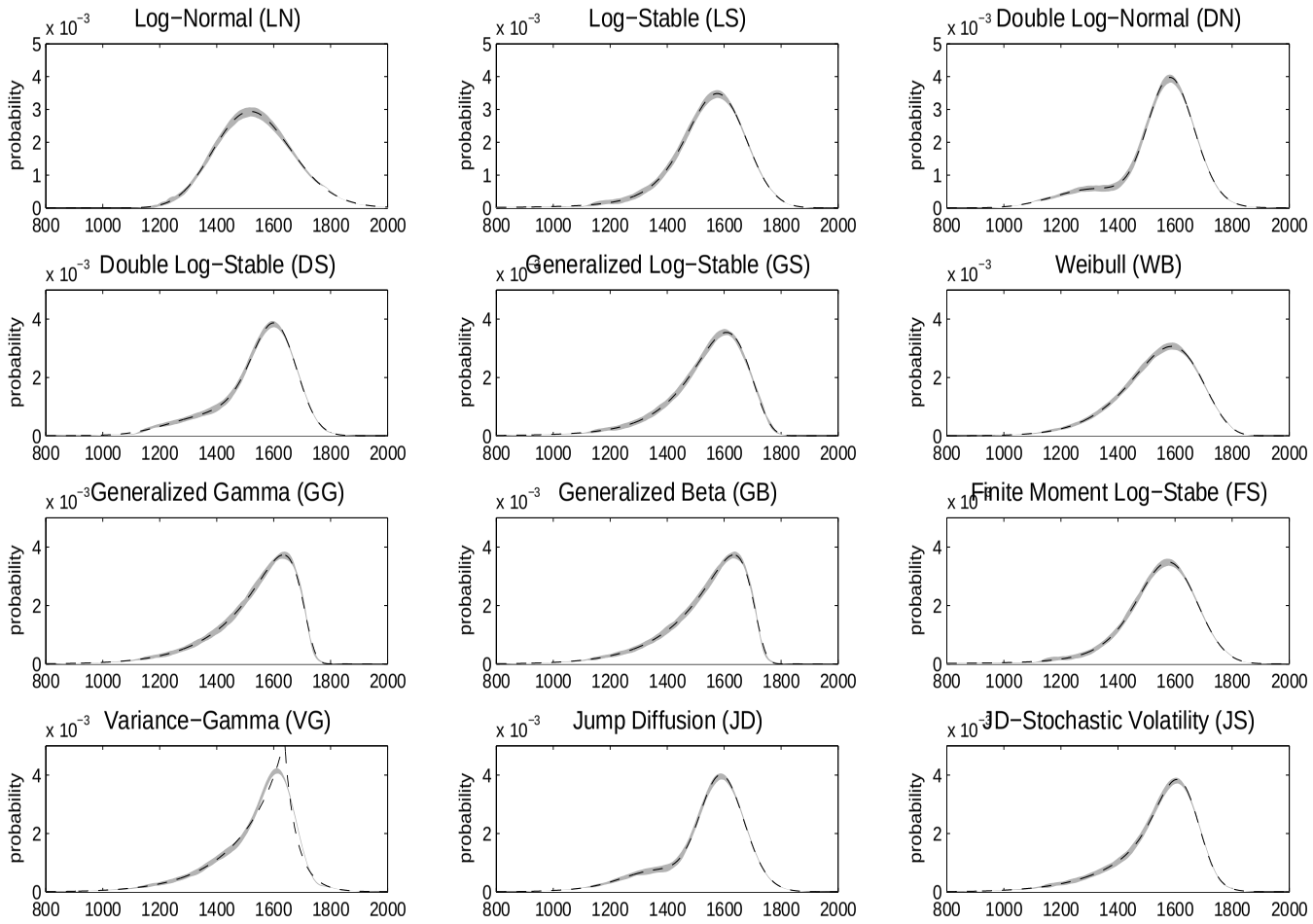

Figure 4.5: BSP method: Monte Carlo Experiments. The dashed lines are true RNM PDFs and the grey areas are the ranges of estimated RNM PDFs by the BSP method.

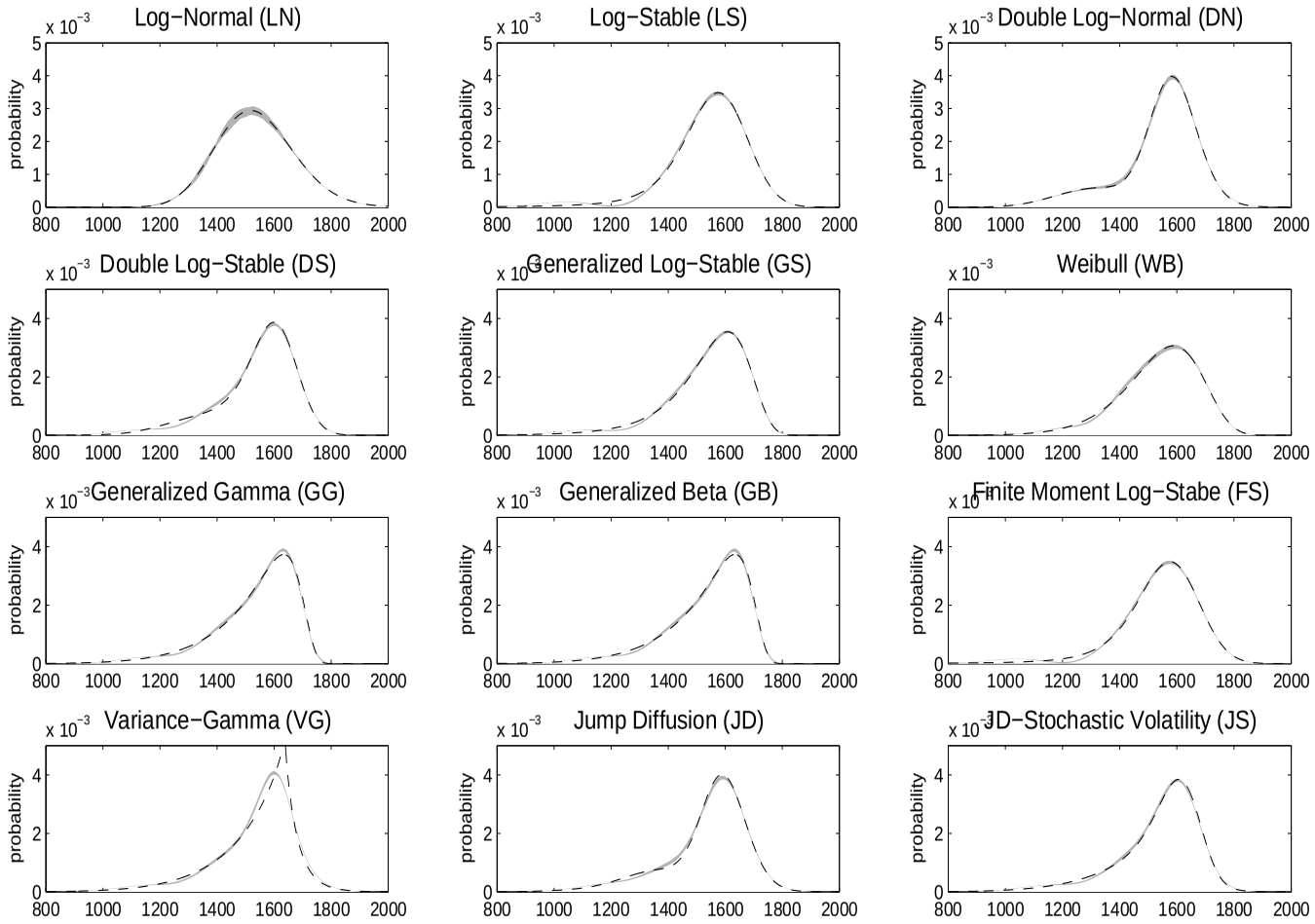

Figure 4.6: SML method: Monte Carlo Experiments. The dashed lines are true RNM PDFs and the grey areas are the ranges of estimated RNM PDFs by the SML method.

Actual RNM	BSP Method	SML Method
LN	0.0006	0.0000
LS	0.0013	0.0305
DN	0.0001	0.0000
DS	0.0013	0.0073
GS	0.0000	0.0042
WB	0.0002	0.0019
GG	0.0000	0.0020
GB	0.0000	0.0020
FS	0.0013	0.0305
VG	0.0004	0.0050
JD	0.0000	0.0016
JS	0.0000	0.0019
AVG	0.0004	0.0072

Note: The KLIC divergences are computed based on 12 sets of cross-section of the OTM option prices from the 12 hypothetical actual RNM PDF for each method.

Table 4.1: Kullback-Leibler Information Criterion (KLIC) Divergence

	BSP Method			SML Method		
Scenario	RMISE	RISB	RIV	RMISE	RISB	RIV
LN	0.0229	0.0091	0.0210	0.0194	0.0024	0.0192
LS	0.0200	0.0068	0.0188	0.0466	0.0459	0.0082
DN	0.0213	0.0114	0.0180	0.0192	0.0162	0.0102
DS	0.0233	0.0149	0.0180	0.0502	0.0495	0.0087
GS	0.0253	0.0116	0.0225	0.0373	0.0363	0.0087
WB	0.0189	0.0048	0.0183	0.0350	0.0333	0.0105
GG	0.0304	0.0204	0.0226	0.0422	0.0410	0.0101
GB	0.0309	0.0207	0.0229	0.0419	0.0407	0.0099
FS	0.0199	0.0068	0.0187	0.0465	0.0458	0.0081
VG	0.1214	0.1202	0.0175	0.1593	0.1591	0.0087
JD	0.0223	0.0138	0.0176	0.0440	0.0430	0.0096
JS	0.0229	0.0134	0.0185	0.0379	0.0368	0.0090
AVG	0.0316	0.0211	0.0195	0.0483	0.0458	0.0101

Note: The RMISE is decomposed as $\text{RMISE}^2(\hat{p}) = \text{RISB}^2(\hat{p})+\text{RIV}^2(\hat{p})$. The RMISEs are computed based on 500 simulated sets of cross-section data on S&P 500 index options with 2 months to maturity under the 12 scenarios for each method

Table 4.2: Root Mean Integrated Squared Errors (RMISE)

CHAPTER 5

CONCLUSION

The risk-neutral measure of the future asset prices can be estimated from the currently observed cross-section of option prices with the same time-to-maturity. The estimated RNM of the asset prices provides valuable information about the market's expectations on the future movement of asset prices.

This dissertation develops two new parametric and nonparametric methods for estimating risk-neutral measures, and investigates empirical performance of parametric RNM estimation methods.

The generalized two-factor log-stable option pricing model in Chapter 2 is a highly integrated approach to evaluating contingent claims in the sense that it provides the state prices, the pricing kernel, and the risk neutral measure explicitly. The RNM can be simply derived by adjusting the FM for the state-contingent value of the numeraire. Under generalized two-factor log-stable uncertainty the RNM is expressed as a convolution of two exponentially tilted stable distributions, while the FM itself is a pure stable distribution. Furthermore, the generalized two-factor log-stable RNM has a very flexible parametric form for approximating other probability distributions. Thus, this model also provides a considerably accurate tool for estimating the RNM from the observed option prices even though the generalized two-factor log-stable assumption might not be satisfied.

The empirical results of the RNM estimation from the S&P 500 index options shows that the generalized two-factor log-stable model gives better performance than the Black-

Scholes log-normal model, the finite moment log-stable model and the orthogonal log-stable model in fitting the observed option prices. Moreover, the distributional assumption for the generalized stable model is consistent with the implied volatility structure, which violates the lognormal assumption of the Black-Scholes model.

In Chapter 2, I implement 12 parametric RNM estimation methods by means of the closed form of RNM distributions or RNM characteristic functions. I then compared the empirical performance of the 12 parametric RNM estimation methods under three criteria—the root mean squared error (RMSE) for the goodness-of-fit, likelihood ratio (LR) for the model selection, and the root mean integrated squared error (RMISE) for the accuracy and stability of the estimated RNMs.

The empirical results show that the generalized two-factor log-stable model in Chapter 2 outperforms other alternative parametric RNM estimation methods. The RMSEs and the LR tests indicate that the generalized two-factor log-stable model and the jump diffusion model with stochastic volatilities dominate other models. However, the jump diffusion model with stochastic volatilities model is vulnerable to over-fitting problems due to a large number of parameters. Our Monte-Carlo experiments reveal that the jump diffusion with stochastic volatilities suffers from serious over-fitting problems and also show that the generalized two-factor log-stable model outperforms the alternatives.

In Chapter 4, I propose a new nonparametric RNM estimation method which overcomes the problems with the smoothed implied volatility smile (SML) method which is the most widely used nonparametric technique for estimating RNMs. In this new approach, I model the RNM CDF using quartic B-spline with power tails. With the power tails, the estimated RNM has nonnegative tail probabilities and also reflects information about true tail probabilities. Since the RNM CDFs are constructed using quartic B-spline functions, the resulting RNM PDFs have continuity C^2. The use of B-spline also improves computational efficiency and reduces the number of spline parameters. The advantage of constructing the RNM CDF with power tails is that the sum of RNM probabilities is guaranteed to be unity.

We also choose the optimum number of knots so that our method avoids both overfitting and oversmoothing.

Our nonparametric approach involves solving a highly nonlinear optimization problem with a number of constraints due to the power tails. It is computationally difficult and inaccurate to estimate the B-spline part of the CDF and the power tails simultaneously. To improve computational efficiency and accuracy we develop a 3-step RNM estimation technique: (i) estimate the power tail parameters; (ii) select the optimum number of the knots; and (iii) estimate the B-spline control points. The 3-step estimation procedure transforms a nonlinear optimization problem into a convex quadratic programming which is efficiently solved by numerical optimization software.

The Monte-Carlo experiments suggest that the BSP method performs considerably better than the SML method as a technique for estimating option implied RNM. The SML method violates the no-arbitrage constrains, and is also significantly biased, particularly under the scenarios that the true RNM is a fat-tailed distribution. In contrast, the BSP method always produces arbitrage-free RNM estimators, and almost perfectly recovers the actual RNM PDFs for all hypothetical distributional assumptions.

APPENDIX A

DERIVATION OF THE GENERALIZED TWO-FACTOR LOG-STABLE RNM

A.1 Derivation of (2.18)

The joint distribution of v_N and v_A can be expressed as

$$\begin{aligned} h(v_N, v_A) &= h(v_N, v_N + z) \\ &= \frac{1}{|c_{N1}c_{A2} - c_{N2}c_{A1}|} f_{U_1U_2}(u_1, u_2), \end{aligned} \tag{A.1}$$

where $f_{U_1U_2}(u_1, u_2)$ is the joint distribution of two factors u_1 and u_2.

Since

$$\begin{aligned} z &\equiv \log S_T = v_A - v_N \\ &= -(c_{N1} - c_{A1})u_1 - (c_{N2} - c_{A2})u_2 + \delta \end{aligned} \tag{A.2}$$

and

$$\begin{aligned} u_1 &= -\frac{c_{N2} - c_{A2}}{c_{N1} - c_{A1}}u_2 - \frac{1}{c_{N1} - c_{A1}}z + \frac{1}{c_{N1} - c_{A1}}\delta \\ &= -\frac{c_{N2} - c_{A2}}{c_{N1} - c_{A1}}u_2 - \frac{1}{c_{N1} - c_{A1}}(z - \delta), \end{aligned} \tag{A.3}$$

the log marginal utility of numerarie v_N can be written as follows:

$$\begin{aligned} v_N &= c_{N1}\left(-\frac{c_{N2}-c_{A2}}{c_{N1}-c_{A1}}u_2 - \frac{1}{c_{N1}-c_{A1}}(z-\delta)\right) + c_{N2}u_2 \\ &= \left(\frac{c_{N2}c_{N1}-c_{N2}c_{A1}-c_{N1}c_{N2}+c_{N1}c_{A2}}{c_{N1}-c_{A1}}u_2\right) - \frac{c_{N1}}{c_{N1}-c_{A1}}(z-\delta) \\ &= -\frac{c_{N2}c_{A1}-c_{N1}c_{A2}}{c_{N1}-c_{A1}}u_2 - \frac{c_{N1}}{c_{N1}-c_{A1}}(z-\delta) \end{aligned} \tag{A.4}$$

By substituting (A.1), (A.2) and (A.4) into (2.12), we have

$$\begin{aligned} q(z) &= \frac{1}{EU_N}\int_{-\infty}^{\infty} e^{v_N} h(v_N, v_N+z)dv_N \\ &= \frac{1}{EU_N}\int_{-\infty}^{\infty} e^{-\frac{c_{N2}c_{A1}-c_{N1}c_{A2}}{c_{N1}-c_{A1}}u_2 - \frac{c_{N1}}{c_{N1}-c_{A1}}(z-\delta)} \cdot \\ &\quad \frac{1}{|c_{N1}c_{A2}-c_{N2}c_{A1}|} f_{U_1U2}(u_1,u_2)\left|\frac{|c_{N1}c_{A2}-c_{N2}c_{A1}|}{c_{N1}-c_{A1}}\right| du_2 \\ &= \frac{1}{|c_{N1}-c_{A1}|}\frac{1}{EU_N}\int_{-\infty}^{\infty} e^{-\frac{c_{N2}c_{A1}-c_{N1}c_{A2}}{c_{N1}-c_{A1}}u_2 - \frac{c_{N1}}{c_{N1}-c_{A1}}(z-\delta)} \cdot \\ &\quad f_{U_1U_2}\left(-\frac{z-\delta+(c_{N2}-c_{A2})u_2}{c_{N1}-c_{A1}}, u_2\right) du_2. \end{aligned} \tag{A.5}$$

By using (A.3), the joint distribution of u_1 and u_2 can be expressed as:

$$\begin{aligned} & f_{U_1U_2}\left(-\frac{z-\delta+(c_{N2}-c_{A2})u_2}{c_{N1}-c_{A1}}, u_2\right) \\ = \;& s(u_2;\alpha,-1,1,0)\, s\left(-\frac{z-\delta+(c_{N2}-c_{A2})u_2}{c_{N1}-c_{A1}};\alpha,-1,1,0\right) \\ = \;& |c_{N1}-c_{A1}| s(u_2;\alpha,-1,1,0)\, s(z;\alpha,\mathrm{sgn}(c_{N1}-c_{A1}),|c_{N1}-c_{A1}|,\delta+(c_{N2}-c_{A2})u_2) \end{aligned} \tag{A.6}$$

Plugging (A.6) into (A.5), we finally have the stable RNM pdf:

$$\begin{aligned} q(z) &= \frac{1}{EU_N}\int_{-\infty}^{\infty} e^{-\frac{c_{N2}c_{A1}-c_{N1}c_{A2}}{c_{N1}-c_{A1}}u_2-\frac{c_{N1}}{c_{N1}-c_{A1}}(z-\delta)}\cdot s(u_2;\alpha,-1,1,0) \\ & \quad s(z;\alpha,\mathrm{sgn}(c_{N1}-c_{A1}),|c_{N1}-c_{A1}|,\delta-(c_{N2}-c_{A2})u_2)du_2. \end{aligned} \tag{A.7}$$

A.2 Proof of (2.19) and Derivation of (2.20)

The generalized two-factor log-stable RNM is a convolution of two exponentially tilted stable distributions:

$$q(z) = \overset{2}{\underset{j=1}{\circledast}} ts_{\mathrm{sgn}(c_{Nj}-c_{Aj})}\left(z_j;\alpha,|c_{Nj}-c_{Aj}|,\delta_j,\left|\frac{c_{Nj}}{c_{Nj}-c_{Aj}}\right|\right)$$

Proof.

From (A.7), the CF of the generalized two-factor log-stable RNM is written as:

$$\begin{aligned} cf_q(t) &= \int_{-\infty}^{\infty} e^{itz}q(z)dz \\ &= \frac{1}{EU_N}\int_{-\infty}^{\infty} e^{-\frac{c_{N2}c_{A1}-c_{N1}c_{A2}}{c_{N1}-c_{A1}}u_2+\frac{c_{N1}}{c_{N1}-c_{A1}}\delta}s(u_2;\alpha,-1,1,0)\cdot \\ & \quad \int_{-\infty}^{\infty} e^{-\left(\frac{c_{N1}}{c_{N1}-c_{A1}}-it\right)z}\, s(z;\alpha,\mathrm{sgn}(c_{N1}-c_{A1}),|c_{N1}-c_{A1}|,\delta-(c_{N2}-c_{A2})u_2)dz\,du_2. \end{aligned} \tag{A.8}$$

Using the properties of sign function, we have:

$$\text{I.} \quad -\left(\frac{c_{N1}}{c_{N1}-c_{A1}} - it\right)z$$
$$= \; -\operatorname{sgn}(c_{N1}-c_{A1})\left(\left|\frac{c_{N1}}{c_{N1}-c_{A1}}\right| - \operatorname{sgn}(c_{N1}-c_{A1})it\right)z \tag{A.9}$$

$$\text{II.} \quad \left(-\frac{c_{N2}c_{A1}-c_{N1}c_{A2}}{c_{N1}-c_{A1}} + \operatorname{sgn}(c_{N1}-c_{A1})(c_{N2}-c_{A2})\left(\left|\frac{c_{N1}}{c_{N1}-c_{A1}}\right| - \operatorname{sgn}(c_{N1}-c_{A1})it\right)\right)u_2$$
$$= \; (c_{N2}-(c_{N2}-c_{A2}))\,u_2 \tag{A.10}$$

$$\text{III.} \quad -\operatorname{sgn}(c_{N1}-c_{A1})\left(\left|\frac{c_{N1}}{c_{N1}-c_{A1}}\right| - \operatorname{sgn}(c_{N1}-c_{A1})it\right)\delta$$
$$-\left(\left|\frac{c_{N1}}{c_{N1}-c_{A1}}\right| - \operatorname{sgn}(c_{N1}-c_{A1})it\right)^{\alpha}|c_{N1}-c_{A1}|^{\alpha}\sec\left(\frac{\pi\alpha}{2}\right) + \frac{c_{N1}}{c_{N1}-c_{A1}}\delta$$
$$= \delta it - \left(\left|\frac{c_{N1}}{c_{N1}-c_{A1}}\right| - \operatorname{sgn}(c_{N1}-c_{A1})it\right)^{\alpha}|c_{N1}-c_{A1}|^{\alpha}\sec\left(\frac{\pi\alpha}{2}\right) \tag{A.11}$$

By using (A.9), the inner integration term in (A.8) may be written as:

$$\int_{-\infty}^{\infty} e^{-\operatorname{sgn}(c_{N1}-c_{A1})\left(\left|\frac{c_{N1}}{c_{N1}-c_{A1}}\right| - \operatorname{sgn}(c_{N1}-c_{A1})it\right)z} \cdot$$
$$s(z;\alpha,\operatorname{sgn}(c_{N1}-c_{A1}),|c_{N1}-c_{A1}|,\delta-(c_{N2}-c_{A2})u_2)dz$$
$$= \; \exp\Big[-\operatorname{sgn}(c_{N1}-c_{A1})\left(\left|\frac{c_{N1}}{c_{N1}-c_{A1}}\right| - \operatorname{sgn}(c_{N1}-c_{A1})it\right)(\delta-(c_{N2}-c_{A2})u_2)$$
$$-\left(\left|\frac{c_{N1}}{c_{N1}-c_{A1}}\right| - \operatorname{sgn}(c_{N1}-c_{A1})it\right)^{\alpha}|c_{N1}-c_{A1}|^{\alpha}\sec\left(\frac{\pi\alpha}{2}\right)\Big] \tag{A.12}$$

By using (A.10), (A.11), and (A.12), the CF of the RNM may be expressed as:

$$\begin{aligned} cf_q(t) &= \frac{1}{EU_N} e^{\delta it - \left(\left|\frac{c_{N1}}{c_{N1}-c_{A1}}\right| - \mathrm{sgn}(c_{N1}-c_{A1})it\right)^{\alpha} |c_{N1}-c_{A1}|^{\alpha} \sec\left(\frac{\pi\alpha}{2}\right)} \cdot \\ &\qquad \int_{-\infty}^{\infty} e^{c_{N2}-(c_{N2}-(c_{N2}-c_{A2})it)u_2} s(u_2;\alpha,-1,1,0)\, du_2. \end{aligned} \tag{A.13}$$

Let

$$w = (c_{N2} - c_{A2})u_2, \tag{A.14}$$

so that

$$\left|\frac{du_2}{dw}\right| = \frac{1}{|c_{N2} - c_{A2}|}. \tag{A.15}$$

With (A.14) and (A.15), the integral term of (A.13) is written as:

$$\begin{aligned} &\int_{-\infty}^{\infty} e^{c_{N2}-(c_{N2}-(c_{N2}-c_{A2})it)u_2} s(u_2;\alpha,-1,1,0)\, du_2 \\ &= \int_{-\infty}^{\infty} e^{\left(\frac{c_{N2}}{c_{N2}-(c_{N2}-c_{A2}} - it\right)w} s\left(\frac{1}{c_{N2}-c_{A2}} w;\alpha,-1,1,0\right) \frac{1}{|c_{N2}-c_{A2}|}\, dw \\ &= \exp\left[-\left(\left|\frac{c_{N2}}{c_{N2}-c_{A2}}\right| - \mathrm{sgn}(c_{N2}-c_{A2})it\right)^{\alpha} |c_{N2}-c_{A2}|^{\alpha} \sec\left(\frac{\pi\alpha}{2}\right)\right]. \end{aligned} \tag{A.16}$$

By Property 2 of stable distributions, the expected marginal utility of numeraire is

$$\begin{aligned} EU_N &= E\, e^{v_N} = \exp(\delta_2 - c_N^{\alpha} \sec\left(\frac{\pi\alpha}{2}\right)) \\ &= \exp\left(-(c_{N1}^{\alpha} + c_{N2}^{\alpha}) \sec\left(\frac{\pi\alpha}{2}\right)\right). \end{aligned} \tag{A.17}$$

By substituting (A.16), and (A.17) into (A.13), the CF of the RNM is taken to be

$$\begin{aligned} cf_q(t) &= \exp\left\{ i\delta t + |c_{N1}-c_{A1}|^{\alpha}\sec\left(\frac{\pi\alpha}{2}\right)\left[\left|\frac{c_{N1}}{c_{N1}-c_{A1}}\right|^{\alpha} - \left(\left|\frac{c_{N1}}{c_{N1}-c_{A1}}\right| - \mathrm{sgn}(c_{N1}-c_{A1})it\right)^{\alpha}\right] \right. \\ &\quad \left. + |c_{N2}-c_{A2}|^{\alpha}\sec\left(\frac{\pi\alpha}{2}\right)\left[\left|\frac{c_{N2}}{c_{N2}-c_{A2}}\right|^{\alpha} - \left(\left|\frac{c_{N2}}{c_{N2}-c_{A2}}\right| - \mathrm{sgn}(c_{N2}-c_{A2})it\right)^{\alpha}\right]\right\}. \end{aligned}$$

Finally, the log CF of the RNM is

$$\begin{aligned} \log cf_q(t) &= i\delta t + |c_{N1}-c_{A1}|^{\alpha}\sec\left(\frac{\pi\alpha}{2}\right)\left[\left|\frac{c_{N1}}{c_{N1}-c_{A1}}\right|^{\alpha} - \left(\left|\frac{c_{N1}}{c_{N1}-c_{A1}}\right| - \mathrm{sgn}(c_{N1}-c_{A1})it\right)^{\alpha}\right] \\ &\quad + |c_{N2}-c_{A2}|^{\alpha}\sec\left(\frac{\pi\alpha}{2}\right)\left[\left|\frac{c_{N2}}{c_{N2}-c_{A2}}\right|^{\alpha} - \left(\left|\frac{c_{N2}}{c_{N2}-c_{A2}}\right| - \mathrm{sgn}(c_{N2}-c_{A2})it\right)^{\alpha}\right]. \end{aligned} \tag{A.18}$$

An exponentially tilted stable distribution

$$\begin{aligned} & ts_{\mathrm{sgn}(c_{Nj}-c_{Aj})}\left(z;\alpha,|c_{Nj}-c_{Aj}|,\delta_j,\left|\frac{c_{Nj}}{c_{Nj}-c_{Aj}}\right|\right) \\ &= k\, e^{-\mathrm{sgn}(c_{Nj}-c_{Aj})\left|\frac{c_{Nj}}{c_{Nj}-c_{Aj}}\right| z}\, s\left(x;\alpha,\mathrm{sgn}(c_{Nj}-c_{Aj}),|c_{Nj}-c_{Aj}|,\delta_j\right) \end{aligned}$$

has the CF:

$$\begin{aligned} cf_{ts,j}(t) &= k\int_{-\infty}^{\infty} e^{-\left(\mathrm{sgn}(c_{Nj}-c_{Aj})\left|\frac{c_{Nj}}{c_{Nj}-c_{Aj}}\right|-it\right)z}\, s\left(z;\alpha,\mathrm{sgn}(c_{Nj}-c_{Aj}),|c_{Nj}-c_{Aj}|,\delta_j\right)dz \\ &= k\, e^{-\left(\mathrm{sgn}(c_{Nj}-c_{Aj})\left|\frac{c_{Nj}}{c_{Nj}-c_{Aj}}\right|-it\right)\delta_j - \left(\left|\frac{c_{Nj}}{c_{Nj}-c_{Aj}}\right|-\mathrm{sgn}(c_{Nj}-c_{Aj})it\right)^{\alpha}|c_{Nj}-c_{Aj}|^{\alpha}\sec\left(\frac{\pi\alpha}{2}\right)}. \end{aligned}$$

Since

$$cf_{ts,j}(0) \;=\; k\,\exp\Big[-\operatorname{sgn}(c_{Nj}-c_{Aj})\left|\frac{c_{Nj}}{c_{Nj}-c_{Aj}}\right|\delta_j - \left|\frac{c_{Nj}}{c_{Nj}-c_{Aj}}\right|^{\alpha}|c_{Nj}-c_{Aj}|^{\alpha}\sec\left(\frac{\pi\alpha}{2}\right)\Big] \equiv 1,$$

we must have

$$k \;=\; \exp\Big[\operatorname{sgn}(c_{Nj}-c_{Aj})\left|\frac{c_{Nj}}{c_{Nj}-c_{Aj}}\right|\delta_j + \left|\frac{c_{Nj}}{c_{Nj}-c_{Aj}}\right|^{\alpha}|c_{Nj}-c_{Aj}|^{\alpha}\sec\left(\frac{\pi\alpha}{2}\right)\Big],$$

hence

$$cf_{ts,j}(t) = \exp\left\{i\delta_j t + |c_{Nj}-c_{Aj}|^{\alpha}\sec\left(\frac{\pi\alpha}{2}\right)\left[\left|\frac{c_{Nj}}{c_{Nj}-c_{Aj}}\right|^{\alpha} - \left(\left|\frac{c_{Nj}}{c_{Nj}-c_{Aj}}\right| - \operatorname{sgn}(c_{Nj}-c_{Aj})it\right)^{\alpha}\right]\right\}.$$

Finally, the log CF of the tilted stable distribution is

$$\log cf_{ts,j}(t) \;=\; i\delta_j t + |c_{Nj}-c_{Aj}|^{\alpha}\sec\left(\frac{\pi\alpha}{2}\right)\left[\left|\frac{c_{Nj}}{c_{Nj}-c_{Aj}}\right|^{\alpha} - \left(\left|\frac{c_{Nj}}{c_{Nj}-c_{Aj}}\right| - \operatorname{sgn}(c_{Nj}-c_{Aj})it\right)^{\alpha}\right]. \tag{A.19}$$

Combining (A.18) and (A.19), we have

$$\log cf_q(t) \;=\; \sum_{j=1}^{2}\log cf_{ts,j}(t).$$

Since the log CF of the convolution of two densities is the sum of their respective log CFs, the generalized RNM $q(z)$ is such a convolution of two exponentially tilted stable densities. □

APPENDIX B

DERIVATION OF THE OPTION PRICING FUNCTION UNDER THE B-SPLINE RNM CDF WITH POWER TAILS

I. The case $K < K_1$

$$
\begin{aligned}
& C(K;\mathbf{c},\boldsymbol{\theta}) \\
= \;& e^{-r_f T}\int_K^{\infty} x\,R'(x)\,dx - Ke^{-r_f T}\int_K^{\infty} R'(x)\,dx \\
= \;& e^{-r_f T}\left[\int_K^{\infty} x\,R'(x)\,dx - K\left(1-R(K)\right)\right] \\
= \;& e^{-r_f T}\left[\int_K^{K_1} \rho_1\lambda_1 x^{\lambda_1}dx + \int_{K_1}^{K_N} x\sum_{i=1}^{n-5} c_i B_{i,4}^{(1)}(x)dx + \int_{K_N}^{\infty} \rho_2\lambda_2 x^{-\lambda_2}dx - K\left(1-\rho_1 K^{\lambda_1}\right)\right] \\
= \;& e^{-r_f T}\left[\frac{\rho_1\lambda_1}{\lambda_1+1}\left(K_1^{\lambda_1+1}-K^{\lambda_1+1}\right) + \int_{K_1}^{K_N} x\sum_{i=1}^{n-5} c_i B_{i,4}^{(1)}(x)dx + \frac{\rho_2\lambda_2}{\lambda_2-1}K_N^{-\lambda_2+1} - K\left(1-\rho_1 K^{\lambda_1}\right)\right] \\
= \;& e^{-r_f T}\left[\sum_{i=1}^{n-5} c_i\int_K^{K_N} x\,B_{i,4}^{(1)}(x)\,dx + \frac{\rho_1\lambda_1}{\lambda_1+1}K_1^{\lambda_1+1} + \frac{\rho_2\lambda_2}{\lambda_2-1}K_N^{-\lambda_2+1} + \frac{\rho_1}{\lambda_1+1}K^{\lambda_1+1} - K\right] \qquad \text{(B.1)}
\end{aligned}
$$

$$
\begin{aligned}
& P(K;\mathbf{c},\boldsymbol{\theta}) \\
= \;& -e^{-r_f T}\int_0^{K} x\,R'(x)\,dx + Ke^{-r_f T}\int_0^{K} R'(x)\,dx \\
= \;& -e^{-r_f T}\left[\int_0^{K} x\,R'(x)\,dx + KR(K)\right] \\
= \;& -e^{-r_f T}\left[\int_0^{K} \rho_1\lambda_1 x^{\lambda_1}\,dx + K\left(\rho_1 K^{\lambda_1}\right)\right] \\
= \;& e^{-r_f T}\left[-\frac{\rho_1\lambda_1}{\lambda_1+1}K^{\lambda_1+1} + \rho_1 K^{\lambda_1+1}\right] \;=\; e^{-r_f T}\frac{\rho_1}{\lambda_1+1}K^{\lambda_1+1} \qquad \text{(B.2)}
\end{aligned}
$$

II. The case $K_1 \geq K \geq K_N$

$$
\begin{aligned}
& C(K;\mathbf{c},\boldsymbol{\theta}) \\
= \;& e^{-r_f T}\int_K^{\infty} x\,R'(x)\,dx - Ke^{-r_f T}\int_K^{\infty} R'(x)\,dx \\
= \;& e^{-r_f T}\int_K^{\infty} x\,R'(x)\,dx - Ke^{-r_f T}\,(1-R(K)) \\
= \;& e^{-r_f T}\int_K^{K_N} x\sum_{i=1}^{n-5} c_i B_{i,4}^{(1)}(x)\,dx + e^{-r_f T}\int_{K_N}^{\infty} \rho_2\lambda_2 x^{-\lambda_2}\,dx - Ke^{-r_f T}\left(1-\sum_{i=1}^{n-5} c_i B_{i,4}(K)\right) \\
= \;& e^{-r_f T}\int_K^{K_N} x\sum_{i=1}^{n-5} c_i B_{i,4}^{(1)}(x)\,dx + e^{-r_f T}\,\frac{\rho_2\lambda_2}{\lambda_2-1}K_N^{-\lambda_2+1} - Ke^{-r_f T}\left(1-\sum_{i=1}^{n-5} c_i B_{i,4}(K)\right) \\
= \;& e^{-r_f T}\sum_{i=1}^{n-5} c_i\int_K^{K_N} x\,B_{i,4}^{(1)}(x)\,dx + e^{-r_f T}\,\frac{\rho_2\lambda_2}{\lambda_2-1}K_N^{-\lambda_2+1} - Ke^{-r_f T}\left(1-\sum_{i=1}^{n-5} c_i B_{i,4}(K)\right) \\
= \;& e^{-r_f T}\sum_{i=1}^{n-5} c_i\int_K^{K_N} x\,B_{i,4}^{(1)}(x)\,dx + e^{-r_f T}\,\frac{\rho_2\lambda_2}{\lambda_2-1}K_N^{-\lambda_2+1} - Ke^{-r_f T} + e^{-r_f T}\left(\sum_{i=1}^{n-5} c_i K B_{i,4}(K)\right) \\
= \;& e^{-r_f T}\left[\sum_{i=1}^{n-5} c_i\left(KB_{i,4}(K) + \int_K^{K_N} x\,B_{i,4}^{(1)}(x)\,dx\right) + \frac{\rho_2\lambda_2}{\lambda_2-1}K_N^{-\lambda_2+1} - K\right] \qquad \text{(B.3)}
\end{aligned}
$$

$$
\begin{aligned}
& P(K;\mathbf{c},\boldsymbol{\theta}) \\
= \;& -e^{-r_f T}\int_0^{K} x\,R'(x)\,dx + Ke^{-r_f T}\int_0^{K} R'(x)\,dx \\
= \;& -e^{-r_f T}\int_0^{K} x\,R'(x)\,dx + Ke^{-r_f T}R(K) - e^{-r_f T}\int_0^{K_1} \rho_1\lambda_1 x^{\lambda_1}\,dx - e^{-r_f T}\int_{K_1}^{K} x\sum_{i=1}^{n-5} c_i B_{i,4}^{(1)}(x)\,dx \\
& + Ke^{-r_f T}\sum_{i=1}^{n-5} c_i B_{i,4}(K) \\
= \;& -e^{-r_f T}\,\frac{\rho_1\lambda_1}{\lambda_1+1}K_1^{\lambda_1+1} - e^{-r_f T}\int_{K_1}^{K} x\sum_{i=1}^{n-5} c_i B_{i,4}^{(1)}(x)\,dx + Ke^{-r_f T}\sum_{i=1}^{n-5} c_i B_{i,4}(K) \\
= \;& -e^{-r_f T}\,\frac{\rho_1\lambda_1}{\lambda_1+1}K_1^{\lambda_1+1} - e^{-r_f T}\sum_{i=1}^{n-5} c_i\int_{K_1}^{K} x\,B_{i,4}^{(1)}(x)\,dx + Ke^{-r_f T}\sum_{i=1}^{n-5} c_i B_{i,4}(K) \\
= \;& e^{-r_f T}\left[\sum_{i=1}^{n-5} c_i\left(KB_{i,4}(K) - \int_{K_1}^{K} x\,B_{i,4}^{(1)}(x)\,dx\right) - \frac{\rho_1\lambda_1}{\lambda_1+1}K_1^{\lambda_1+1}\right] \qquad \text{(B.4)}
\end{aligned}
$$

III. The case $K_N < K$

$$
\begin{aligned}
& P(K;\mathbf{c},\boldsymbol{\theta}) \\
= \; & -e^{-r_f T}\int_0^K x\,R'(x)\,dx + Ke^{-r_f T}\int_0^K R'(x)\,dx \\
= \; & -e^{-r_f T}\int_0^K x\,R'(x)\,dx + Ke^{-r_f T}R(K) \\
= \; & -e^{-r_f T}\int_0^{K_1} \rho_1\lambda_1 x^{\lambda_1}\,dx - e^{-r_f T}\int_{K_1}^{K_N} x\sum_{i=1}^{n-5} c_i B_{i,4}^{(1)}(x)\,dx - e^{-r_f T}\int_{K_N}^{K} \rho_2\lambda_2 x^{-\lambda_2}\,dx \\
& +Ke^{-r_f T}\left(1-\rho_2 K^{-\lambda_2}\right) \\
= \; & -e^{-r_f T}\frac{\rho_1\lambda_1}{\lambda_1+1}K_1^{\lambda_1+1} - e^{-r_f T}\int_{K_1}^{K} x\sum_{i=1}^{n-5} c_i B_{i,4}^{(1)}(x)\,dx + e^{-r_f T}\frac{\rho_2\lambda_2}{\lambda_2-1}\left(K^{-\lambda_2+1}-K_N^{-\lambda_2+1}\right) \\
& +e^{-r_f T}\left(K-\rho_2 K^{-\lambda_2+1}\right) \\
= \; & -e^{-r_f T}\frac{\rho_1\lambda_1}{\lambda_1+1}K_1^{\lambda_1+1} - e^{-r_f T}\sum_{i=1}^{n-5} c_i\int_{K_1}^{K} x\,B_{i,4}^{(1)}(x)\,dx + e^{-r_f T}\frac{\rho_2\lambda_2}{\lambda_2-1}\left(K^{-\lambda_2+1}-K_N^{-\lambda_2+1}\right) \\
& +e^{-r_f T}\left(K-\rho_2 K^{-\lambda_2+1}\right) \\
= \; & e^{-r_f T}\left[-\sum_{i=1}^{n-5} c_i K B_{i,4}(K) - \frac{\rho_1\lambda_1}{\lambda_1+1}K_1^{\lambda_1+1} + \frac{\rho_2\lambda_2}{\lambda_2-1}\left(K^{-\lambda_2+1}-K_N^{-\lambda_2+1}\right) + \left(K-\rho_2 K^{-\lambda_2+1}\right)\right] \\
= \; & e^{-r_f T}\left[-\sum_{i=1}^{n-5} c_i K B_{i,4}(K) - \frac{\rho_1\lambda_1}{\lambda_1+1}K_1^{\lambda_1+1} - \frac{\rho_2\lambda_2}{\lambda_2-1}K_N^{-\lambda_2+1} + \frac{\rho_2}{\lambda_2-1}K^{-\lambda_2+1} + K\right] \qquad \text{(B.5)}
\end{aligned}
$$

$$
\begin{aligned}
& C(K;\mathbf{c},\boldsymbol{\theta}) \\
= \; & e^{-r_f T}\int_K^{\infty} x\,R'(x)\,dx - Ke^{-r_f T}\int_K^{\infty} R'(x)\,dx \\
= \; & e^{-r_f T}\int_K^{\infty} x\,R'(x)\,dx - Ke^{-r_f T}\left(1-R(K)\right) \\
= \; & e^{-r_f T}\int_K^{\infty} \rho_2\lambda_2 x^{-\lambda_2}\,dx - Ke^{-r_f T}\left(1-(1-\rho_2 K^{-\lambda_2})\right) \\
= \; & e^{-r_f T}\left[\frac{\rho_2\lambda_2}{\lambda_2-1}K^{-\lambda_2+1} - \rho_2 K^{-\lambda_2+1})\right] \\
= \; & e^{-r_f T}\frac{\rho_2}{\lambda_2-1}K^{-\lambda_2+1} \qquad \text{(B.6)}
\end{aligned}
$$

Combining (B.1), (B.3), and (B.5) yields the call price function:

$$
\begin{aligned}
& C(K;\mathbf{c},\boldsymbol{\theta}) \\
= \;& e^{-r_f T}\left[\sum_{i=1}^{n-5} c_i \int_K^{K_N} x\, B_{i,4}^{(1)}(x)dx + \frac{\rho_1\lambda_1}{\lambda_1+1}K_1^{\lambda_1+1} + \frac{\rho_2\lambda_2}{\lambda_2-1}K_N^{-\lambda_2+1} + \frac{\rho_1}{\lambda_1+1}K^{\lambda_1+1} - K\right] I_{[0,K_1)}(K) \\
+ \;& e^{-r_f T}\left[\sum_{i=1}^{n-5} c_i \left(KB_{i,4}(K) + \int_K^{K_N} x\, B_{i,4}^{(1)}(x)\,dx\right) + \frac{\rho_2\lambda_2}{\lambda_2-1}K_N^{-\lambda_2+1} - K\right] I_{[K_1,K_N]}(K) \\
+ \;& e^{-r_f T}\frac{\rho_2}{\lambda_2-1}K^{-\lambda_2+1}\, I_{(K_N,\infty]}(K)
\end{aligned}
$$

Similarly, combining (B.2), (B.4), and (B.6) yields the put price function:

$$
\begin{aligned}
& P(K;\mathbf{c},\boldsymbol{\theta}) \\
= \;& e^{-r_f T}\,\frac{\rho_1\lambda_1}{\lambda_1+1}K^{\lambda_1+1}\, I_{[0,K_1)}(K) \\
+ \;& e^{-r_f T}\left[\sum_{i=1}^{n-5} c_i \left(KB_{i,4}(K) - \int_{K_1}^{K} x\, B_{i,4}^{(1)}(x)\,dx\right) + \frac{\rho_1\lambda_1}{\lambda_1+1}K_1^{\lambda_1+1}\right] I_{[K_1,K_N]}(K) \\
+ \;& e^{-r_f T}\left[-\sum_{i=1}^{n-5} c_i KB_{i,4}(K) - \frac{\rho_1\lambda_1}{\lambda_1+1}K_1^{\lambda_1+1} - \frac{\rho_2\lambda_2}{\lambda_2-1}K_N^{-\lambda_2+1} + \frac{\rho_2}{\lambda_2-1}K^{-\lambda_2+1} + K\right] I_{(K_N,\infty]}(K).
\end{aligned}
$$

APPENDIX C

DERIVATION OF THE QUADRATIC PROGRAM FOR B-SPLINE RNM ESTIMATION

C.1 Loss function

$$
\begin{aligned}
L_\omega &= \sum_{i=1}^{N} \left(V(K_i) - V(K_i; \mathbf{c}|\boldsymbol{\theta}^*)\right)^2 + \omega \int_{K_1}^{K_N} \left[R'''(x; \mathbf{c}|\boldsymbol{\theta}^*)\right]^2 dx \\
&= \epsilon^\top \epsilon + \omega \int_{K_1}^{K_N} \left[R'''(x; \mathbf{c}|\boldsymbol{\theta}^*)\right]^2 dx
\end{aligned}
$$

where

$$
\epsilon = \mathbf{V} - \hat{\mathbf{V}}|\boldsymbol{\theta}^*
$$

$$
\mathbf{V} = \begin{bmatrix} V(K_1) \\ \\ \\ \vdots \\ \\ \\ V(K_N) \end{bmatrix} = \begin{bmatrix} P(K_1) \\ \vdots \\ P(K_p) \\ \\ C(K_{p+1}) \\ \vdots \\ C(K_N) \end{bmatrix},
$$

$$\hat{\mathbf{V}}|\boldsymbol{\theta}^* = \begin{bmatrix} V(K_1;\mathbf{c}|\boldsymbol{\theta}^*) \\ \\ \vdots \\ \\ V(K_N;\mathbf{c}|\boldsymbol{\theta}^*) \end{bmatrix} = \begin{bmatrix} P(K_1;\mathbf{c}|\boldsymbol{\theta}^*) \\ \vdots \\ P(K_p;\mathbf{c}|\boldsymbol{\theta}^*) \\ \\ C(K_{p+1};\mathbf{c}|\boldsymbol{\theta}^*) \\ \vdots \\ C(K_N;\mathbf{c}|\boldsymbol{\theta}^*) \end{bmatrix}.$$

C.1.1 Sum of Squared Errors (SSE)

Using the option price functions (4.22) and (4.22), we have

$$C(K_i;\mathbf{c}|\boldsymbol{\theta}^*) = e^{-rT}\left[\sum_{j=1}^{n-5} c_i\left(K_i B_{j,4}(K_j) + \int_{K_i}^{K_N} x\, B_{j,4}^{(1)}(x)\,dx\right) + \frac{\rho_2^*\lambda_2^*}{\lambda_2^*-1}K_N^{-\lambda_2^*+1} - K_i\right],$$

$$P(K_i;\mathbf{c}|\boldsymbol{\theta}^*) = e^{-rT}\left[\sum_{j=1}^{n-5} c_j\left(K B_{j,4}(K) - \int_{K_1}^{K} x\, B_{j,4}^{(1)}(x)\,dx\right) + \frac{\rho_1^*\lambda_1^*}{\lambda_1^*+1}K_1^{\lambda_1^*+1}\right],$$

whence

$$\hat{\mathbf{V}}|\boldsymbol{\theta}^* = \begin{bmatrix} \mathbf{c}'\mathbf{M_1} - e^{-rT}\frac{\rho_1^*\lambda_1^*}{\lambda_1^*+1}K_1^{\lambda_1^*+1} \\ \vdots \\ \mathbf{c}'\mathbf{M_p} - e^{-rT}\frac{\rho_1^*\lambda_1^*}{\lambda_1^*+1}K_1^{\lambda_1^*+1} \\ \\ \mathbf{c}'\mathbf{H_{p+1}} + e^{-rT}\left(\frac{\rho_2^*\lambda_2^*}{\lambda_2^*-1}K_N^{-\lambda_2^*+1} - K_{p+1}\right) \\ \vdots \\ \mathbf{c}'\mathbf{H_N} + e^{-rT}\left(\frac{\rho_2^*\lambda_2^*}{\lambda_2^*-1}K_N^{-\lambda_2^*+1} - K_N\right) \end{bmatrix},$$

where

$$\mathbf{M_i} = e^{-rT}\begin{bmatrix} K_i B_{1,4}(K_i) - \int_{K_1}^{K_i} x\, B_{1,4}^{(1)}(x)\,dx \\ \vdots \\ K_i B_{n-5,4}(K_i) - \int_{K_1}^{K_i} x\, B_{n-5,4}^{(1)}(x)\,dx \end{bmatrix},$$

$$\mathbf{H_i} = e^{-rT}\begin{bmatrix} K_i B_{1,4}(K_i) + \int_{K_i}^{K_N} x\, B_{1,4}^{(1)}(x)\,dx \\ \vdots \\ K_i B_{n-5,4}(K_i) + \int_{K_i}^{K_N} x\, B_{n-5,4}^{(1)}(x)\,dx \end{bmatrix}.$$

Let

$$\mathbf{W} = \begin{bmatrix} P(K_1) + e^{-rT}\frac{\rho_1^*\lambda_1^*}{\lambda_1^*+1}K_1^{\lambda_1^*+1} \\ \vdots \\ P(K_p) + e^{-rT}\frac{\rho_1^*\lambda_1^*}{\lambda_1^*+1}K_1^{\lambda_1^*+1} \\ \\ C(K_{p+1}) - e^{-rT}\left(\frac{\rho_2^*\lambda_2^*}{\lambda_2^*-1}K_N^{-\lambda_2^*+1} - K_{p+1}\right) \\ \vdots \\ C(K_N) - e^{-rT}\left(\frac{\rho_2^*\lambda_2^*}{\lambda_2^*-1}K_N^{-\lambda_2^*+1} - K_N\right) \end{bmatrix} \quad \text{and} \quad \mathbf{G} = \begin{bmatrix} \mathbf{M_1'} \\ \vdots \\ \mathbf{M_p'} \\ \\ \mathbf{H_{p+1}'} \\ \vdots \\ \mathbf{H_N'} \end{bmatrix},$$

then

$$\begin{aligned} \epsilon &= \mathbf{V} - \hat{\mathbf{V}}|\boldsymbol{\theta}^* \\ &= \mathbf{W} - \mathbf{G}\mathbf{c} \\ \epsilon^\top\epsilon &= (\mathbf{W} - \mathbf{G}\mathbf{c})^\top(\mathbf{W} - \mathbf{G}\mathbf{c}) \\ &= \mathbf{c}^\top\mathbf{G}^\top\mathbf{G}\mathbf{c} - 2\mathbf{W}^\top\mathbf{G}\mathbf{c} + \mathbf{W}^\top\mathbf{W}. \end{aligned} \tag{C.1}$$

C.1.2 Roughness penalty

$$\begin{aligned}\int_{K_1}^{K_N} \left[R'''(x;\mathbf{c}|\boldsymbol{\theta}^*)\right]^2 dx &= \int_{K_1}^{K_N} \left[\mathbf{c}^\top \mathbf{B}^{(\mathbf{3})}(x)\right]^2 dx \\ &= \int_{K_1}^{K_N} \mathbf{c}^\top \mathbf{B}^{(\mathbf{3})}(x)\mathbf{B}^{(\mathbf{3})}(x)^\top \mathbf{c}\, dx \end{aligned} \tag{C.2}$$

where

$$\mathbf{B}^{(\mathbf{3})}(x) = \begin{bmatrix} B_{1,4}^{(3)}(x) \\ B_{2,4}^{(3)}(x) \\ \vdots \\ B_{n-6,4}^{(3)}(x) \\ B_{n-5,4}^{(3)}(x) \end{bmatrix}.$$

Since

$$\begin{aligned}\int_{x_i}^{x_{i+1}} \mathbf{c}^\top \mathbf{B}^{(\mathbf{3})}(x)\mathbf{B}^{(\mathbf{3})}(x)^\top \mathbf{c}\, dx &= \gamma_{i+1}^3 - \gamma_i^3 \\ &= \frac{h}{3}\left(\gamma_i^2 + \gamma_i\,\gamma_{i+1} + \gamma_{i+1}^2\right),\end{aligned}$$

where $\gamma_i \equiv R'''(x_i;\mathbf{c}|\boldsymbol{\theta}^*) = \mathbf{c}^\top \mathbf{B}^{(\mathbf{3})}(x_i)$,

the equation (C.2) can be written as a matrix form:

$$\begin{aligned}\int_{K_1}^{K_N} \mathbf{c}^\top \mathbf{B^{(3)}}(x)\mathbf{B^{(3)}}(x)^\top \mathbf{c}\, dx &= \sum_{i=5}^{n-5}\left[\int_{x_i}^{x_{i+1}} \mathbf{c}^\top \mathbf{B^{(3)}}(x)\mathbf{B^{(3)}}(x)^\top \mathbf{c}\, dx\right] \\ &= \sum_{i=5}^{n-5}\left[\frac{h}{3}\left(\gamma_i^2 + \gamma_i\,\gamma_{i+1} + \gamma_{i+1}^2\right)\right] \\ &= \mathbf{c}^\top \mathbf{D}^\top \mathbf{R}\mathbf{D}\mathbf{c}. \end{aligned} \tag{C.3}$$

where

$$\mathbf{R} = \begin{bmatrix} \frac{h}{3} & \frac{h}{6} & 0 & 0 & \dots & 0 \\ \frac{h}{6} & \frac{2h}{3} & \frac{h}{6} & 0 & \dots & 0 \\ 0 & \frac{h}{6} & \ddots & \ddots & \ddots & \vdots \\ 0 & 0 & \ddots & \ddots & \frac{h}{6} & 0 \\ \vdots & \vdots & \ddots & \frac{h}{6} & \frac{2h}{3} & \frac{h}{6} \\ 0 & 0 & \dots & 0 & \frac{h}{6} & \frac{h}{3} \end{bmatrix},$$

$$\mathbf{D} = \begin{bmatrix} B_{1,4}^{(3)}(x_5) & \cdots & B_{n-5,4}^{(3)}(x_5) \\ \vdots & \vdots & \vdots \\ B_{1,4}^{(3)}(x_{(n-4)}) & \cdots & B_{n-5,4}^{(3)}(x_{n-4}) \end{bmatrix},$$

By combining (C.1) and (C.3),

$$\begin{aligned} L_\omega &= \sum_{i=1}^{N}\left(V(K_i) - V(K_i;\mathbf{c}|\boldsymbol{\theta}^*)\right)^2 + \omega\int_{K_1}^{K_N}\left[R'''(x;\mathbf{c}|\boldsymbol{\theta}^*)\right]^2 dx \\ &= \mathbf{c}^\top\left[\mathbf{G}^\top\mathbf{G} + \omega\mathbf{D}^\top\mathbf{R}\mathbf{D}\right]\mathbf{c} - 2\mathbf{W}^\top\mathbf{G}\mathbf{c} + \mathbf{W}^\top\mathbf{W}. \end{aligned}$$

Thus, the optimization problem (4.30) is equivalent to the following quadratic program:

$$\min_{\mathbf{c}\in\mathbb{R}^{n^*-5}} \quad L_\omega = \frac{1}{2}\mathbf{c}^\top\mathbf{Q}\mathbf{c} + \mathbf{F}\mathbf{c},$$

where

$$\begin{aligned}\mathbf{Q} &= \mathbf{G}^\top\mathbf{G} + \omega\mathbf{D}^\top\mathbf{R}\mathbf{D},\\ \mathbf{F} &= -\mathbf{W}^\top\mathbf{G}.\end{aligned}$$

C.2 Constratints for the B-spline RNM CDF with Power Tails

C.2.1 End Points Conditons

By differentiating the B-spline basis function at knot points, the knot values of the B-spline basis function up to the 2nd derivative are given by:

$$B_{j,4}(x) = \begin{cases} \frac{1}{24} & x = x_{j+1} \\ \frac{11}{24} & x = x_{j+2} \\ \frac{11}{24} & x = x_{j+3} \\ \frac{1}{24} & x = x_{j+4} \end{cases} \tag{C.4}$$

$$B^{(1)}_{j,4}(x) = \begin{cases} \frac{1}{6h} & x = x_{j+1} \\ \frac{1}{2h} & x = x_{j+2} \\ -\frac{1}{2h} & x = x_{j+3} \\ -\frac{1}{6h} & x = x_{j+4} \end{cases} \tag{C.5}$$

$$B^{(2)}_{j,4}(x) = \begin{cases} \frac{1}{2h^2} & x = x_{j+1} \\ -\frac{1}{2h^2} & x = x_{j+2} \\ -\frac{1}{2h^2} & x = x_{j+3} \\ \frac{1}{2h^2} & x = x_{j+4} \end{cases} \tag{C.6}$$

By using the knot values of the B-spline basis (C.4), (C.5), and (C.6), the RNM can be written as:

$$\begin{aligned} R(x_j) &= \sum_{i=1}^{n-5} c_i B_{i,4}(x_j) \\ &= c_{j-4}B_{j-4,4}(x_j) + c_{j-3}B_{j-3,4}(x_j) + c_{j-2}B_{j-2,4}(x_j) + c_{j-1}B_{j-1,4}(x_j) \\ &= \frac{c_{j-4} + 11c_{j-3} + 11c_{j-2} + c_{j-1}}{24} \end{aligned} \tag{C.7}$$

$$\begin{aligned} R'(x_j) &= \sum_{i=1}^{n-5} c_i B^{(1)}_{i,4}(x_j) \\ &= c_{j-4}B^{(1)}_{j-4,4}(x_j) + c_{j-3}B^{(1)}_{j-3,4}(x_j) + c_{j-2}B^{(1)}_{j-2,4}(x_j) + c_{j-1}B^{(1)}_{j-1,4}(x_j) \\ &= \frac{-c_{j-4} - 3c_{j-3} + 3c_{j-2} + c_{j-1}}{6h} \end{aligned} \tag{C.8}$$

$$\begin{aligned} R''(x_j) &= \sum_{i=1}^{n-5} c_i B^{(2)}_{i,4}(x_j) \\ &= c_{j-4}B^{(2)}_{j-4,4}(x_j) + c_{j-3}B^{(2)}_{j-3,4}(x_j) + c_{j-2}B^{(2)}_{j-2,4}(x_j) + c_{j-1}B^{(2)}_{j-1,4}(x_j) \\ &= \frac{c_{j-4} - c_{j-3} - c_{j-2} + c_{j-1}}{2h^2} \end{aligned} \tag{C.9}$$

With the knot values of the RNM (C.7), (C.8), and (C.9), the end point conditions (4.10)-(4.15) can be expressed as:

$$\begin{aligned} \frac{c_1 + 11c_2 + 11c_3 + c_4}{24} &= \rho_1 K_1^{\lambda_1} \\ \frac{-c_1 - 3c_2 + 3c_3 + c_4}{6h} &= \rho_1 \lambda_1 K_1^{\lambda_1 - 1} \\ \frac{c_1 - c_2 - c_3 + c_4}{2h^2} &= \rho_1 \lambda_1 (\lambda_1 - 1) K_1^{\lambda_1 - 2} \end{aligned}$$

$$\begin{aligned} \frac{c_{n-8} + 11c_{n-7} + 11c_{n-6} + c_{n-5}}{24} &= 1 - \rho_2 K_N^{-\lambda_2} \\ \frac{-c_{n-8} - 3c_{n-7} + 3c_{n-6} + c_{n-5}}{6h} &= \rho_2 \lambda_2 K_N^{-\lambda_2 - 1} \\ \frac{c_{n-8} - c_{n-7} - c_{n-6} + c_{n-5}}{2h^2} &= -\rho_2 \lambda_2 (\lambda_2 + 1) K_N^{-\lambda_2 - 2} \end{aligned}$$

The end point conditions (4.10)-(4.15) can then be written as a matrix form:

$$\begin{bmatrix} 1 & 11 & 11 & 1 & 0 & \dots & 0 & 0 & 0 & 0 & 0 \\ -1 & -3 & 3 & 1 & 0 & \dots & 0 & 0 & 0 & 0 & 0 \\ 1 & -1 & -1 & 1 & 0 & \dots & 0 & 0 & 0 & 0 & 0 \\ 0 & 0 & 0 & 0 & 0 & \dots & 0 & 1 & 11 & 11 & 1 \\ 0 & 0 & 0 & 0 & 0 & \dots & 0 & -1 & -3 & 3 & 1 \\ 0 & 0 & 0 & 0 & 0 & \dots & 0 & 1 & -1 & -1 & 1 \end{bmatrix} \begin{bmatrix} c_1 \\ c_2 \\ \vdots \\ c_{n-6} \\ c_{n-5} \end{bmatrix} = \begin{bmatrix} 24\rho_1 x_0^{\lambda_1} \\ 6h\rho_1\lambda_1 x_0^{\lambda_1-1} \\ 2h^2\rho_1\lambda_1(\lambda_1-1)x_0^{\lambda_1-2} \\ 24(1-\rho_2 x_n^{-\lambda_2}) \\ 6h\rho_2\lambda_2 x_n^{-\lambda_2-1} \\ -2h^2\rho_2\lambda_2(\lambda_2+1)x_n^{-\lambda_2-2} \end{bmatrix}$$

C.2.2 Non-negative probability condition

By using (C.8), the non-negative probability condition (4.16) can be expressed as:

$$\begin{aligned} R'(x_j) &= \sum_{i=1}^{n-5} c_i B_{i,4}^{(1)}(x_j) \\ &= c_{j-4}B_{j-4,4}^{(1)}(x_j) + c_{j-3}B_{j-3,4}^{(1)}(x_j) + c_{j-2}B_{j-2,4}^{(1)}(x_j) + c_{j-1}B_{j-1,4}^{(1)}(x_j) \\ &= \frac{-c_{j-4} - 3c_{j-3} + 3c_{j-2} + c_{j-1}}{6h} \geq 0, \quad j = 6, \dots, n-5. \end{aligned} \tag{C.10}$$

The equation (C.10) can then be written as a matrix form:

$$\begin{bmatrix} 0 & -1 & -3 & 3 & 1 & 0 & 0 & 0 & \dots & 0 \\ 0 & 0 & -1 & -3 & 3 & 1 & 0 & 0 & \dots & 0 \\ \vdots & \vdots & & \ddots & \ddots & \ddots & \ddots & \vdots & \vdots & \vdots \\ 0 & \dots & 0 & 0 & -1 & -3 & 3 & 1 & 0 & 0 \\ 0 & \dots & 0 & 0 & 0 & -1 & -3 & 3 & 1 & 0 \end{bmatrix} \begin{bmatrix} c_1 \\ c_2 \\ \vdots \\ c_{n-6} \\ c_{n-5} \end{bmatrix} \geq \mathbf{0}$$

C.2.3 Mean-Forward Price Equaility Condition

The mean-forward price equality condition (4.20) is given by:

$$\begin{aligned}
S^0 e^{rT} &= E^Q(x) \\
&= \int_0^\infty x R'(x)\,dx \\
&= \int_0^{K_1} \rho_1 \lambda_1 x^{\lambda_1}\,dx + \int_{K_1}^{K_N} x \sum_{i=1}^{n-5} c_i B_{i,4}^{(1)}(x)\,dx + \int_{K_N}^{\infty} \rho_2 \lambda_2 x^{-\lambda_2}\,dx \\
&= \int_0^{K_1} \rho_1 \lambda_1 x^{\lambda_1}\,dx + \sum_{i=1}^{n-5} c_i \int_{K_1}^{K_N} x\, B_{i,4}^{(1)}(x)\,dx + \int_{K_N}^{\infty} \rho_2 \lambda_2 x^{-\lambda_2}\,dx \\
&= \frac{\rho_1 \lambda_1}{\lambda_1 + 1} K_1^{\lambda_1 + 1} + \sum_{i=1}^{n-5} c_i \int_{K_1}^{K_N} x\, B_{i,4}^{(1)}(x)\,dx + \frac{\rho_2 \lambda_2}{\lambda_2 - 1} K_N^{-\lambda_2 + 1} \qquad \text{(C.11)}
\end{aligned}$$

The equation (C.11) can then be written as a matrix form:

$$\left[\int_{K_1}^{K_N} x\, B_{1,4}^{(1)}(x)\,dx \ldots \int_{K_1}^{K_N} x\, B_{n-5,4}^{(1)}(x)\,dx\right] \begin{bmatrix} c_1 \\ c_2 \\ \vdots \\ c_{n-6} \\ c_{n-5} \end{bmatrix} = S_0 e^{rT} - \frac{\rho_1 \lambda_1}{\lambda_1 + 1} K_1^{\lambda_1 + 1} - \frac{\rho_2 \lambda_2}{\lambda_2 - 1} K_N^{-\lambda_2 + 1}$$

BIBLIOGRAPHY

Aït-Sahalia, Y., Duarte, J., 2003. Nonparametric Option Pricing under Shape Restrictions. Journal of Econometrics 116, 9-47.

Aït-Sahalia, Y., Lo, A., 1998. Nonparametric Estimation of State-price Densities Implicit in Financial Asset Prices. Journal of Finance 53, 499-547.

Aït-Sahalia, Y., Lo, A., 2000. Nonparametric Risk Management and Implied Risk Aversion. Journal of Econometrics 94, 9-51.

Akaike, H., 1973. Information Theory and an Extension to the Likelihood Ratio Principle, in B. N. Petrov and F. Csaki, eds.: Proceedings of the Second International Symposium of Information Theory

Andersen, A.B., Wagener, T., 2002. Extracting Risk Neutral Probability Densities by Fitting Implied Volatility Smiles: Some Methodological Points and an Application to the 3M Euribor Futures Option Prices. Working Paper No. 198. European Central Bank.

Anderson, M., Lomakka, M., 2005. Evaluating implied RNDs by some new confidence interval estimation techniques. Journal of Banking and Finance 29, 1535-1557.

Bahra, B., 1997. Implied Risk-neutral Probability Density Functions from Option Prices: Theory and Application. Working paper, Bank of England.

Bakshi, G., Cao, C., Chen, J., 1997. Empirical Performance of Alternative Option Pricing Models. Journal of Finance 52, 2003-2049.

Bates, D., 1991. The Crash of '87: Was It Expected? The Evidence from Options Markets. Journal of Finance 46, 1009-1044.

Bates, D., 1996. Testing Option Pricing Model, in: G.S Maddala and C.R. Rao (eds.), Handbook of Statistics, Vol. 14, Elsevier, North Holland 1996, 567-611.

Bates, D., 1996. Jumps and Stochastic Volatility: Exchange Rate Processes Implicit in

Deutsche Mark Options. Review of Financial Studies 9, 69-107.

Black, F., Scholes, M., 1973. The Pricing of Options and Corporate Liabilities. Journal of Political Economy 81, 637-654.

Bliss, R., Panigirtzoglou, N., 2002. Testing the Stability of Implied Probability Density Functions. Journal of Banking and Finance 26, 381-422.

Bondarenko, O., 2003. Estimation of Risk Neutral Densities using Positive Convolution Approximation. Journal of Econometrics 116, 85-112.

Bookstaber, R.M., McDonald, J.B., 1987. A General Distribution for Describing Security Price Returns. Journal of Business 60, 1987.

Breeden, D., Litzenberger, R., 1978. Prices of State Contingent Claims Implicit in option Prices. Journal of Business 51, 621-652.

Bu, R., Hadri, K., 2007. Estimating Option Implied Risk-Neutral Densities using Spline and Hypergeometric Functions. Econometrics Journal, Forthcoming.

Buchen, P., Kelly, M., 1996. The Maximum Entropy Distribution of an Asset Inferred from Option Prices. Journal of Financial and Quantitative Analysis 31, 143-159.

Campa, J.M., Chang, P.H.K., Reider, R.L., 1998. Implied Exchange Rate Distributions: Evidence from OTC Option Markets. Journal of International Money and Finance 17, 117-160.

Carr, P., Madan, D., 1999. Option valuation Using the Fast Fourier Transform. Journal of Computational Finance 2, 61-73.

Carr, P., Wu, L., 2003. The Finite Moment Log Stable Process and Option Pricing. Journal of Finance 58. 753-777.

Cartea, A., and Howison, S., 2002. Distinguished Limits of Lévy-Stable Processes, and Applications to Option Pricing. mimemo, University of Oxford Mathematical Institute.

Chang, P.H., and Melick, W., 1999. Background Note, in: Estimating and Interpreting Probability Density Functions-Proceedings of a Workshop held at the BIS on 14 June 1999. Bank for International Settlements.

Clews, R., Panigirtzoglou, N., Proudman, J., 2000. Recent developments in extracting information from options markets. Bank of England Quarterly Bulletin 40(1), 50-60.

Cox, J., Ross, S., 1976. The Valuation of Options for Alternative Stochastic Processes.

Journal of Financial Economics 3, 145-166.

Engle, R.F., Mustafa, C., 1992. Implied ARCH Models from Options Prices, Journal of Econometrics 52, 289-311.

de Boor, C., 1978. A Practical Guide to Splines. Springer-Verlag, 113-115.

Dekel, E., Lipman, B., Rustichini, A., 2001. A Unique Subjective State Space for Unforeseen Contingencies. Econometrica 69, 891-934.

Fama., E., 1963. Mandelbrot and the stable paretian hypothesis. Journal of Business 36(4), 420-429.

Fengler, M.R., 2005. Arbitrage-Free Smoothing of the Implied Volatility Surface. SFB 649 Economic Risk Discussion Paper 2005-019.

Gereben, A., Extracting Market Expectations from Option Prices. Reserve Bank of New Zealand: Bulletin 65(1), 43-52.

Gul, F., Pesendorfer, W., 2004. Random Expected Utility. mimemo. Princeton University.

Hales, S.J., 1997. Valuation of Foreign Currency Options with the Paretian Stable Option Pricing Model. Ph.D. dissertation, Ohio State University Department of Economics.

Heston, S., 1993. Closed-form Solution for Options with Stochastic Volatility, with Application to Bond and Currency Options, Review of Financial Studies 6, 327-343.

Jackwerth, J., 1999. Option Implied Risk-neutral Distributions and Implied Binomial Trees: a Literature Review. Journal of Derivatives 7, 66-82.

Jackwerth, J., Rubinstein, M., 1996. Recovering Probability Distributions from Option Prices. Journal of Finance 51, 1611-31.

Kreps, D., 1979. A Preference for Flexibility. Econometrica 47, 565-576.

Kullback, S., Leibler, R.A., 1951, On Information and Sufficiency. Annals of Mathematical Statistics 22, 79-86.

Lee, S.H., 2008. Parametric RNM Estimation: A Horse Race. mimemo. The Ohio State University.

Longstaff, F.A., 1995. Option Princing and the Martingale Restriction. Review of Financial Studies 8, 1091-1124.

Madan, D.B., Carr, P., Chang, E., 1998. The Variance Gamma Process and Option Pricing. European Financial Review 2, 79-105.

Madan, D.B. Milne, F., 1991. Option Pricing with VG Martingale Components. Mathematical Finance 1, 39-55.

Malz, A.M., 1997. Estimating the Probability Distribution of the Future Exchange Rate from Options Prices. Journal of Derivatives 5, 18-36.

Mandelbrot, B., Taylor, H.M., 1967. On the Distribution of Stock Price Differences. Operations Research 15, 1057-1062.

Markose, S., Alentorn, A., 2005. The Generalized Extreme Value Distribution (GEV), Implied Tail Index and Option pricing. Working paper, University of Essex.

McCulloch, J.H., 1971. Measuring the Term Structure of Interest Rates, Journal of Business 44, 19-31.

McCulloch, J.H., 1975. The Tax-Adjusted Yield Curve. Journal of Finance 30, 811-30.

McCulloch, J.H., 1978. The Pricing of Short-Lived Options When Price Uncertainty is Log-Symmetric Stable. Working Paper 89, Boston College.

McCulloch, J.H., 1985. Interest-Risk Sensitive Deposit Insurance Premia: Stable ACH Estimates. Journal of Banking and Finance 9, 137-156.

McCulloch, J.H., 1987. Foreign Exchange Option Pricing with Log-Stable Uncertainty. in: S.J. Khoury and A. Ghosh (eds). Recent Developments in International Banking and Finance, Vol.1, ed. by. Lexington, MA: Lexington, 231-245.

McCulloch, J.H., 1996. Financial Applications of Stable Distributions. in: G.S Maddala and C.R. Rao (eds.), Handbook of Statistics, Vol. 14, Elsevier, North Holland 1996, 393-425.

McCulloch, J.H., 2003. The Risk-Neutral Measure and Option Pricing under Log-Stable Uncertainty. mimemo. Ohio State University

McCulloch, J.H., Lee, S.H. 2006. Estimation of the Risk Neutral Measure with the Stable Option Pricing Model. mimemo. Ohio State University

Melick, W.R., Thomas, c.P., 1997. Recovering an Assets Implied PD from Option Prices: An application to Crude Oil during the Gulf Crisis. Journal of Financial and Quantitative Analysis 32, 91-115.

Merton, R.C., 1976. Option Pricing when Underlying Stock Returns are Discontinuous. Journal of Financial Economics 3, 125-144.

Monterio, A.M., Tütüncü, R., Vicente, L.N., 2005. Recovering Risk-Neutral Probability Density Functions from Options Prices using Cubic Splines and Ensuring Nonnegativity. mimemo. Carnegie Mellon University.

Naik, V., Lee, M., 1999. General Equilibrium Pricing of Options on Market Portfolio with Discontinuous Returns. Review of Financial Study 3, 393-521.

Rebanoto, R., 1999. Volatility and Correlations in the Pricing of Equity, FX and Interest-Rate Options. New York, NY: John Wiley & Sons, Inc.

Ritchey, R.J. 1990. Call Option Valuation for Discrete Normal Mixtures. Journal of Financial Research 13, 285-296.

Rosenberg, J., 1998. Pricing Multivariate Contingent Claims using Estimated Risk-Neutral Density Functions. Journal of International Money and Finance 17, 229-247.

Ross, S., 1976. Options and effciency. Quarterly Journal of Economics 90, 75-89.

Rosenberg, J., Engle, R., 2002. Empirical pricing kernels. Journal of Financial Economics 64, 341-372.

Savickas, R., 2002. A Simple Option-Pricing Formula. The Financial Review 37, 207-226.

Scott, L., 1997. Pricing Stock Options in a Jump-Diffusion Model with Stochastic Volatility and Interest Rates: Applications of Fourier Inversion Methods. Mathmatical Finance 7, 413-424.

Schwartz, G., 1978, Estimating the Dimension of a Model, Annals of Statistics 6, 461-464.

Shimko, D.C., 1993. Bounds of Probability, Risk 6, 33-37.

Söderlind, P., 2000. Market Expectation in the UK before and after the ERM Crisis. Economica 67, 1-18.

Stutzer, M., 1996. A Simple Nonparametric Approach to Derivative Security Valuation. Journal of Finance 51, 1633-1652.

Tunaru, R., Albota, G., 2005. Estimating Risk Neutral Density with a Generalized Gamma

Distribution. Working paper, City University, London.

Zolotarev, V.M., 1986. One-Dimensional Stable Laws. Vol. 65 in Translations of Mathematical Monographs. American Mathematical Society. (1983 Russian original).

Vinogradov, V., 2002. On a Class of Lévy Processes Used to Model Stock Price Movements with Possible Downward Jumps. Mathematical Reports of the Academy of Science [Canada], 24, 152-159.

Vuong, Q.H., 1989. Likelihood Ratio Tests for Model Selection and Non-nested Hypotheses. Econometrica 57, 307-333.